TÉCNICO LISBOA

Cardiac differentiation of human induced Pluripotent Stem Cells in Vertical-Wheel bioreactors

Inês Alexandra Brites Ribeiro

Thesis to obtain the Master of Science Degree in

Biological Engineering

Supervisor: Doctor Carlos André Vitorino Rodrigues

Examination Committee

Chairperson: Professor Maria Margarida Fonseca Rodrigues Diogo
Supervisor: Doctor Carlos André Vitorino Rodrigues
Member of the Committee: Professor Ana Margarida Pires Fernandes Platzgummer

December 2021

Preface

The work presented in this thesis was performed at the Institute for Bioengineering and Biosciences of Instituto Superior Técnico (Lisbon, Portugal), during the period March-November 2021, under the supervision of Doctor Carlos Rodrigues.

Declaration

I declare that this document is an original work of my own authorship and that it fulfills all the requirements of the Code of Conduct and Good Practices of the Universidade de Lisboa.

Acknowledgements

I would like to express my gratitude to everyone who supported me throughout this thesis.

Firstly, I would like to thank my supervisor, Doctor Carlos Rodrigues, for introducing me to Stem Cell Engineering Research Group (SCERG) and the fascinating field of stem cells, and for his guidance and support during this work. Thank you for providing moments to share and discuss ideias, not only within our own group, but also with experts in the field of bioprocess economics, Professor Frederico Ferreira and Doctor Cátia Bandeiras, to whom I would also like to express my gratitude.

Diogo Nogueira, my ”unofficial” supervisor, I could not thank you enough for all your help during this journey. You were incredible and taught me about stem cell culture with the greatest patience. Thank you also for being a friend and cheering me up whenever I felt demotivated or things weren't going so well in the lab. You really made this journey more cheerful with your constant happiness and positivity. I will never forget those funny moments when we played cards and Nintendo Switch after a long day of work.

I also want to thank my lab colleague, William Salvador, who I'm deeply glad and honoured to have met. You were incredibly supportive throughout this time and a really good friend. Thank you for cheering me up, for your patience and for sharing with me your vast knowledge, not only in thesis related subjects, but other interesting subjects, such as philosophy, poetry and music. This adventure would not be the same without you. I wish you all the best and I hope to share many more good moments with you in the future.

A special thank you to my friends in TFIST, Tuna Feminina do Instituto Superior Técnico, who were really supportive and caring. All the music and happiness shared with you were extremely important during this period. You will always represent a second family to me.

To my friends from Biological Engineering, thank you for being excellent colleagues and friends during the past 5 years. I wish you all the luck and success to your future careers and personal lives.

I could not forget to mention the support of my family and best friends, who were always therefor me both in good and bad moments and always believed in my potential. I know I can count on you inevery aspect of my life and I'm lucky that I'm surrounded by such incredible people. To those who left too early, my grandparents, I will always hold you tightly in my heart. You shaped who I am today and I'm sure you are very proud of me wherever you are.

Finally, I would like to thank for the funding received from the FCT granted to the projects CardioWheel (PTDC/EQU-EQU/29653/2017) and SMART (PTDC/EQU-EQU/3853/2020), as well as to the Research Unit iBB - Institute for Bioengineering and Biosciences (UIDB/04565/2020 and UIDP/04565/2020) and to i4HB - the Associate Laboratory Institute for Health and Bioeconomy (LA/P/0140/2020).

Abstract

Human induced pluripotent stem cell-derived cardiomyocytes (hiPSC-CMs) have great potential for applications in regenerative medicine, disease modeling and drug development, since they can be generated in a shorttime and in large quantities. Vertical-Wheel Bioreactors (VWBRs) have a gentle agitation system, beingpromising for the large-scale production of shear-stress sensitive cells, unlike the commonly used stirred tank bioreactors (STBRs). An economic model for the production of hiPSC-CMs in 3L VWBRs allowed toidentify the reagents and the maturation phase as the main cost drivers. The minimum working volume ofthe bioreactor was found to be a limitation for some autologous processes, because of increased costs related to an excessive production of hiPSC-CMs arising from using a greater volume than necessary. Further studies conducted in VWBRs are necessary to assess the application of lower cell densities, together with the optimization of other parameters (e.g agitation speed), to avoid excess production costswhile not compromising differentiation efficiency. Allogeneic therapies cost/dose were found to be lowerthan for autologous therapies at different scales. Additionally, hiPSCs were cultured in lab with three different culture media (mTesR1, E8 or B8) and differentiated into CMs via modulation of the canonical Wnt pathway in two distinct culture media (RPMI/B27 or CDM3). All conditions generated far lower percentages of CMs (up to 32.60% $cTnT^+$ cells) than the 80-98% $cTnT^+$ cells obtained in the original protocol after 15 days of differentiation, which might be associated with the lack of cell growth and adhesion to Matrigelsubstrate.

Keywords: cardiomyocytes, induced pluripotent stem cells, Vertical-Wheel bioreactors, economic model, cardiac differentiation, canonical Wnt signaling pathway

Resumo

Cardiomiócitos derivados de células estaminais pluripotentes induzidas (hiPSC-CMs) apresentam potencial para diversas aplicações em medicina regenerativa, modelação de doenças e desenvolvimento de fármacos, porque podem ser gerados em pouco tempo e grandes quantidades. Os biorreatores Vertical-Wheel (VWBRs) possuem um sistema de agitação gentil, sendo promissores para a produção em larga escala de células sensíveis a tensões de corte, contrariamente aos reatores de tanque agitado (STBRs) commumente utilizados. Um modelo económico da produção de hiPSC-CMs em VWBRs de 3L permitiu identificar os reagentes e a maturação como as principais fontes de custo. O volume mínimo de trabalho do reator constitui uma limitação para alguns processos autólogos, devido a maiores custos com o excesso de produção causado pela obrigatoriedade de respeitar esse critério. Estudos em VWBRs são necessários para avaliar a aplicação de menores densidades celulares, juntamente com a otimização de outros parâmetros, para evitar custos de produção excessivos sem comprometer a eficiência de diferenciação. Os custos/dose de processos alogénicos são menores que os custos/dose de processos autólogos em diferentes escalas. Adicionalmente, hiPSCs foram cultivadas em laboratório em três meios de cultura diferentes (mTesR1, E8 ou B8) e diferenciadas em CMs por meio da modulação da via Wnt canónica em dois meios de cultura (RPMI/B27 ou CDM3) em monocamada. Todas as condições geraram percentagens muito mais baixas de CMs (até 32,6% células $cTnT^{+}$) que os 80-98% de células $cTnT^{+}$ obtidas no protocolo original após 15 dias de diferenciação, o que pode estar associado ao baixo crescimento celular e adesão ao Matrigel.

Keywords: cardiomiócitos, células pluripotentes induzidas, biorreatores Vertical-Wheel, modelo económico, diferenciação cardíaca, via de sinalização Wnt canónica

Contents

List of Figures

List of Tables

List of abbreviations

2D	two-dimensional
3D	three-dimensional
AA	ascorbic acid
ATP	adenosine triphosphate
bFGF	basic fibroblast growth factor
BMP	bone morphogenic protein
BSA	bovine serum albumin
β-TrCP	β-transducin repeat containing E3 ubiquitin protein ligase
CICR	Ca^{2+} induced Ca^{2+} release
CiPA	Comprehensive in Vitro Proarrythmia Assay
CDM3	chemically defined medium 3
CHD	coronary heart disease
CHO	chinese hamster ovary
CK	caseine kinase
CMs	cardiomyocytes
CoG	cost of goods
CPP	critical process parameters
CQA	critical quality attributes
CVDs	cardiovascular diseases
CVPCs	cardiovascular progenitor cells
DC	destruction complex
DKK1	Dickkopf homolog 1
DMEM	Dulbecco's modified Eagle's medium
DO	dissolved oxygen
DS	dextran sulfate
Dsh	Dishevelled
E8	Essential 8
EB	embryoid body
ECC	excitation-contraction coupling

ECM	extracellular matrix
ECs	endothelial cells
EHT	engineered heart tissue
EMA	European Medicines Agency
ESCs	embryonic stem cells
FACS	fluorescence-activated cell sorting
FBS	foetal bovine serum
FCB	flow cytometry buffer
FCS	foetal calf serum
FDA	Food and Drug Administration
FGF	fibroblast growth factor
FHF	first heart field
FI	fold increase
Flk	fetal liver kinase
Fz	Frizzled
GATA	GATA-binding protein
GFP	green fluorescent protein
GMP	good manufacturing practices
HCN4	hyperpolarization-activated cyclic nucleotide gated channel 4
HSA	human serum albumin
hESCs	human embryonic stem cells
hESC-CMs	human embryonic stem cell derived cardiomyocytes
hESC-CVPCs	human embryonic stem cell derived cardiovascular progenitor cells
hiPSC-CMs	human induced pluripotent stem cell derived cardiomyocytes
hPSCs	human pluripotent stem cells
hPSC-CMs	human pluripotent stem cell derived cardiomyocytes
ICM	inner cell mass
Ig	immunoglobulin
IGF	insulin-like growth factor
iPSCs	induced pluripotent stem cells
iPSC-CMs	induced pluripotent stem cell derived cardiomyocytes
Isl	LIM-homebox transcription factor islet
IWP	inhibitor of the Wnt production
KDR	kinase domain receptor
KLF	Krüppel-like factor
KO-SR	KnockOut Serum Replacement
LEF	lymphoid enhancer factor
LRP	lipoprotein receptor-related protein

LVEF	left ventricular ejection fraction
MACS	magnetic-activated cell sorting
MEA	microelectrode array
mEF	mouse embryonic fibroblast
MESP1	mesoderm posterior transcription factor 1
MHC	myosin heavy chain
MI	myocardial infarction
NGS	neural goat serum
NRG	neuroregulin
OCT	octamer-binding transcription factor
PDGFR-α	platelet derived growth factor receptor alpha
PFA	paraformaldehyde
PP2A	protein phosphatase 2A
PSCs	pluripotent stem cells
QbD	quality by design
qRT-PCR	real-time quantitative reverse transcription polymerase chain reaction
QTPP	quality target product profile
ROCK	rho-associated coiled-coil protein kinase
RPMI	Roswell Park Memorial Institute
RWB	rotating wall bioreactor
Sca	stem cell antigen
SCF	stem cell factor
SHF	second heart field
SIRPA	signal-regulatory protein alpha
SMCs	smooth muscle cells
sMHC	sarcomeric myosin heavy chain
SOX	sex determining region Y-box
SR	sarcoplasmic reticulum
SSEA	stage-specific embryonic antigen
STBRs	stirred tank bioreactor
TCA	trycarboxilic acid
TCF	T cell factor
TGF	transforming growth factor
TNNT2	cardiac troponin T type 2
TRA	tumour rejection antigen
T-tubules	transverse tubules
ULA	ultra low attachment
VCAM	vascular cell adhesion molecule

VEGF	vascular endothelial growth factor
VEGFR	vascular endothelial growth factor receptor
WNT	wingless-type mouse mammary tumour virus integration site
VWBR	Vertical-Wheel™ bioreactor

1 Introduction

1.1 Stem Cells

Stem cells are unspecialized cells of the body that are able to self-renew or differentiate into specialized cells. They can replace damaged cells in a living organism. [1] [2] [3]

1.1.1 Classification of stem cells

Stem cells are classified according to their differentiation potential as totipotent, pluripotent, multipotent or unipotent (Figure 1.1). These cells can then become somatic terminally differentiated cells, such as cardiac cells and neurons. [1] [2] [3]

Totipotent cells (e.g zygote) have the highest differentiation potential and can give rise to cells of the entire organism, including extraembryonic tissues. [1] [2] [3]

After a few days of development, zygote turns into a blastocyst, which comprises an outer layer (trophoblast) that surrounds an inner cell mass (ICM) and a fluid-filled cavity called blastocoel. The cells from the ICM are called embryonic stem cells (ESCs). These cells are pluripotent, since they can give rise to cells from the three germ layers (mesoderm, endoderm and ectoderm), but not to extraembryonic tissues. Another example of pluripotent stem cells (PSCs) is induced pluripotent stem cells (iPSCs), which are artificially generated from somatic cells. [1] [3]

Multipotent stem cells have lower differentiation capability than PSCs, being able to generate cells of specific cell lineages. For instance, heamatopoietic stem cells are multipotent, since they can only give rise to blood cells. [1] [2] [3]

Unipotent stem cells can divide repeatedly, but are only able to form one cell type (e.g dermatocytes). [1] [2] [3]

1.1.2 Pluripotent Stem Cells

As previously referred, PSCs are able to differentiate towards cells of the three germ layers. PSCs can be divided into ESCs and iPSCs, which, theoretically, can propagate indefinitely, being an unlimited source for replacing lost or damaged tissues. [1] [2]

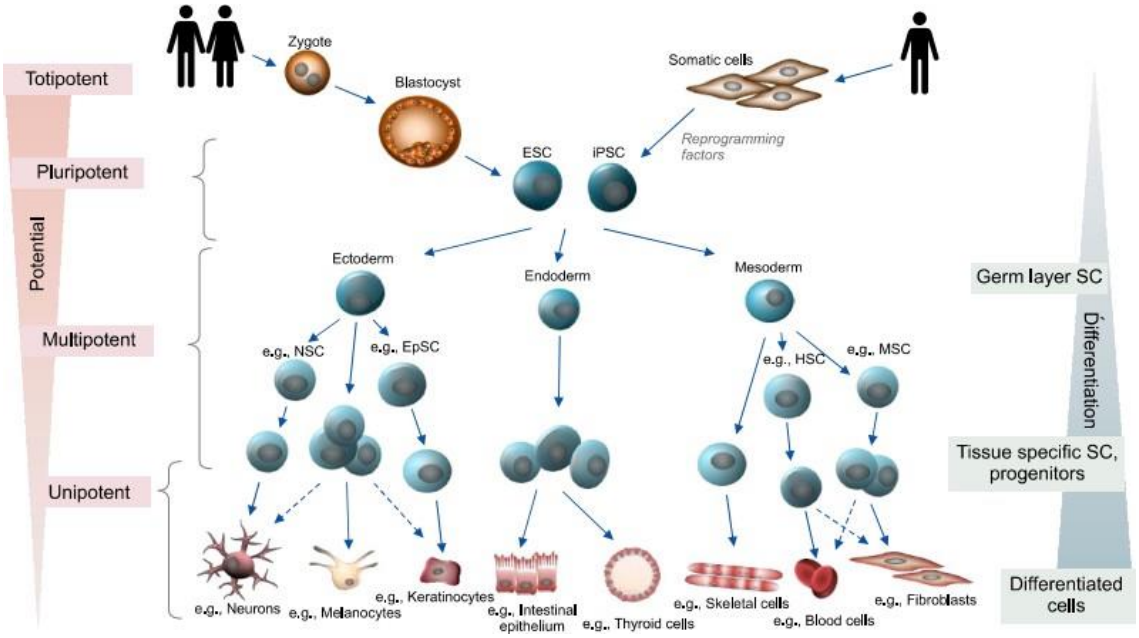

Figure 1.1: Differentiation potential of stem cells. ESC: embryonic stem cell, iPSC: induced pluripotent stem cell, NSC: neural stem cell, EpSC: epidermal stem cell, HSC: hematopoietic stem cell, MSC: mesenchymal stem cell. Adapted from [3]

1.1.2.1 Embryonic stem cells vs. Induced pluripotent stem cells

ESCs were first isolated in 1981 from the ICM of mouse developing blastocysts by Evans and Kaufman [4] and Gail Martin [5]. While in the study of Evans and Kaufman, ICM cells were cultured on a feeder layer of mouse embryonic fibroblasts (mEFs) in Dulbecco's modified Eagle's medium (DMEM) supplemented with 10% fetal calf serum and 10% new-born calf serum [4], in the study of Gail Martin ICM cells were cultured on mEFs with embryonic carcinoma cells conditioned media [5]. In both studies, isolated cells demonstrated the capability to differentiate into several cell types and ability to form teratocarcinomas when injected into mice. [4] [5]

In 1998, Thomson et. al. obtained, for the first time, human embryonic stem cells (hESCs) from the ICM of blastocysts from *in vitro* fertilization. Cells were cultured on irradiated mEFs in DMEM medium supplemented with 20% fetal bovine serum (FBS), 1 mM glutamine, 0.1 mM β-mercaptoethanol and 1% non-essential amino acids. Generated cells expressed high levels of telomerase activity, pluripotent cell surface markers (such as stage-specific embryonic antigen (SSEA)-4), normal karyotypes and the ability to produce teratomas after injection into immunodeficient mice. [6]

The high proliferation capacity *in vitro* and the ability to generate cells from the three germ layers render ESCs very promising for several therapeutical applications. However, these cells can form teratomas when injected into a host and prior differentiation of ESCs is needed to avoid teratoma formation. Furthermore, the isolation of ESCs causes some ethical concerns, due to the destruction of embryos. [1] [2]

iPSCs were first derived in 2006 when Yamanaka and Takahashi discovered the possibility of reprograming somatic cells back into a pluripotent state. Mouse embryonic or adult fibroblasts were retrovirally transduced with four transcription factors: octamer-binding transcription factor (OCT) 3/4, sex determining

region Y-box (SOX) 2, Krüppel-like factor (KLF) 4 and c-MYC [7]. One year later, Yamanaka, Takahashi and co-workers succeeded in generating human induced pluripotent stem cells (hiPSCs) from adult human fibroblasts by retrovirally transducing the same cocktail of transcription factors. [8] In the same year, Thomson et. al. also succeeded in obtaining hiPSCs from human adult fibroblasts by reprogramming with a different set of transcription factors (Oct3/4, Sox2, Nanog and Lin28) using lentiviruses. [9]

iPSCs can be reprogrammed from several cell sources, such as fibroblasts, peripheral blood cells, keratinocytes, renal epithelial cells from urine, etc. Somatic cells are transfected with Yamanaka's original cocktail of transcription factors or different combinations of reprogramming factors, which can be introduced by integrating viral vector systems (e.g retroviruses and lentiviruses) or integration-free systems, such as non-integrating viral vectors (e.g sendai viruses and adenoviruses), plasmid DNA transfer, recombinant proteins and synthetic mRNAS. However, there are some issues concerning the reprogramming method, namely the low efficiency of existing methods and risk of genetic abnormalities and teratoma formation by integration of retroviral or lentiviral vectors into the host's genome. Therefore, iPSCs should be well characterized before they can be safely used for clinical applications. [1] [2]

Cell source can also affect iPSCs differentiation potential into specific cell lineages. iPSCs present residual methylation from the cell of origin (epigenetic memory), which impacts their differentiation. [2]

Despite some limitations, the advent of iPSCs opened new possibilities in stem cell research. Unlike ESCs, iPSCs cause no ethical concerns, can be patient-specific and thus, biocompatible with the patient, avoiding immune rejection. Apart from regenerative medicine purposes, iPSCs can be also used for disease modeling, drug development and drug toxicity studies. [1] [2]

PSC characterization methods include the expression of pluripotency markers (e.g OCT4, SOX2, etc.), differentiation into all three embryonic germ layers both *in vitro* (by the formation of embryoid bodies) and *in vivo* (by assessing the formation of teratomas in immunodeficient mice) and karyotypic analysis to assess genetic stability. [5] [7]

1.1.3 Applications of stem cells

Stem cells have a plethora of applications, such as cell therapy, tissue engineering, drug screening and disease modelling. [2] [10] [11]

Stem cells can be used to restore tissue function by integrating into the host tissue or by releasing signals that help to restore tissue function without integrating into the host tissue. For example, mesenchymal stem cells (MSCs) appear to provide some paracrine trophic factors that help cardiac regeneration when injected into injured hearts. [10] Stem cells can be also combined with engineered scaffolds using tissue engineering approaches to promote cell adhesion and growth and/or mimicking the target tissue environment by promoting angiogenesis. When transplanted *in vivo*, these tissue constructs are incorporated into the host's tissues, helping to repair damaged tissues. [10] [12]

Human pluripotent stem cells (hPSCs) have been used in the pharmacological industry for drug screening and disease modeling applications. hiPSCs are currently applied to generate disease models for both drug efficacy screening and toxicity assays. These cells do not have the ethical concerns

associated with hESCs and can pave the way for personalized medicine using patient-specific iPSCs. iPSCs can be reprogrammed from somatic cells from patients suffering from a specific disease and then be differentiated into disease-relevant cell types in order to unveil disease cellular mechanisms and further develop new drugs to target these conditions. Gene editing tools can also be applied to correct disease-causing gene mutations in patient-derived iPSCs or introduce specific mutations into non-disease affected wild-type iPSCs to generate isogenic iPSC controls. Three-dimensional (3D) organoids can be made from several hiPSC-derived cell types to mimic human physiology, being promising platforms for disease modelling and drug screening. [11] Regarding drug toxicity, hiPSC-derived cells can also be useful tools to predict more accurately drug cardiotoxicity or hepatotoxicity effects before they reach clinical trials; many drugs have failed in later stages of clinical trials due to unforeseen toxicities in suboptimal screening assays, such as screening in Chinese hamster ovary cells. Many studies have started using hiPSC-derived cardiomyocytes (hiPSC-CMs) and hiPSC-derived hepatic cells to evaluate drug toxicity. [2] [11] [13] For example, the Comprehensive in Vitro Proarrythmia Assay (CiPA) involves using hiPSC-CMs to assess drug effects on cardiac repolarization and more accurately predict the risk of potentially fatal cardiac arrythmia (torsades de pointes) before drugs can reach clinical trials. [13]

Although most clinical trials for Regenerative Medicine applications have relied on the usage of ESCs, one clinical trial has used hiPSC-derived autologous retinal pigmental epithelial cells to treat macular degeneration and the treatment improved patient's vision. The trial was subsequently put on hold due to mutations observed in a second patient's hiPSCs, but it is anticipated to resume. [11] More recently, in 2018, Japan has initiated a clinical trial to treat patients suffering from heart disease with cardiac sheets made of iPSC-CMs. [14]

1.2 Human Heart

1.2.1 Human heart development *in vivo*

The heart is one of the first organs to form and become functional during embryogenesis. It is a four-chambered organ that functions not only to mediate a proper oxygen distribution, but also to transport nutrients and signaling molecules to the entire body. [15] [16] [17] [13]

Most of the knowledge regarding human heart development is based on mammalian models like mouse, due to ethical concerns in using fetuses for these studies. Mouse models are considered accurate models of human cardiac development, despite some differences between them (e.g human heart is 1000 times larger and starts beating around embryonic day 22 in humans vs. embryonic day 9 in mice). Researchers have recently begun to use hPSCs-derived cardiomyocytes (hPSC-CMs) to study heart development, but some limitations still exist, like the fact that they do not reach full maturity. [18] [19]

Figure 1.2 depicts an overview of heart development. Early in embryonic development, the inner cell mass of the blastocyst undergoes gastrulation, giving rise to the three germ layers: ectoderm, mesoderm and endoderm. [15] [17] [16] The heart is comprised of multiple cell lineages that mainly derive from the mesodermal layer and also ectoderm-derived cardiac neural crest cells, which arise from the interaction

of inductive and inhibitory signals between the germ layers. The heart tissue consists of cardiomyocytes (CMs), endothelial cells (ECs) and smooth muscle cells (SMCs). [15] [16] [17] [18] [20] [13]

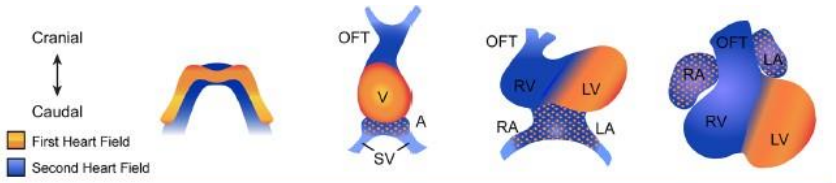

Stage	Cardiac Crescent	Linear Heart Tube	Looping Heart	Chamber Specialization/ Septation
Mouse Embryo Stage	E7.5	E8.0	E9-12	E10+
Human Embryo Stage	Day 15	Day 20	Day 28-30	Day 32+
Key Regulators	GATA4 NKX2.5 MESP1/2 ISL1 BAF60C MEF2C	GATA4 NKX2.5 TBX5 TBX20 MEF2C	GATA4 NKX2.5 TBX5 MEF2C HAND1/2	GATA4 NKX2.5 TBX5 PITX2 TBX1

Figure 1.2: Heart development overview. [17]

Initiation of the gastrulation process and mesoderm induction depends on NODAL, bone morphogenetic protein (BMP), wingless-type mouse mammary tumour virus integration site (WNT) and fibroblast growth factor (FGF) signaling pathways. Mesodermal induction is marked by the expression of the T-box transcription factor T(Brachyury). In order to generate a cardiogenic mesoderm, T^{+} cells require NOTCH-mediated inhibition of canonical Wnt/β-catenin pathway and activation of non-canonical Wnt. Mesoderm posterior transcription factor 1 (MESP1) is thought to be the earliest marker of cardiovascular specification. It downregulates pluripotency gene expression while activates cardiac-specific genes, like Nkx2-5 and GATA-binding protein (GATA)4. These $MESP1^{+}$ cells undergo epithelial-to-mesenchymal transition, migrating billaterally from the primitive streak towards the anterior direction of the embryo, where they will give rise to the two major cardiac progenitor pools: first heart field (FHF) or cardiac crescent and second heart field (SHF) progenitor cells (located medially and dorsally to FHF progenitor cells). SHF progenitor cells demonstrate increased proliferation and delayed differentiation commitment in relation to FHF cells. [13] [15] [17] [16] [20] [21] [22] [23]

During the third week of human embryonic development, FHF cells fuse at the midline to form the linear heart tube, which is comprised of an outer myocardial layer and an inner endocardial layer separated by extracellular matrix (cardiac jelly). The linear heart tube starts beating around embryonic day 22. FHF progenitor cells give rise to the left ventricle and small portions of the atria. [15] [16] [17] [20] [18] [13] [19] By week 4, the linear heart tube undergoes rightward looping and SHF progenitors migrate to the anterior and posterior venous poles of the heart tube, promoting its elongation. These cells differentiate into CMs, ECs and SMCs, contributing to the formation of the right ventricle, septum, inflow and outflow tracts. [15] [16] [17] [20] [18] [19] Other important processes occur, such as the formation of endocardial cushions (precursors to future valvular structures) in the atrioventricular canal and the outflow tract. In this process, endocardial cells undergo epithelial-mesenchymal transition due to myocardial signals in

the cardiac jelly and these mesenchymal cells proliferate and invade the cardiac jelly, giving rise to the endocardial cushions. [15] Apart from endocardium and myocardium, a third layer of cells, which covers the entire heart, is formed: the epicardium. The epicardium is derived from proepicardial cells, which give rise to cardiac fibroblasts, coronary SMCs and a small population of CMs. Some of these cells undergo an epithelial-mesenchymal transition and invade the underlying myocardium to differentiate into cardiac fibroblasts, coronary vessels SMCs and coronary endothelium. [15] [16] [17] [20] [18] [19]

After cardiac looping, cardiac trabeculation occurs. At this stage, luminal projections (trabeculae), consisting of myocardial cells enclosed by the endocardial layer are formed due to paracrine signaling between both layers. This process helps the compaction of the ventricular myocardium, contractility, septation and conductivity. [16] [17] [18] Cardiac neural crest cells also help the septation process, participating in the septation of the outflow tract and giving rise to SMCs within the aortic and pulmonary arteries. Apart from that, they also take part in the formation of heart valves and sensory innervation. [15] [16] [17] [18]

The heart becomes fully formed and functional organ around gestational week 7. [16] [18]

1.2.2 Cardiovascular diseases and traditional therapies

Cardiovascular diseases (CVDs) are the major cause of death in the world. It is estimated that 17.9 million people died from CVDs in 2019, which represents 32% of the global deaths. CVDs are a group of heart and circulatory disorders that include coronary heart disease (CHD), cerebrovascular disease (stroke), rheumatic heart disease, among others. [24]

CHD, also called ischemic heart disease, is the most common cause of death in most western countries. CHD is characterized by reduced blood supply and, thus, lack of oxygenation of the heart muscle due to obstruction of coronary arteries. This leads to myocardial infarction (MI), which is the permanent heart muscle damage. After MI, there is an extensive cardiac remodeling, characterized by ischemia, cardiomyocyte necrosis or apoptosis, inflammation, cardiomyocyte hypertrophy (which results in the enlargement of the left ventricle) and the formation of a fibrotic scar. [25] [26] Cardiac remodeling eventually leads to heart failure (heart's inability to pump blood around the body properly) and, consequently death. [25] [26] [27] [28]

Conventional drug treatments for patients with CVD include anti-thrombotic therapy [24] [25] [26] , which prevent the formation of blood clots by suppressing the formation of thrombin [25] , β-adrenergic receptor blockers [24] [25] [26] [29], which slow the heart rate and prevent arrythmias [29], angiotensin-converting enzyme inhibitors, angiotensin-II receptor blockers or aldosterone antagonists [24] [25] [26] [27] [28] [29] , which inhibit renin-angiotensin-aldosterone system and cause the regression of left ventricular hypertrophy, decrease blood pressure and prevent adverse cardiac remodeling [25] [27] [28], and statins [24] [26] [27], which have an anti-inflammatory action [27] and lower blood cholesterol [29]. Sometimes patients are subjected to surgical procedures, such as balloon angioplasty or stents to prevent coronary stenosis and restore the blood flow, coronary artery bypass graft surgery to increase blood supply to coronary circulation by grafting arteries or veins from other parts of the body to the coronary arteries to

bypass atherosclerotic narrowings, as well as valve repair and replacement procedures. [24] [25] [29]

After a MI, patients with left ventricular dysfunction have a high risk of sudden death due to lethal arrythmias. Thus, they are given implantable cardioverter defibrillators to prevent sudden cardiac death. [27] [28]

In the case of advanced end-stage heart failure, heart transplantation remains the only viable therapy. However, due to the high prevalence of CVDs, there is donor organ shortage and most patients on long wait-lists for cardiac transplant die from heart failure. [30] Cardiac cell therapy is a promising therapeutic alternative to heart transplantation. PSC-derived cardiomyocytes are particularly promising, given the high proliferation capacity and cardiac differentiation potential of PSCs. [13] [31]

1.2.3 Cardiovascular progenitor cells

Cardiovascular progenitor cells (CVPCs) are mesoderm-derived cells characterized by their restricted differentiation potential into the three cardiac cell types: CMs, SMCs and ECs. [32] [33] [34] [35]

Human heart has a very limited regenerative capacity, being 0.5-1% of CMs renewed every year. [35] Several populations of endogenous CVPCs in adult mammalian hearts have been identified, but these cells account only for 1-2% of the cell number in the heart. CVPCs can be obtained in large numbers from PSCs, being suitable for cell-based therapies, disease modelling, drug screening and heart development models. In particular, hiPSC-derived CVPCs allow the creation of patient-specific disease models and autologous cell therapies, avoiding immune rejection by the host. It should be noted that no cell-type specific markers are yet known for CVPCs. Thus, in the future, it will be crucial to define the molecular identity of CVPCs, in order to more finely control lineage commitment to distinct cardiac entities. [32] [33]

MESP1 is the earliest marker of cardiac progenitors and marks a progenitor population preceding the FHF and SHF progenitors. This transcription factor activates downstream key cardiogenic transcription factors, such as Nkx2-5,GATA4, Mef2c and LIM-homebox transcription factor islet (Isl)-1. [32] [33] [34] [35] [18]

Spater and colleagues identified the hyperpolarization-activated cyclic nucleotide gated channel 4 (HCN4), which is a voltage-gated ion channel of the conduction system, as a specific marker of FHF. [18] [36] Isl-1 has been previously regarded as a specific marker for SHF progenitors, but it was detected at the cardiac crescent stage, suggesting that it is also expressed in FHF progenitors. [34] [18] $Isl-1^{+}$ cells are found in the embryonic and postnatal human hearts, but not in adult human hearts. [34]

Stage-specific embryonic antigen-1 (SSEA-1) has also been proposed as an early cardiac progenitor marker. [35] [37] $SSEA-1^{+}$ cells can give rise to cells of both FHF and SHF and differentiate into CMs, SMCs and ECs. Since it is a surface marker, $SSEA-1^{+}$ cells can be isolated by fluorescence-activated cell sorting (FACS). [37]SSEA-1 has been used as sorting marker for hESC-derived cardiac progenitors (hESC-CVPCs) in a clinical trial developed by Menasché et. al. to treat a patient with heart failure. [38] This study is mentioned later in Section 1.3.6.

Vascular endothelial growth factor receptor (VEGFR)2 encoded by fetal liver kinase (*Flk*)-1, also known as kinase domain protein receptor (*KDR*), has been shown to mark early CVPC populations. [33] [34]

[35] [18] [39] Yang et. al. identified a population of $KDR^{low}/c-Kit^{-}$ CVPCs derived from hESCs which were able to differentiate into CMs, SMCs and ECs *in vitro* or when transplanted into mice. [39]

Platelet derived growth factor receptor alpha (PDGFR-α) was also shown to mark CVPCs. [33] [35] [18] Chong et. al. found strong expression of PDGFR-α in the interstitial cells of the epicardium, myocardium, endocardium and coronary smooth muscle both in human fetal and diseased adult hearts. Isolated $PDGFR-^{+}$ cells from human fetal hearts could give rise to SMCs and ECs *in vitro*, but not CMs, which suggested a possible role of these progenitors to promote vascularization or limit fibrosis in injured hearts. [40]

Cell-surface protein signal-regulatory protein alpha (SIRPA) has been shown to be expressed in CVPCs. [33] [41] In a study using hESC-derived $Nkx2\text{-}5^{GFP}$ (a fusion gene that encodes for the transcription factor Nkx2-5 and the green fluorescent protein (GFP) when the Nkx2-5 promoter is activated) cells, most $Nkx2\text{-}5^{+}$ cells were also $SIRPA^{+}$ cells. A population with more restricted differentiation potential expressing vascular cell adhesion molecule (VCAM)1, $Nkx2-5^{+}$ $SIRPA^{+}$ $VCAM1^{+}$ cells, arose from $Nkx2-5^{+}$ $SIRPA^{+}$, giving predominantly rise to cardiac troponin T type 2 (*TNNT2*) positive cells (84.2±6.8% $TNNT2^{+}$ cells), which is a marker characteristic of CMs. [41]

Stem cell factor (SCF) receptor c-Kit has been suggested as a CVPC marker and several studies identified an endogenous cardiac $c\text{-}Kit^{+}$ population in human heart. [32] [33] [34] Bearzi et. al. reported the differentiation of human cardiac $c\text{-}Kit^{+}$ cells isolated by FACs into CMs, SMCs and ECs *in vitro* and after transplantation into immunodeficient mice. [42] However, there is some controversy among the scientific community about whether or not to regard $c\text{-}Kit^{+}$ cells as CVPCs. Studies in mice have shown that resident $c\text{-}Kit^{+}$ cells have little cardiomyogenic potential and contribute mostly to the recovery of post-MI damaged hearts by revascularization. [43] [44] $c\text{-}Kit^{+}$ cells include $c\text{-}Kit^{+}/CD45^{+}$ cardiac mast cells and $c\text{-}Kit^{+}/CD31^{+}/CD34^{+}$ endothelial progenitor cells. Only a small percentage of $c\text{-}Kit^{+}$($c\text{-}Kit^{+}/tryptase^{-}/CD45^{-}/CD31^{-}/CD34^{-}$) cells can give rise to CMs, ECs and SMCs. [13]

A population of stem-cell antigen (Sca)-1 positive cells has been identified in adult murine hearts and human $Sca\text{-}1^{+}$ cells were isolated from the heart with the rodent antibody. [34] [13] $Sca\text{-}1^{+}$ cells differentiate into CMs, SMCs and ECs and exhibit *in vivo* cardiomyogenic regenerative potential. [13] [45]

1.3 Process Development

1.3.1 Culture platforms for expansion and differentiation of hPSCs into CMs

As mentioned before, hPSCs can be used for a wide range of applications, such as drug screening, disease modelling and cellular therapies. These applications require the production of high cell numbers. For example, it is estimated that doses in the order of 1×10^9 hPSC-derived cardiomyocytes (hPSC-CMs) are required to treat patients with heart injury. Therefore, it is vital to establish scalable, defined, robust and economically viable processes for the production of hPSC-based products. [13]

1.3.1.1 2D culture systems

Monolayer cell culture on two-dimensional (2D) platforms, such as tissue culture plates or T-Flasks, has been widely established, either for hPSC expansion or hPSC differentiation into CMs. The cells grow on the surface of matrices, such as Matrigel™, recombinant proteins (e.g. laminin) or syntheticpolymers. This method is a standard procedure in all laboratories and allows for an easy observation ofcell quality under a microscope, as well as easy medium changes. [46]

In order to generate large cell numbers for the aforementioned applications, a scale-out approach can be done, where multiple vessels are used to achieve the required cell numbers. Nevertheless, this is very space-, time-, cost-, labor-consuming and restricts the online monitoring of culture parameters. [47] [48] [49] Moreover, these systems inadequately mimic the *in vivo* physiological 3D microenvironment. [48] [50] In static culture conditions, there are also gradients of media components, waste metabolite products, paracrine factors and gases. All these factors result in a high cellular heterogeneity and low production yields. [50] [49]

With the objective to overcome space and labor-associated problems using the “scale-out” approach, multilayered flasks with online monitoring of culture parameters (e.g. pH and dissolved oxygen (DO)) were developed. However, more studies are required to demonstrate their feasibility for large-scale production of hPSCs and also hPSC-CMs. [49]

1.3.1.2 3D culture systems

3D culture systems, namely bioreactors, are promising alternatives for the large production of hPSCs and also hPSC-CMs. These systems allow the homogeneous distribution of oxygen and nutrients to the culture and are equipped with probes and control systems to monitor and maintain important culture parameters, like temperature, pH and DO. Another advantage of bioreactors is that a variety of feeding regimes can be applied, namely batch, repeated-batch, fed-batch, and perfusion. [48] [50]

Regarding 3D culture formats, cells can be cultured either in the form of aggregates, attached to microcarriers or microencapsulated. [47] [48] [51] [52] [50] [49]

In aggregate cultures, cells are inoculated to bioreactors in the form of single cells or cell clumps and form aggregates. This culture format resembles the cells natural microenvironment and support hPSC growth and viability without the need of matrices. Differentiation can also be induced by changing expansion medium to a lineage-specific differentiation medium. However, it is necessary to control aggregate size due to diffusional limitations of nutrients, growth factors and oxygen in the center of the aggregates, which can lead to necrosis or spontaneous differentiation when their diameter is larger than 300 µm. [48] [50] [49]

Cells can also grow in 3D attached to microcarriers made of different materials (e.g polystyrene, gelatin, glass), which can be coated with matrices (e.g. Matrigel, laminin, vitronectin) to promote cell adhesion. The advantages of using microcarriers are their large surface area/volume ratio available for cell growth, facilitating scale-up. Notwithstanding, the need to detach cells from microcarriers by enzymatic or mechanical dissociation leads to high cell losses; biodegradable and biocompatible microcarriers can

eliminate this problem and cells attached to microcarriers can be directly transplanted into patients. Cells attached to microcarriers are also susceptible to high hydrodynamic shear stress inside the bioreactor, which can compromise cell viability, pluripotency maintenance or differentiation. Furthermore, fabrication of microcarrier beads and respective coatings can be costly. [48] [50] [49]

Microencapsulating cells inside a biomaterial (e.g hydrogels) protects cells from shear stress inside the bioreactor and avoids clumping that can occur in microcarrier or aggregate-based cultures. The biomaterials can be engineered to mimic specific cell niches and provide cues for self-renewal or differentiation into a specific lineage. [48] [50] Some hydrogels are thermo-responsive and cells can be released by changing the temperature. Others are cellulose-based and cells are released via enzymatic treatment. [46] As with biocompatible microcarriers, biocompatible capsules can be used for regenerative medicine purposes. The disadvantages of using this culture format are the difficult cell recovery and the high manufacturing costs of the biomaterials. [49]

1.3.1.2.1 Bioreactor platforms Stirred tank bioreactors (STBRs) and rotating wall bioreactors (RWBs) are the most commonly used bioreactors for hPSC production. STBRs are widely established in bio-pharmaceutical industry for the production of recombinant proteins from mammalian cell lines, such as Chinese hamster ovary. These bioreactors are equipped with impellers that induce uplift current against gravity, keeping cell aggregates or microcarriers in suspension, while providing homogeneous distribution of nutrients and growth factors throughout the bioreactor. Additionally, they are eqquiped with probes to assess important culture parameters, such as pH, temperature and DO, and can include further control systems for cell-density assessment and metabolite concentration. Another advantage of these platforms is the ease of scaling-up using stepwise increments in reactor vessel dimensions. [53] As for RWBs, the rotation of their cylindrical vessel along with its longitudinal horizontal axis, creates a microgravity environment under a laminar flow and provides efficient mixing and homogeneous cell cultures. One bottleneck of STBRs is that, to maintain cells in suspension, high agitation rates are required, exposing cells to high hydrodynamic shear stress. While RWBs provide efficient mixing and homogeneous cell cultures with low shear stress, they have limited volume capability. Therefore, Vertical-Wheel™ bioreactors (VWBRs) were developed to overcome these problems and allow for large-scale production of shear-sensitive cells such as hiPSCs and their derived products.

1.3.1.2.1.1 Vertical-Wheel™ Bioreactors VWBRs are composed by a large vertical wheel impeller, which rotates around a horizontal axis and provides both radial and axial agitation, and a U-shaped bottom (Figure 1.3), which prevents cells from settling. Since the vertical wheel occupies a large area of the vessel, its rotational energy is dissipated to the liquid over a large contact area, resulting in minimum gradients of turbulent energy dissipation rate and gentle mixing, as opposed to STBRs, in which their small impeller rotation at high speeds causes a wide range of local turbulent energy dissipation rates. These unique features of VWBRs allow uniform particle suspension and mass transfer and efficient particle suspension under low agitation speeds and, therefore, low shear stress, creating a favorable culture environment for shear-sensitive, anchorage-dependent cells. When higher shear is needed, it can be done by simply increasing the impeller

speed. Bioreactor vessels are single-use and thus, avoid the risk of potential cross-contaminations while reducing labor. [54] [55] [56] [57]

VWBR models can have two different agitation mechanisms: MagDrive technology, in which rotation is controlled by magnetic coupling between VWBR impeller and the base unit [58], and AirDrive technology, in which agitation is driven by the force of gas bubbles from the sparger at the vessel bottom [59]. Furthermore, VWBRs are available at different scales, being available from 100 mL to 80 L (MagDrive VWBRs) and from 3L to 500 L (AirDrive VWBRs). [58] [59] Starting from 3L scale, VWBRs are embedded with a control unit to allow automated control of culture conditions.[54]

Recently, Borys et. al. demonstrated by computational fluid dynamics (CFD) that there is an homogeneous distribution of hydrodynamic forces throughout the VWBR, which provides a low shear stress culture environment to shear-sensitive cells such as hiPSCs. Moreover, hiPSCs were expanded as aggregates in VWBRs, achieving over 30-fold expansion in 6 days without compromising cell quality. [55]

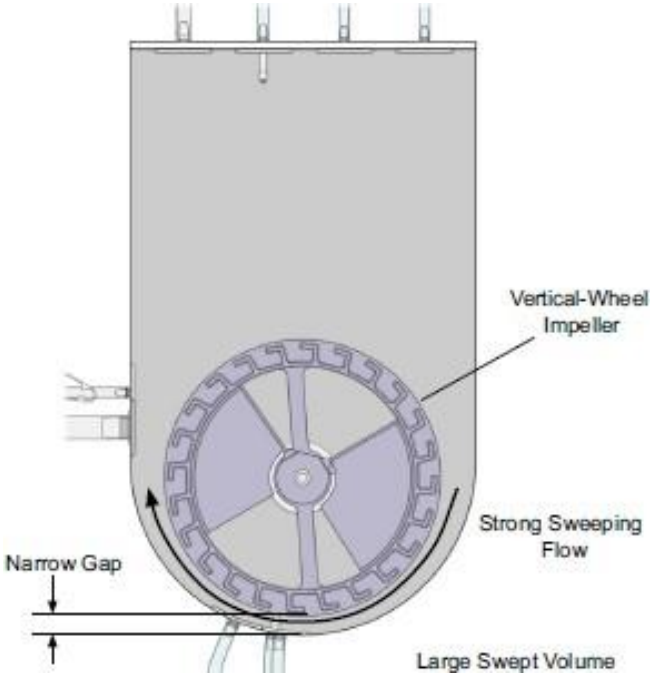

Figure 1.3: Key features of the Vertical-Wheel™ Bioreactor. [57]

1.3.2 Pluripotent stem cell culture

Maintenance of pluripotency depends on several factors that together promote and control cell self-renewal. The extracellular environment, soluble factors, cell-cell interactions, physical forces and physicochemical factors are the key factors that control stem cell fate. [50] Pluripotency is dependent on the complex interaction between several signal transduction pathways, such as transforming growth factor beta (TGF-β) superfamily, receptor tyrosine kinase signaling (downstream of basic fibroblast growth factor (bFGF)) and pathways involving insulin-like growth factors (IGFs). [49]

Traditionally, hPSCs were cultivated on feeder-cell based layers, most commonly proliferation-inactivated mEFs feeder layers, supplemented with foetal bovine/calf serum (FBS/FCS) or animal-derived growth

factors. [47] These cells produce important extracellular matrix (ECM) proteins and growth factors critical for the maintenance of pluripotency, such as TGF-β1, activin A and bone morphogenic protein (BMP)-4. [49] However, feeder cell-based matrices present some limitations for the large-scale production of hPSCs, namely the limited proliferation capacity of feeder cells, low efficiency to support pluripotency after several passages, high risk of contamination by zoonotic or human pathogens and immune rejection, rendering these systems unsuitable for clinical applications. Furthermore, feeder-based systems are undefined and inconsistencies in hPSC culture arise from differential expression and secretion of ECM proteins and growth factors essential for pluripotency maintenance among different feeder cells. [47] [51] [50] [49]

Matrigel™ was one of the first feeder-free alternatives to be developed and was reported to maintain hESC cultures for several passages in combination with mEF-conditioned media. This substrate is produced by Engelbreth-Holm-Swarm mouse sarcoma cells and is composed of ECM proteins, such as laminin, entactin, collagen IV and heparan sulphate proteoglycans, in addition to growth factors. Nevertheless, both Matrigel™ and mEF-conditioned media can introduce xenogeneic contaminants and lot-to-lot variability, impairing the use of hPSCs cultured in these systems for therapeutic applications. [47] [51] [50]

Thus, efforts have been made to develop xenogeneic-free and defined culture conditions for the *in vitro* culture of hPSCs that enable to understand the biology of hPSCs and the factors involved in pluripotency, while culturing cells in compliance with prospective clinical applications. [47] [48] [51] [50] For example, proprietary Knockout Serum Replacement (KSR) was developed in an attempt to overcome lot-to-lot variation caused by undefined serum containing medium and is the standard medium used for the culture of hPSCs in mEFs. [47] Alternative substrates to Matrigel™ and feeder cells have also been explored, like the use of recombinant human proteins (e.g laminin or vitronectin) and synthetic substrates (e.g Synthemax (Corning)). [47] [48] [51] [52] [50] [60] [53]

DMEM/F12 is the standard basal media used in hPSC culture, which is a combination of DMEM, a nutrient-rich formulation for mammalian cells, and Ham's F-12 Nutrient Mixture (F-12), a serum-free formulation optimized for the culture of Chinese hamster ovary (CHO) cells. [47] [48] Apart from the basal medium, supplements are added to the culture medium to improve cell growth and help maintaining pluripotency. mTesR1 is a widely used medium in hPSC culture, being composed of DMEM/F12 basal medium and other factors, such as bovine serum albumin (BSA), vitamins, antioxidants, minerals, lipids, and growth factors. There are also commercially available xeno-free options, like TeSR2 (xeno-free version of mTesR1 which contains human serum albumin (HSA) instead of BSA) and Essential 8 (E8). E8, which does not contain either HSA or BSA, is completely xeno-free and chemically defined, making it suitable for clinical applications. It is composed of only eight components: DMEM/F12 basal medium, sodium bicarbonate, insulin, transferrin, ascorbic acid (AA), selenite, and the growth factors bFGF and TGF-β1, essential for the maintenance of pluripotency. Culture medium is the main cost driver in hPSC culture and the presence of thermosensitive growth factors like bFGF, which degrades at 37°, leads to high production costs due to the need of daily medium exchanges, which is time-consuming as well. For these reasons, a novel medium formulation, B8, which is based on E8 formulation was designed by Kuo et. al. In this medium, components concentrations were optimized and neuroregulin (NRG)1 was added to the

original formulation to enhance cell growth. Additionally, a thermostable version of fibroblast growth factor (FGF)2, FGF2-G3, was incorporated, enabling a weekend-free feeding schedule without compromising cell growth. Furthermore, the capability of maintaining pluripotency in long term (over 100 passages) was demonstrated for 34 hiPSC lines. The in-lab generation of codon-optimized recombinant proteins FGF2, TGF-β3 and NRG1 expressed by *Escherichia coli* allowed a significant reduction of medium cost (15 €/L, which is approximately 3% of commercial media cost). [47] [48] [60]

Regarding cell passaging, hPSCs can be passaged manually using a pipette tip or a cell scraper, enzymatically (using enzymes such as TrypLE and Accutase) or using chelants, such as ethylenediaminetetraacetic acid (EDTA), that bind calcium and magnesium cations that participate in cell-cell and cell-matrix interactions mediated by cadherins and integrins. [48] [61] Enzymatic dissociation into single cells leads to poor cell survival due to dissociation-induced apoptosis. Rho-associated protein kinase (ROCK) is responsible for the shape and movement of cells by acting on the cytoskeleton. Single cell dissociation induces ROCK-mediated actomyosin hyperactivation (blebbing) and apoptosis. ROCK inhibitors, such as small molecule Y-27362 and thiazovivin, have been used to enhance cell survival of hPSCs during single cell dissociation. [47] [50] [48] Alternatively, EDTA dissociates hPSCs as cell clumps and there is no need of using ROCK inhibitors. Furthermore, it is a quick procedure and does not pose increased risks of genomic instability of iPSCs, as opposed to enzymatic-based methods. [61] [62]

Several studies have reported the feasibility of the expansion of hPSCs as aggregates in bioreactors. For instance, Nogueira et. al. reported the expansion of hiPSCs as aggregates in PBS MINI 0.1 VWBRs for the first time, using mTeSR1 and mTeSR3D culture media, in a repeated batch or fed-batch mode, respectively, as well as dextran sulfate (DS) supplementation. DS is a polysulfated compound that has been shown to have an anti-aggregation effect via surface charge modulation and antiapoptotic activity. [48] [63] In Nogueira and co-workers study, DS supplementation allowed about a 2-fold increase in maximum cell number using both media. A maximum cell density of $2.3\pm0.2 \times 10^6$ was obtained in mTeSR1 media supplemented with DS. Importantly, hiPSCs retained their pluripotency characteristics and differentiation potential after expansion. [64] Recently, Manstein et. al. applied a perfusion feeding strategy together with *in silico* modeling to optimize the culture conditions for hPSC aggregates expansion in STBRs. An efficient control of process limiting parameters, such as pH, DO, glucose and lactate levels and osmolality, boosted cell density at the end of the process to a previously unmatched value of 35×10^6 cells/mL after 7 days of expansion from an inoculation density of 5×10^5 cells/mL, achieving 5.25×10^9 hPSCs in a 150 mL scale while retaining pluripotency, differentiation potential and karyotype stability. The fact that such a high number of cells can be obtained in a short period of time enables reduced media requirements and, therefore, less media associated costs. [65]

1.3.3 Differentiation of pluripotent stem cells into cardiomyocytes

The main strategies that have been described for differentiation of hPSCs into CMs are embryoid body (EB) formation, inductive co-culture and monolayer culture systems (Figure 1.4). [46] [21] [66] Each approach allows the generation of CMs with variable efficiencies. Cardiac differentiation efficiency is dependent

on several factors, such as cell line, cell density, aggregate size in the case of aggregate differentiation and timing and dose of supplementation with small molecules in the case of protocols that resort to small molecules. [67] [68]

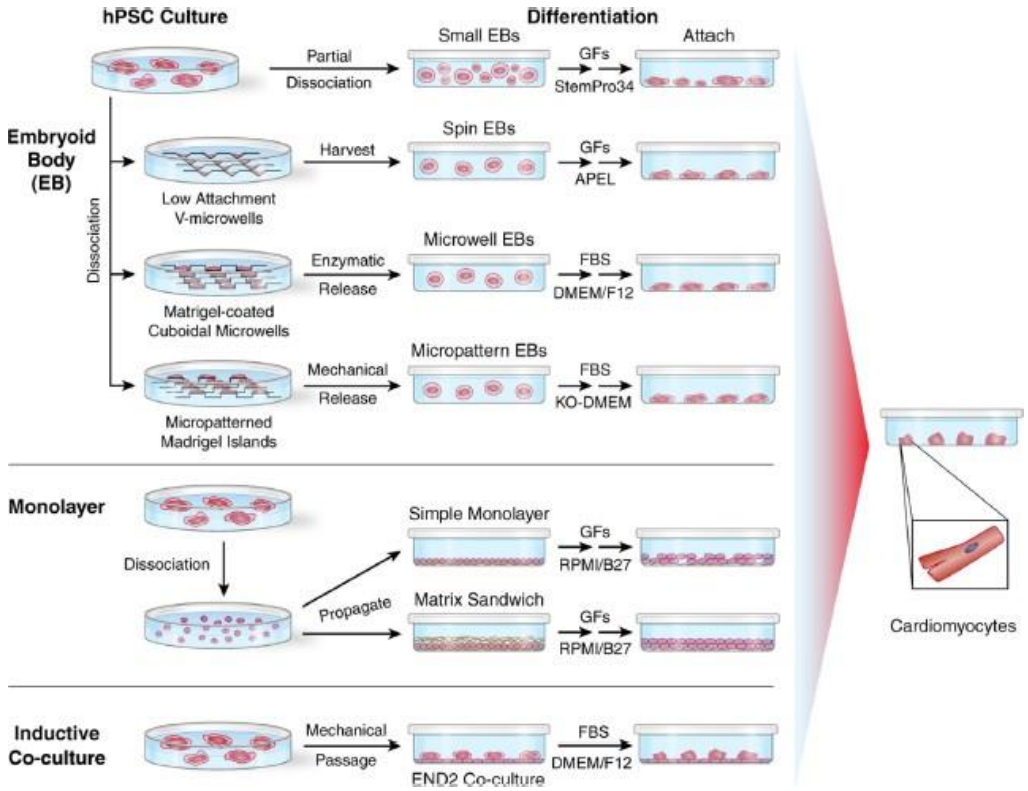

Figure 1.4: Main strategies for cardiac differentiation of hPSCs. hPSCs can be differentiated as embryoid bodies, monolayer culture and inductive co-culture. Cardiac differentiation can be induced by supplementing commonly used media for differentiation (StemPro34, APEL, DMEM/F12, KO-DMEM, RPMI/B27) with growth factors (GFs) in a stage-specific manner, fetal bovine serum (FBS) or small molecules. In embryoid body cultures, PSCs are induced into aggregates composed of cells of the three germ layers; cell aggregate size can be controlled by using microwells with forced aggregation, microwells to first expand hPSC colonies to a defined size, and micropatterned colonies of defined sizes. In monolayer cultures, hPSCs are typically cultured on mEF-conditionedmedia or mTesR1 under Matrigel. In inductive co-culture approaches, hPSCs are co-cultured withvisceral endoderm-like cells, taking advantage of endoderm-derived signals to promote cardiac differentiation. APEL: albumin, polyvinyl alcohol, essential lipids; KO: knockout; RPMI: Roswell Park Memorial Institute 1640 basal medium.

EBs are round 3D aggregates formed by PSCs that contain cells of the three germ layers. [21] The presence of beating cells in embryoid bodies was first shown in 2001 in EBs derived from hESCs from the H9 line. hESC colonies grown on top of the mEF feeder layers were dispersed into small clumps using collagenase IV and were suspended in nonadherent plastic petri dishes in 20% FCS supplemented differentiation medium. The EBs were plated on gelatin-coated culture dishes, where they were observed for the appearance of spontaneous contractions. [66] [22] [69] Although this method was not very efficient in generating CMs (< 1% CMs), it is still widely used to test spontaneous differentiation of hPSC lines into cells of the three germ layers. [66] By applying specific conditions, PSCs can be induced to generate EBs with a greater amount of CMs. Thus, based on the knowledge from heart development *in vivo*, several

protocols rely on the addition of growth factors involved in normal cardiac development, such as BMP4, Activin A, FGF2, Wnt agonists and antagonists, in a timely and concentration-dependent manner to direct cardiac differentiation or small molecules that have the same role. [66] [21] [22] [39]. In these protocols, hPSCs are induced to go from a primitive streak-like stage to a cardiac mesoderm stage, followed by the formation of CVPCs and ultimately CMs. For example, in 2008, Yang. et. al. established a serum-free protocol based on the sequential supplementation of Activin A, BMP4, vascular endothelial growth factor (VEGF), Dickkopf homolog 1 (DKK1) and bFGF for the generation of human embryonic stem cell-derived embryoid bodies. With this protocol they were able to generate a KDR^{low} $/c-kit^{-}$ population capable of differentiating into CMs, ECs and vascular SMCs *in vitro* and after transplantation *in vivo* to mice. These cells can generate populations of more than 50% contracting CMs when plated in monolayer cultures. Activin A and BMP4 are responsible for mesodermal induction, DKK1 (WNT inhibitor) induces cardiac mesoderm, VEGF promotes the expansion and maturation of the KDR^{+} population and bFGF promotes the expansion of mesodermal cells, as well as expansion of the developing cardiovascular lineages. [21] [39] [66] [21] EB size control is important for the reproducibility of differentiation. Therefore, forced aggregation techniques are employed to obtain controlled-size EBs.[66] [21] [22] These techniques include microwells with forced aggregation (centrifugation), microwells to first expand hPSC colonies to a defined size and micropatterned hPSC colonies of defined sizes. (Figure 1.4) [22] Regarding culture media, these protocols use commercially available media such as DMEM/F12 or knockout (KO)-DMEM supplemented with FBS and APEL (albumin, polyvinyl alcohol, essential lipids) or StemPro-34 in combination with growth factors. Both APEL and StemPro-34 are serum-free; APEL media contains human recombinant proteins (albumin, transferrin and insulin), it is xeno-free and was developed for the formation of spin EBs, while StemPro-34 is a serum-free medium which was first used to culture hematopoietic progenitors. [22]

In inductive co-culture approaches, hPSCs are co-cultured with visceral endoderm-like cells, taking advantage of endoderm-derived signals to promote cardiac differentiation. [66] [23]

Monolayer differentiation approaches rely on the temporal supplementation of cardiogenic growth factors and/or small molecules like in EB protocols. [66] [46] [21] PSCs are typically cultured on mEF-conditioned media or mTesR1 under Matrigel and differentiated in DMEM/F12 or Roswell Park Memorial Institute (RPMI) 1640 basal medium (the most commonly used) with B27 supplement. [70] [71] [72] [73] RPMI 1640 is a serum-free medium that was originally developed for culture of human leukocytes. [74]

The first monolayer protocols established for the differentiation of hPSCs into CMs were not very efficient. For example, in the work of Laflamme et. al., the sequential treatment with Activin A and BMP4 typically yielded around 30% CMs and only with a Percoll gradient centrifugation step was the purity increased up to 80%. [21] [70] Therefore, one method aiming to improve monolayer differentiation efficiency consists on the application of a Matrigel sandwich protocol, which was described by Zhang et. al. In this method, hPSCs are cultured as monolayers on Matrigel-coated plates in mTeSR1 medium. Subsequently, when cells reach 90% confluence, they are overlayed with a mixture of mTesR1 medium and Matrigel, forming a matrix sandwich. When cells reach a 100% confluence, they are treated for 24h with basal medium of RPMI/B27 minus insulin supplement (because insulin is known to inhibit early cardiogenesis) containing activin A and Matrigel, followed by treatment with BMP4 and bFGF for 4 days

in the same basal medium. At day 5, the medium is changed to RPMI/B27 complete supplement. By applying a combination of ECM and growth factors, this method enabled the generation of CMs with high purity from multiple hPSC lines (40-98% depending on the cell line). The application of a Matrigel sandwich promoted the epithelial-to-mesenchymal transition that some epiblast cells undergo during gastrulation, increasing cardiac differentiation efficiency. [21] [22] [23] [75]

One of the most efficient cardiac differentiation protocols to date was developed by Lian et. al. This protocol is based on the temporal modulation of the canonical Wnt pathway (reviewed in detail in Section 1.3.3.1) using small molecules and allowed the generation of up to 98% CMs with high reproducibility. Wnt signaling pathway plays a very important role in the heart development; its activation is required for the mesendodermal patterning of the primitive streak, while its subsequent inactivation is important for the formation of cardiac mesoderm. The protocol developed by Lian et. al. relies on the usage of RPMI 1640 medium supplemented with B27, which contains animal origin components, such as BSA, and should be replaced by xeno-free medium for clinical application purposes. [66] [46] Burridge et. al. developed a chemically defined and xeno-free medium for cardiac differentiation, which they termed chemically defined medium 3 (CDM3), consisting of just three components: the basal medium RPMI 1640, L-ascorbic acid 2-phosphate and rice-derived recombinant human albumin (RHA). The use of RHA over BSA/HSA avoids xenogeneic issues and batch-to-batch variations, while reducing costs. CDM3 was effective in generating CMs in 11 hiPSC lines along with temporal modulation of the Wnt pathway with small molecules, producing up to 95% *TNNT* 2^{+} CMs. The use of a chemically defined and simple medium formulation not only allows a reproducible differentiation of hPSCs into CMs, but it also allows to screen for factors that skew cardiac subtype specification into atrial, ventricular or nodal cells. [76]

Some studies report the differentiation of hPSCs aggregates or in microcarries into CMs in bioreactors. For instance, Laco et. al. reported a fully integrated process of hiPSC expansion, differentiation into CMs via canonical Wnt modulation, purification using lactate-free medium and recovery in microcarrier stirred tank bioreactors, generating CMs with high purity (>96% Troponin T). [67] Halloin et. al. demonstrated the feasibility of producing CMs from hPSC aggregates in stirred tank bioreactors in the chemically defined media CDM3, obtaining about 1×10^{6} CMs/mL after 10 days. [68]

1.3.3.1 Differentiation by temporal modulation of the canonical WNT signaling pathway

Wnt signaling is highly conserved throughout the animal kingdom and has an important role in embryonic developmental processes and maintenance of adult tissues, such as cell-fate determination, proliferation and motility. [77] [78] [79] It can be divided into three signaling pathways: the canonical, non-canonical and Ca^{2+} pathways. Mutations in Wnt pathways are associated to several growth-related pathologies and cancer. The canonical Wnt pathway plays an important role in cardiac development and it is schematically represented in Figure 1.5.

When Wnt/β-catenin pathway is off, β-catenin is targeted for degradation by a destruction complex (DC) of proteins in the cytoplasm, including Axin, APC, the serine/threonine kinases glycogen synthase kinase (GSK)3 and caseine kinase (CK)1, protein phosphatase 2A (PP2A) and the E3-ubiquitin ligase β-TrCP. β-catenin is phosphorylated by CK1 and GSK3, which allows it to be targeted for ubiquination by

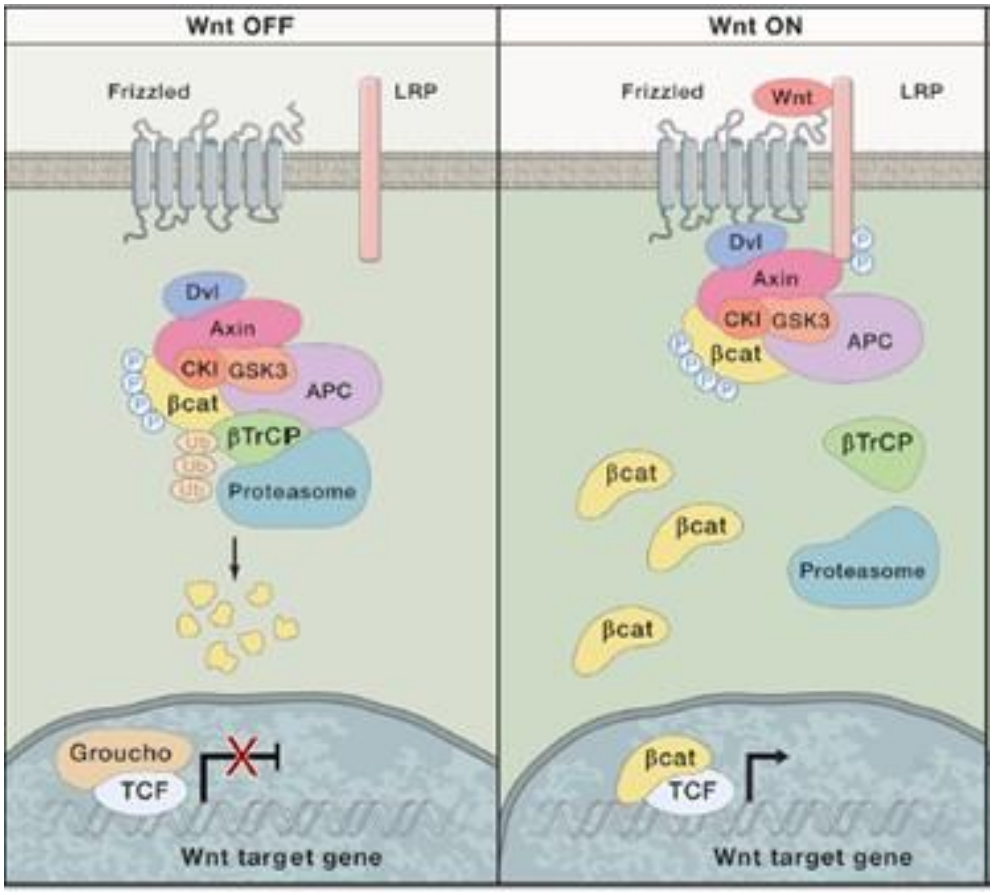

Figure 1.5: Canonical Wnt signaling pathway. Adapted from [79]

β-TrCP. After ubiquitination, β-catenin is degraded by the proteasome. In the nucleus, Groucho binds to T cell factor (TCF), inhibiting the transcription of Wnt target genes. On the other hand, when this pathway is activated, Wnt proteins bind to the Frizzled (Fz)/ lipoprotein receptor-related protein (LRP) and activate the cytoplasmic phosphoprotein Dishevelled (Dsh). The DC is relocalized to the cell membrane and Dsh induces the Axin-mediated phosphorylation of LRP by GSK3 and CK1. Ubiquitination of phosphorylated β-catenin is blocked, which causes the DC to become saturated by phosphorylated β-catenin and the accumulation of stabilized non-phosphorylated β-catenin in the cytoplasm. Stabilized β-catenin can subsequently be translocated into the nucleus, where it binds to LEF/TCF (lymphoid enhancer factor/T cell factor) family of transcription factors, activating Wnt target genes. [77] [78] [79]

Lian and co-workers developed a highly efficient protocol based on the temporal modulation of the canonical Wnt signaling pathway to derive CMs from hPSCs under defined, growth factor-free conditions. Initially, hPSCs are cultured on Matrigel™ or Synthemax-coated plates in mTesR1 medium until reaching full confluency. Subsequently, mTesR1 is replaced by RPMI/B27 medium minus insulin containing a GSK3 inhibitor, such as small molecule CHIR99021, to allow for the accumulation of β-catenin in the cytoplasm and its association in the nucleus with TCF/LEF transcription factors, activating transcription of target genes and inducing the formation of mesendoderm cells. After 24 hours (day 1), medium is changed without the presence of the GSK3 inhibitor. At day 3, canonical Wnt signaling is inhibited by adding inhibition of the Wnt production (IWP) 2 or 4. [71] [72] These molecules inhibit Porcupine, which is a protein

responsible for the palmitoylation of Wnt proteins, a process that is required for their functionalization. [77] [78] [79] By inhibiting canonical Wnt signaling mesendoderm progenitor cells are induced towards a cardiac fate. At day 5, Wnt inhibitor is removed from the culture by changing the medium to RPMI/B27 minus insulin. Starting from day 7, medium is switched to RPMI/B27 and medium changes occur every 3 days. Only by modulating this pathway it was possible to consistently generate populations of up to 98% CMs with a high yield of 15 CMs per hPSC input. [71] [72] This method is very advantageous in relation to others presented in Section 1.3.3: it is technically simple, scalable, chemically defined, a purification step can be avoided due to the high purity of the generated populations of CMs and the use of chemically synthesized small molecules instead of growth factors provides more reproducible results among several cell lines, while reducing costs. [22] [71] [72] Wnt signaling regulates other autocrine and paracrine signals involved in cardiomyocyte specification, including members of TGF-β superfamily. Differentiation efficiency depends on timing and dose of Wnt pathway modulators. [71] [72]

1.3.4 Purification of pluripotent stem cell derived cardiomyocytes

Despite the improvements in protocols for generating CMs from hPSCs with some studies reporting derivation of cell populations with high percentages of CMs, it is important that pure populations of hPSC-CMs are obtained for their application in regenerative medicine, drug discovery and disease modeling. Particularly, it is crucial for cardiac cell therapy purposes to separate hPSC-CMs from undifferentiated hPSCs, which could otherwise lead to the formation of teratomas. Having pure populations of hPSC-CMs is also important to better understand and test the performance of new drugs and their toxicity. Therefore, several methods have been developed to purify hPSC-CMs, including Percoll density gradient centrifugation, the use of genetically engineered hPSC lines, nongenetic methods that use a mitochondrial dye, surface protein-based enrichment, the lactate method and miRNA switches. [80]

Percoll density gradient centrifugation is a simple, easy and inexpensive method to enrich hPSC-CMs populations. Xu et. al. demonstrated the purification of hESC-derived EBs that underwent FBS-based cardiac differentiation by Percoll density gradient centrifugation. H7-derived CMs were dissociated and subjected to a discontinuous Percoll gradient (one layer containing 40.5% Percoll and other containing 58.5% Percoll). After centrifugation, one layer of cells (fraction I) could be observed above the 40.5% Percoll layer and another layer of cells (fraction III) between the 40.5% Percoll layer (fraction II) and the 58.5% Percoll layer (fraction IV). The highest percentages of beating cells were observed in fractions III and IV, containing an average of 36% and 70% sarcomeric myosin heavy chain (sMHC) positive cells, respectively. Fraction IV represented a 4-fold enrichment in relation to the unpurified cell population, which contained an average of 17% sMHC-positive cells. [81] Laflamme et. al. also demonstrated the enrichment of hESC-derived CMs (hESC-CMs) populations differentiated as EBs by sequential treatment with Activin A and BMP4 by Percoll density gradient centrifugation. There was an enrichment of cultures with around 30% CMs after differentiation to an average of 83% CMs after Percoll density gradient centrifugation. Purified CMs were transplanted into infarcted heart rats in combination with a cocktail of pro-survival factors to limit CM death after transplantation. The transplanted CMs improved cardiac

function and no teratomas were observed. [70] Despite its advantages, Percoll method is not very efficient, unspecific and it is not scalable. [80]

Some methods rely on the use of genetically engineered hPSC lines that express a drug resistant gene or fluorescent reporter gene in the presence of a cardiac specific promoter. The obtainment of hPSC-CMs enriched populations can be achieved by drug selection, eliminating cells that do not express the drug resistant gene, or by FACS to isolate cells expressing the fluorescent reporter gene. [80] Klug et. al. reported for the first time this strategy, where they transfected a fusion gene comprising an aminoglycoside phosphotransferase gene driven by a α-cardiac MHC promoter. After differentiation and antibiotic selection with G418, highly pure populations (up to 99% purity) of CMs were obtained. [82] However, the major limitation of these methods is the genetic manipulation by viral or nonviral transfection/transduction methods to introduce the reporter or drug resistance genes into the host genome, hindering their use for therapeutic applications. [80]

Surface protein-based enrichment approaches rely on the use of antibodies against specific surface markers and sorting the target cells by FACS or magnetic-activated cell sorting (MACS). Although no specific surface markers for CMs have been reported, these approaches are highly specific and sensitive and several surface markers can be used simultaneously to isolate target cells. [80] Dubois et. al. identified SIRPA in cardiac precursors and hPSC-CMs. By performing FACS with an antibody against SIRPA, they could isolate populations of up to 98% cardiac troponin T-positive cells. [83] Elliot and co-workers used NKX2.5/eGFP hESCs to generate hPSC-CMs and sorted them by their NKX2.5 expression. They found that both SIRPA and VCAM-1 were significantly upregulated in NKX2.5/*eGFP*$^{+}$ cells and concluded thata purer population of hPSC-CMs could be obtained by performing sorting them with both cell surface markers. [35]

Toyhama et. al. developed a purification method, called lactate method, that is based on the differences in metabolism between CMs and non-CMs, including undifferentiated cells. While CMs have high numbers of mitochondria and can uptake lactate via tricarboxylic acid (TCA) cycle to generate adenosine triphosphate (ATP) in the absence of glucose, non-CMs are mainly dependent on glycolysis to obtain energy and cannot survive without the presence of glucose by using lactate as an alternative energy source. Based on these metabolic differences, the authors changed the differentiation medium of PSC-derived CMs to a glucose-depleted medium containing lactate, which allowed for the enrichment of cultures consisting of 10% CMs to up to 99% CMs with a recovery of 74.4%. Transplantation of purified cells to immunocompromised mice did not cause the formation of teratomas. The simplicity of the lactate method, high efficiency, relativelylow cost and scalability makes it a powerful tool for the purification of hPSC-CMs. [80] [84]

miRNA switches are synthetic mRNA sequences with a recognition sequence for miRNA and an open reading frame encoding a desired gene that can be a fluorescence gene or a cell death gene. In cells of interest, miRNA sequence in miRNA switches binds to miRNA expressed in those cells, suppressing the translation of the fluorescence or cell death gene. Thus, the cell type of interest is distinguished from other cell types that express that gene. [80] Miki et. al. demonstrated the high purification of populations of hPSC-CMs using miRNA switches miR-1-, miR-208a-, and miR-499a-5p tagged with blue fluorescence protein (BFP). miRNA switches encoding the apoptosis inducer Bim enriched for cardiomyocytes without

cell sorting. hPSCs-CMs were purified at more than 95% efficiency, whereas when performing sorting by cell surface markers SIRPA or VCAM1 the proportion of $cTnT^+$ cells ranged between 60% and 85%. Moreover, miRNA switches were shown to have the potential to purify other cell types, such as endothelial cells, hepatocytes, and insulin producing cells differentiated from hPSCs. [85]

1.3.5 Maturation of pluripotent stem cell derived cardiomyocytes

Despite considerable progress, most cardiac differentiation protocols generate cells with fetal-like properties. In order to generate reliable disease models and to perform developmental studies from hPSC-CMs or even to safely transplant these into patients for cell-replacement therapies without the risk of arrythmias, it is important to generate more adult-like CMs *in vitro*. [86] [87]

Adult CMs have rod-like shape, organized and aligned sarcomeres, and are multinucleated/tetraploid cells. These cells also display well developed transverse tubules (T-Tubules) and sarcoplasmic reticulum (SR), allowing an efficient and fast excitation-contraction coupling (ECC) by Ca^{2+} induced Ca^{2+} release (CICR). In contrast, fetal CMs and CMs are small round mononucleated cells with misaligned sarcomeres. Furthermore, they lack T-tubules and show an underdeveloped SR, making ECC slow. Regarding metabolism, whereas mature CMs have well developed mitochondria and rely on fatty acid β-oxidation for energy production, fetal-like CMs typically rely on glycolysis to obtain energy (around 80% of energy is produced by glycolysis). Prenatal heart growth is mostly driven by cardiomyocyte proliferation, while during the postnatal period and the first decade in humans is driven by CM increase in size (hypertrophy), which is in parallel with the loss in proliferation capacity that is observed in more mature CMs *in vitro*. [86] [87]

Many researchers have pursued different strategies to improve hPSC-CMs maturity, such as prolonged culture time, co-culture with other cell types and chemical, mechanical or electrical stimuli. [86] [87]

Prolonging culture time was the first strategy used to improve PSC-CMs maturity. Kamakura et. al. maintained hiPSC-CMs differentiated as EBs throughout 1 year. The long-term culture promoted the structural maturation of CMs, with 360-day-old EBs having more organized and packed myofibrils and the presence of Z-, A-, H-, I- and M-bands (the latter being indicative of myofibrillar maturation), whereas 14-day-old EBs presented less and unaligned myofibrils with immature Z-bands and no presence of A-, H-, I- and M-bands. $MLC2v^+/MLC2a^-$ cells ratio also increased throughout time, which is indicative of maturing ventricular CMs, since MLC2a expression in immature ventricular $MLC2v^+$ cells decreases with maturation. Despite the evidences of maturation, this was not homogeneous.[88] More recently, Fukushima et. al. generated highly purified populations of CMs (>95%) derived from the differentiation by canonical Wnt pathway of a mesodermal population (PDGFRα-positive cells isolated by MACs at day 5) and maintained in culture for over 200 days. These cells exhibited gradual structural and electrophysiological maturation with visible T-tubules at day 231 and were mostly ventricular-type. [89] The disadvantage of long-term culture is that is very time-consuming and therefore impractical from an economic perspective. [86] [87]

Another strategy to promote CMs maturation is related with medium supplementation. Horikoshi et. al. demonstrated that a fatty-acid rich, glucose-free medium promoted metabolic and structural maturation

of hiPSC-CMs, which presented more aligned sarcomeres, enhanced mitochondrial oxidative capacity, stronger capability of using fatty acids as energy sources and better adaptability to switch to glucose as energy source when needed. [90] Cao and co-workers reported the role of AA in enhancing the cardiac differentiation and maturation of mouse PSCs and hiPSC-CMs. AA induces collagen synthesis,which promotes CVPC proliferation via mitogen-activated protein kinase kinase (MEK)/extracellular signal-regulated kinase (ERK) 1/2 pathway. [91] Parikh et. al. showed that supplementation of the culture medium with thyroid and glucocorticoid hormones (triiodothyronine and dexamethasone, respectively) following by further maturation on a Matrigel mattress led to the formation of hiPSC-CMs with an extensive T-tubule network, allowing a better CICR and ECC. [92]

Other researchers have strived to improve maturation by modulating the substrate in which cells grow. For example, Ribeiro et. al. cultured single hPSC-CMs on a 10 kPa polyacrylamide substrate and Matrigel rectangular micropattern in order to simulate physiological stiffness and shape. This strategy led to an increase in electrophysiological and structural maturation with presence of T-tubules. [93]

Culture format also plays a key role in maturation. Branco et. al. showed that expanding hiPSCs as aggregates before cardiac differentiation induces transcriptional changes related to hypoxic response that favour priming towards mesendoderm and allow a more efficient and faster differentiation in comparison to 2D cultures. [94] Other 3D systems, such as engineered heart tissues (EHTs) and organoids, have been shown to boost maturation, due to the combination of hPSC-CMs and other cell types, such as fibroblasts. [87]

Several studies have focused on providing mechanical and/or electrical stimuli to improve maturity. Ronaldson-Bouchard et. al. combined electrical and mechanical stimulation by subjecting hPSC-derived EHTs (composed of hiPSC-CMs and fibroblasts embedded in a fibrin hydrogel) to an ‘intensity training’ in which cells are electrically stimulated at a frequency increasing from 2 Hz to 6 Hz during 2 weeks followed by 1 week at 2 Hz, and mechanically stretched between two pillars. They showed that tissues containing early-stage hiPSC-CMs have better responsiveness to stimuli than tissues comprising later-stage hiPSC-CMs. The formers exhibited great structural and electrophysiological maturity with an extensive T-tubule network. [95]

hPSC-CM maturation has also been achieved by transplantation to normal or injured heart of rats and non-human primates. Some studies are mentioned in Section 1.3.6.

Despite considerable progress, none of the aforementioned methods generated cells with full maturity, since maturation is a complex phenomenon regulated by multiple signaling pathways. There is still need to uncover the mechanisms that lead to maturation, in which omics approaches (e.g transcriptomics) and bioinformatics will have a fundamental role. In addition, it will be important to understand what is the optimal degree of maturity for each hPSC-CM application. [86] [87]

1.3.6 Pre-clinical studies and clinical trials using PSC-derived cardiac progenitors and cardiomyocytes

Different types of stem cells and their derivatives, such as PSCs, skeletal myoblasts, mesenchymal stem cells and cardiac stem cells, have been proposed for cardiac regeneration purposes. Although there is no consensus about which is the best option, PSC-derived CVPCs and CMs are promising candidates, due to the high proliferation capacity of PSCs and their great cardiac differentiation capacity. [96] In this section, some examples of preclinical studies and clinical trials using iPSC or ESC-derived CVPCs and CMs are given.

The first preclinical studies essentially focused on the direct injection of PSC-CMs into the infarcted heart of animal models, such as rats, mice and pigs. [97] For example, Laflamme et. al. reported the engraftment of hESC-CMs into infarcted rat hearts together with a cocktail of pro-survival factors to prevent CM death after transplantation. This treatment resulted in reduced ventricular dilation and global contractile function improvement in comparison with controls receiving noncardiac hESC-derived cells or the pro-survival cocktail only. [70]

Despite the promising results obtained from small animal models studies, some controversial results were obtained in studies using non-human primate models. Chong et. al. injected 1×10^9 hESC-CMs into the myocardium of non-human primate models that suffered myocardial ischemia followed by reperfusion. Grafts enabled an extensive remuscularization of the heart with electromechanical coupling to the host and perfusion by host vasculature. However, in contrast to small animal models studies, non-fatal ventricular arrythmias were observed in monkeys, probably due to the immature phenotype of the injected cells. The results from this study show the importance of using larger animal models to more closely resemble human heart response, due to significant differences in heart size and rate between small animals and humans. [22]

One of the main challenges in cell-based therapy is the low rate of stem cell retention, which impairs engraftment of cells into the host cardiac tissue. Therefore, researchers started to develop bioengineering strategies to improve survival and functionality of engrafted cells instead of directly injecting them. Some of these strategies include cell patches and EHTs. [97]

In 2015, Menasché et. al. reported the first clinical application of a highly purified population of hESC-derived CVPCs (99% $SSEA\text{-}1^+$ cells) embedded into a fibrin patch and implanted into the heart of a patient suffering from severe ischemic left ventricle dysfunction. After 3 months, the patient's left ventricular ejection fraction (LVEF) increased from 26% to 36% and new-onset contractility in the patch-treated area was evident. No complications such as arrythmias, tumor formation or immunorejection were observed. [38]

EHTs aim at mimicking the heart environment to help cell growth, differentiation and survival when transplanted to repair the damaged cardiac tissue of a living organism and can also be used as platforms for drug screening and disease modeling. Therefore, natural and/or biosynthetic materials, decellularized extracellular matrices or 3D printing techniques are used to provide a cardiac ECM-like scaffold for cells to enhance cell growth and communication. [97] In addition, these constructs support the maturation of CMs,

as evidenced in the work from Ronaldson-Bouchard (see section 1.3.5). [97] [95] Very recently, Redd et. al. reported the development of engineered perfusable microvascular constructs, wherein hESC-derived ECs were seeded into patterned micro-channels and a surrounding collagen matrix. These microchannels underwent extensive remodeling and anastomosed with *de novo* vascularity formed by endothelial cells. When transplanted into infarcted rat hearts perfusable microvascular constructs integrated better with the host coronary vasculature than non-perfusable constructs. Furthermore, transplantation of the perfusable grafts containing hESC-derived CMs supported their survival, showing the importance of vascularization for the design of EHTs. [98]

Although most studies have used ESC-derived cells, several studies have started to use iPSC-derived cardiac cells. In 2018, Japan´s government approved the first application of iPSCs in treating patients suffering from heart disease. The study consists in the transplantation of cardiac sheets made of iPSC-CMs to three patients. As yet, no results of this clinical trial were published. [14]

1.3.6.1 Considerations for clinical applications of pluripotent stem cell derived cardiomyocytes

Despite encouraging results from preclinical and clinical studies, there are still some challenges preventing the clinical translation of PSC-CM therapy for cardiac diseases. In this section are reviewed the main considerations that should be taken into account before applying PSC-CMs into clinical applications.

First of all, it is important to expand and differentiate PSC lines under clinical-grade, good manufacturing practices (GMP). These GMP criteria have been established by regulatory agencies such as the European Medicines Agency (EMA) and Food and Drug Administration (FDA), implying the development of standardized procedures and quality controls throughout the entire process of product development to ensure safety. For example, it is more desirable to establish xeno-free cultures, due to the risk of infection with animal-derived components upon transplantation, and to use virus-free integrating techniques for the generation of clinical-grade iPSCs. [99] [13]

One problem when transplanting PSC-CMs into infarcted hearts is the low graft survival, due to the poorly vascular and pro-inflammatory environment of the infarct scar. As mentioned before, engraftment efficiency can be improved, for instance, by delivering cells in a cocktail of pro-survival factors or by combining cells and biomaterials through tissue engineering approaches (Section 1.3.6). [13]

Another issue concerning PSC-CM transplantation is immune rejection. Alternatives to immunosuppression could be the use of autologous iPSC-CMs or human leucocyte antigen (HLA)-matched allogeneic PSCs from a large cell bank. Generation and differentiation of patient specific iPSCs can be, nevertheless, time-consuming and cost prohibitively. [100] [96] [99] [13]

One significant challenge in translating PSC-CMs into clinical applications is the risk of graft-related arrythmias. [100] [96] [13] Arrythmias can occur due to the presence of a mixture of cardiac subtypes, including nodal cells that can act as an ectopic pacemaker, immaturity of delivered of cells, which causes that even purified ventricular cardiomyocytes display automaticity, or poor electromechanical integration with the host's heart. [13]

Since PSCs have the ability to form teratomas, there is a risk of teratoma formation when applying PSC-derived cells for therapy. Teratoma formation can arise from the injection of residual undifferentiated

PSCs or malignant transformation of differentiated cells. Therefore, it is important to obtain highly purified populations of PSC-CMs, as well as monitoring PSCs and their derivatives for karyotypic abnormalities. [100] [96] [99] [13]

Regarding the level of differentiation of PSC-derived cardiac cells, there is no consensus whether PSC-derived cardiac progenitors or more mature cells are desirable for transplantation. On one hand, PSC-derived cardiac progenitors have a better proliferation capacity and do not only allow myocardial restoration but also revascularization. On the other hand, although immature cells can further mature *in vivo*, arrythmia risk, even if transiently, is still present. [13]

In order for PSC-CMs based therapies can be applied in a clinical context, extensive preclinical evidence from large-animal models is required. It is necessary to demonstrate the feasibility and efficacy for these cells to improve cardiac function as well as to establish important parameters such as optimal cell dosage, cellular composition, delivery method, assessment of graft-related arrythmias and responsiveness to anti-arrhythmic drugs. [100] [96] [99] [13]

1.4 Bioprocess Economics and Computational decision support tools

1.4.1 Bioprocess design and development

Bioprocess design and development is considerably challenging, especially when it comes to the production of cell and gene therapy (CGT) products. CGT manufacturing is particularly demanding, due to the inherent complexity of live cell products. Factors such as incomplete understanding of their mechanisms of action *in vivo* and high variability of cell-based raw materials make it difficult to define appropriate manufacturing release criteria. Manufacturing failures, which lead to CGT products not meeting requirements, can have a large financial impact, preventing products from reaching the market. Regulatory agencies have stringent requirements in terms of process manufacturing and control, as well as product quality, which, when not met, can result in CGT products being held back from regulatory approval. Therefore, bioprocesses should be carefully designed to achieve the desired high productivity and product quality consistently, while ensuring its economic viability. [101] [102] [103] [104]

When designing a process for the production of a CGT product, several considerations should be taken into account, such as manufacturing strategy and GMP compliance, cell therapy modality and product demand forecast. [102] GMP compliance include the use of bioreactors, automation and chemically defined media to reduce product variability and ensure high quality. Contrary to 2D culture systems, bioreactors typically allow for scale-up, online monitoring and control of process parameters, are compatible with different medium exchange regimes, such as perfusion, and various process steps can be integrated in these culture systems, reducing significantly the risk of contamination. [104] [105] The implementation of automation or semi-automation is an important factor to take into regard, because it has some advantages, namely labor reduction, product quality consistency due to reduction of human error and microbiology exposures. [104] Chemically defined and animal-component free products are also being increasingly

used to ensure consistency and product quality. [106] As for cell therapy modalities, there are two types: autologous and allogeneic therapies. In autologous cell therapies, patients receive their own cells to treat a wide range of conditions, whereas in allogeneic modalities, cells are sourced from specially recruited donors to treat several people. While allogeneic products can benefit from economies of scale due to manufacture scale-up (i.e one batch can be used to produce many patient doses, thus reducing labor costs per dose), autologous products can only benefit from scale-out when demand increases, since each batch produces cells to treat a single patient. The fact that autologous process can only benefit from scale-out results in high COGs associated with increased labor costs, which can possibly be alleviated with implementation of automation. Another challenge in the production of autologous products is donor variability, which hampers process characterization and must be well understood to guarantee product quality; this challenge is reduced in allogeneic processes, since process standardization can be achieved by always using cells from the same donor pool. [102]

Any modification to process culture conditions (e.g media formulation, moving from tissue culture plates to bioreactors, process automation), can affect cell phenotype and critical product attributes. [104] Quality by Design (QbD) is a commonly applied framework for strategic process development and manufacturing. QbD consists on integrating scientific knowledge and risk analysis to process development by understanding the influence of changes on key factors that affect product quality, which guides decision-making while helping reducing process costs. [102] [101] QbD approaches consist of process discovery, characterization and development in an iterative way to refine the design space as knowledge evolves. [106] The first step in QbD is to define the quality target product profile (QTPP), which describes the properties of the desired product, such as identity, potency (i.e desired functionality) and purity, in order to ensure its safety and efficacy. Secondly, the critical quality attributes (CQA) that influence the QTPP and, therefore, product safety and efficacy, are defined. In their own turn, CQA have associated critical process parameters (CPP), such as growth kinetics, cell maturity, physicochemical parameters (e.g pH, dissolved oxygen, temperature) and growth factors concentration. These CPP are defined through the use of prior knowledge, mechanistic modeling or experimentation. The next phase is quantifying the effect of varying these CPP on the process's CQA and establishing a design space, which corresponds to the parameter operating range over which a process can be optimized to ensure product quality and safety. Control strategies are then defined in order to maintain CPP within the design space. As process knowledge evolves and correlations between process inputs and outputs are better known, there is an iterative refinement of the design space. Dividing manufacturing processes in several building blocks (modules) can help in a more rapid iterative optimization by allowing independent optimization of each block when CQAs for their inputs and outputs are clearly defined. Through the use of this framework, an extensive process knowledge is gained, paving the way to developers to incorporate new technologies into the process. [101]

1.4.2 Bioprocess economic models

Bioprocess economic models are built by modeling processes through the combination of design equations and mass and energy balances to model each unit operation and, at the same time, integrating equations to determine process COGs. Bioprocess models can be divided into static or dynamic, deterministic or stochastic and mechanistic or data-driven models. [107] [108]

Static models are simple models that are particularly useful for cost estimates at an early stage of process development. They are used to determine cost breakdown and to assess the sensitivity of COG to key process parameters. On the other hand, dynamic models describe time-dependent operations and, as opposed to static models, account for delays that occur due to resource constraints. Discrete-event simulation models are suitable for stem cell manufacture modeling, since the system state can be updated as events (i.e process stages) occur and the model can capture parallel events. [107] [108]

Deterministic models measure uncertainty in COG by applying a sensitivity analysis to key variables simply by measuring the impact of ±x% changes in those variables in the resulting COGs. Conversely, stochastic models incorporate uncertainty based on the likelihood of occurrence of each input. A commonly used method in stochastic models is Monte Carlo simulation, where input values are randomly sampled from probability distributions in each simulation run to determine probability distributions of the model outputs, thereby allowing to identify the range of possible outcomes and the probability of exceeding a certain threshold. [107] [108] [109]

Mechanistic models are based on first-principle mechanisms to describe process behaviour when there is a substantial amount of knowledge about it. When developing such models, data is necessary for parameter estimation and for model validation. These models are divided further into kinetics-based models, which typically use systems of ordinary differential equations to describe cell metabolism dynamics (e.g variations of the Monod equation), and flux-based models, which describe genome-level behaviour of cell metabolism at steady-state, being suitable to describe processes in which cell genome is modified to achieve a certain behaviour. As opposed to mechanistic models, data-driven models are exclusively based on experimental data to describe the relationships between process inputs and outputs. While these models are merely descriptive and do not explain observed phenomena, they are, nevertheless, invaluable, since they can capture important process information in a relatively simple way. [103]

Typically, bioprocess economic models are built resorting to computational decision support tools, which are of great value to design manufacturing processes and assess how important process parameters impact on the COGs for a given demand. These tools allow the optimization of process design and manufacturing parameters in order to achieve the lowest COG for a required demand in a fast, safe and less expensive way. [108] [110]

Some studies have used computational decision support tools for stem cell manufacturing, using commercial flowsheeting software, such as SuperPro Designer™, or using custom-made code in programming languages, such as Python. System uncertainty can be included either using deterministic or stochastic parameters. When using deterministic parameters, input parameters can be changed by the user to employ sensitivity analysis and assess their impact on process COG, whereas when using

stochasticity inputs parameters are randomly sampled from probabilistic distributions. [108] [110] Table 1.1 summarizes the existent stem cell bioprocess economic models so far.

Most stem cell bioprocess economic models present in Table 1.1 are data-driven, except for two mechanistic models ([116], [117]), and are either stochastic or deterministic. Typically, these models focus on the following case studies:

1. Impact of switching from manual bioprocesses to automation in the process COGs.
2. Impact of scaling-up in the process COGs.
3. Sensitivity analysis to process parameters to identify strategies to increase the likelihood of process cost-effectiveness.
4. Stochastic modeling to assess the robustness of a process in terms of COGs.
5. Incorporation of bioprocess economic models with a discrete state-transition Markov model to assess the cost-effectiveness of a stem-cell based therapy over a traditional therapy for a certain disease.

Table 1.1: Stem cell bioprocess economic models. AT: adipose tissue; BM: bone marrow; hESC: human embryonic stem cell; hiPSC: human induced pluripotent stem cell; hiPSC-CM: human induced pluripotent stem cell-derived cardiomyocytes; HSC- hematopoietic stem cell; HUC: human umbilical cord; MSC: mesenchymal stem cell; PSC: pluripotent stem cell; RBC: red blood cell; UC: umbilical cord.

Cell type	Case Study	Reference
hiPSCs	Economic analysis of automated vs. non-automated hiPSC production	[111]
PSC-derived *β*cells	Evaluation of the cost efectiveness of treating type 1 diabetes with PSC-derived *β*cells against treatment with intensive insulin therapy using a bioprocess economic model combined with a disease state transition model	[112]
hESC-derived *β*cell progenitors	Evaluation of the cost-effectiveness of stem cell-based *β*cell replacement therapy to treat diabetes in relation to intensive insulin therapy using a discrete-state transition Markov model	[113]
Autologous hiPSC-derived neurons	Identification of the most cost-effective process configuration for the production of hiPSC-derived neurons for drug screening using a bioprocess economic model combined with a brute-force search algorithm	[114]
hiPSC-derived photoreceptor progenitors	Assessment of the key cost drivers of processes using different afinity purification technologies across different cell doses and purification yields	[115]
hiPSC-CMs	Selection of the best process design in terms of equipment configuration and economic parameters for the production of hiPSC-CMs	[116]
Erythroblasts	Deterministic mechanistic model to predict erythroblast growth and find the best compromise between medium exchange regimes, cell density and cell productivity depending on medium and operational costs	[117]
HSC-derived RBCs	Optimization of RBC production using high-fidelity modeling, single variate and multivariate analysis to identify factors that affect production, cost and quality, and bioreactor superstructure optimization	[118]
BM-MSCs	Identification of the most cost-effective expansion technologies for different scales of production of BM-MSCs	[119]
UC-MSCs	Integrated experimental and cost analysis of different culture technologies for UC-MSCs expansion	[120]
Allogeneic MSCs	Identification of the main cost drivers of manufacturing MSCs and comparison between 2D and 3D culture systems	[104]
MSCs	Assessment of the impact of automation, culture medium, staffing costs, donor variability and product transport on the overall COG of MSCs culture	[121]
Allogeneic MSCs	Identification of the most cost-effective process flowsheet configuration (upstream and downstream technologies) at different cell dose sizes, lot sizes and dose demands	[122]
Allogeneic MSCs	Identification of the optimal timing for switching from planar expansion technologies to microcarriers in single-use bioreactors for the expansion of MSCs considering out-of-pocket costs in each stage of product development and risk-adjusted net present value at different market sizes	[123]

Allogeneic MSCs	Comparison of different manufacturing technologies in terms of COGs, robustness, operational and business feasibility under different scale, demand, reimbursement and dose size scenarios for the culture of MSCs	[124]
Autologous BM-MSCs	Assessment of the cost-effectiveness of a process transfer from serum-based media (FBS) to xeno-free medium (human platelet lysate) on the culture of autologous BM-MSCs taking biological variability into account	[125]
HUC and AT-MSCs	Economic evaluation of the process transfer of MSCs culture from T-Flasks to 100 mL Vertical-Wheel^{TM} bioreactors	[126]
Allogeneic BM-MSCs	Evaluation of the manufacturing costs of different doses of MSCs for infusion in cystic fibrosis patients. Comparison of cost effectiveness of using MSCs with modulators in comparison of therapy with modulators at different willingness to pay thresholds using a health economics model	[108]
MSC-derived EVs	Assessment of the most cost-effective technologies for manufacturing EVs at different scales	[127]

2 | Aim of studies

Cardiovascular diseases are the major cause of death in the world, being responsible for 32% of the global deaths in 2019. [24] Conventional drug treatments, such as anti-thrombotic, anti-arrhythmic or anti-inflammatory drugs, have proved inefficient and long wait-lists for cardiac transplant in end-stage heart failure lead to high mortality. After myocardial infarction, one of the most common cardiac disease events, extensive cardiomyocyte death occurs, which compromises the heart's ability to pump blood and eventually leads to death because of the heart's very limited regenerative capacity.

It is estimated that about 1×10^9 cardiomyocytes are required to restore heart function in post-MI patients. [13] hiPSC-CMs are extremely promising for this regenerative medicine purpose, because a high number of cardiac cells can be produced by taking advantage of the high proliferation capacity of hiPSCs. Furthermore, hiPSC-CMs present an exciting possibility for disease modeling, drug screening, cardiotoxicity assays and, as opposed to hESC-CMs, can pave the way for personalized medicine with the generation of patient-specific iPSCs.

To produce the high cell number mentioned above, scalable culture platforms, namely bioreactors, that allow a precise control of the culture environment, are desirable. Differentiation of hiPSCs into CMs has already been demonstrated in STBRs. [67] [68] However, in STBRs, to maintain cells in suspension, high stirring speeds are necessary, which can damage cells because of exposure to high shear stress. On the other hand, VWBRs allow a gentler mixing of cell suspensions with minimal power input, their single-use vessels reduce the risk of cross-contaminations and they are available at small and large scales, rendering them well suited for the large scale production of hiPSC-CMs.

Cell-based therapies are often cost-prohibitive because of high culture medium and quality control costs and other unforeseen costs with failing batches that arise from the process's inherent biological variability. In particular, the differentiation efficiency of hiPSCs is highly affected by several factors, such as cell line, inoculation density and timing and dose of supplementation with small molecules [68], which are responsible for fluctuations in bioprocess costs. Bioprocess economic models help to identify key process cost drivers and to assess how process parameters affect costs, which helps making decisions about how to reduce those costs. [108] [110]

The objective of this thesis was to develop a bioprocess economic model, using Python, of the differentiation of hiPSCs into mature CMs in 3L Vertical-Wheel^{TM} bioreactors to treat post-MI patients undergoing a clinical trial. 3L Vertical-Wheel^{TM} bioreactors were chosen because these provide the necessary scale to produce 1×10^9 CMs per patient and are embedded with a control unit to allow

automated control of culture conditions. Additionally, different culture media formulations were used to generate in-lab hiPSC-CMs as monolayers via modulation of the canonical Wnt pathway. The following research questions were investigated:

1. How do bioprocess parameters, namely step yields, medium performance (RPMI/B27 medium vs. CDM3), batch failure rates, failure detection probability and cell therapy modality (autologous vs. allogeneic) impact process COGs of the production of mature hiPSC-CMs in 3L Vertical-Wheel^{TM} bioreactors?

2. How do culture medium used for expansion (mTesR1, E8, B8) and differentiation (RPMI/B27, CDM3) affect the differentiation efficiency of hiPSCs into CMs?

3 | Materials and Methods

3.1 Bioprocess economics modeling: Production of hiPSC-CMs in Vertical-Wheel Bioreactors

3.1.1 Tool construction

A bioprocess economics model for the production of hiPSC-CMs in VWBRs was developed using Python, an open-source programming language, in Pycharm, an integrated development environment software. This widely used programming language has several available modules for data analysis, such as Pandas, and mathematical functions, such as the math module. Bar charts resulting from COG analysis of different process scenarios were stored as PNG image files.

3.1.2 Bioprocess Design

A process outline of the differentiation of hiPSC aggregates into CMs in Vertical-Wheel™ Bioreactors to treat post-MI patients undergoing a clinical trial is depicted in Figure 3.1. The entire differentiation process occurs inside PBS 3 MAG bioreactors, because these bioreactors provide the necessary scale to produce 1×10^9 CMs per patient and are the smallest scale of bioreactors that are equipped with probes to allow the precise control of culture conditions. Furthermore, the fact that all the process can be integrated in the same culture system can reduce the risk of culture contamination.

While the study of the expansion phase and the respective COGs is out of the scope of this thesis, this step is required to generate sufficient hiPSCs before starting differentiation. To achieve high cell numbers, hiPSCs are typically expanded in 2D culture systems, such as well-plates, and then transferred to bioreactors of increasing working volume. In this case, hiPSCs could first be expanded in well-plates, transferred to 100 mL VWBRs and then to 500 mL VWBRs, before being inoculated to 3L bioreactors.

To start the differentiation phase, hiPSCs aggregates are firstly inoculated inside a PBS 3L VWBR and, afterwards, differentiated into CMs via modulation of the canonical Wnt pathway during 20 days. During the first day of differentiation, aggregates are maintained in differentiation medium (RPMI/B27 or CDM3) supplemented with CHIR, which activates canonical Wnt pathway and allows the mesendodermal priming of hiPSCs aggregates, and Y-27632. From day 1 to 3 canonical Wnt signaling is inhibited by replacing the medium with differentiation medium supplemented with IWP2 to induce cells toward a cardiac fate.

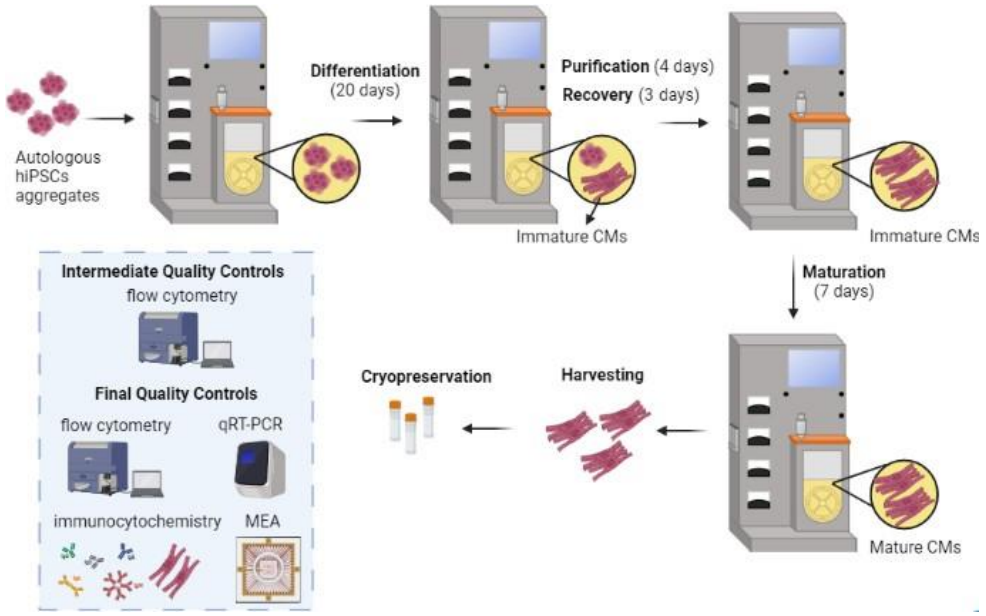

Figure 3.1: Process outline of the production of mature autologous hiPSC-CMs in Vertical-Wheel™ Bioreactors. Autologous hiPSCs aggregates are inoculated inside a PBS 3 MAG bioreactor, where they are differentiated into CMs, purified in lactate-based medium, matured in a fatty-acid rich medium and then harvested in vessel and cryopreserved. 1×10^9 hiPSC-CMs are produced per donor. Intermediate and final quality controls include flow cytometry, real-time quantitative reverse transcription polymerase chain reaction (qRT-PCR), immunocytochemistry and microelectrode array (MEA) assay. Figure adapted from [63] in BioRender.

After that, aggregates continue to be cultured only in the presence of the differentiation medium. [68] Because after the differentiation period some undifferentiated hiPSCs can remain in culture along with CMs, a purification step is needed to remove the undifferentiated hiPSCs. Therefore, after differentiation, cells are purified during 4 days in differentiation medium containing lactate but no glucose, in order to take advantage of the metabolic differences between CMs and non-CMs; whereas CMs can survive in the absence of glucose and uptake lactate via TCA cycle to obtain energy, non-CMs mainly depend on glycolysis to obtain energy and cannot survive without glucose. [84] After purification, a cell recovery period of 3 days occurs. In this period, cells are cultured only in differentiation medium, as this was shown to be important for the generation of purer and functional CMs.[67] Afterwards, hiPSC-CMs are cultured in a fatty-acid rich, glucose-free medium for 7 days to promote their metabolic and structural maturation. [90] Finally, hiPSC-CMs are harvested through an in-vessel enzymatic dissociation. [55] Harvested hiPSC-CMs are cryopreserved with CryoStor CS10 with Y-27632 in liquid nitrogen. [128] Harvesting and cryopreservation steps were assumed to last 1 day together. Quality controls are also performed in key stages throughout the bioprocess, namely after differentiation, after purification and recovery, after maturation and after harvesting. Selected quality controls are flow cytometry, which is performed in each of the aforementioned stages, real-time quantitative reverse transcription polymerase chain reaction (qRT-PCR), immunocytochemistry and microelectrode array (MEA) assay, which are performed after harvesting. [128] [129] [130] The total process duration is 45 days, since MEA assay is the final quality control that takes longer (10 days).

3.1.3 Bioprocess Economics Model

3.1.3.1 Model input parameters

Table 3.1 summarizes all the input parameters that were considered in the model and respective values for the baseline case scenario, which are used by default by the model.

The target cell number of 1×10^9 CMs per donor corresponds to the estimated number that would be required for myocardial regeneration in post-MI patients. [13]

Differentiation efficiency is highly variable with culture conditions and cell line. Published studies regarding the differentiation of PSC aggregates via modulation of the canonical Wnt pathway in stirred tank bioreactors or spinner flasks using either RPMI/B27 or CDM3 as differentiation medium, report differentiation yields between 59.9% and 99%. [128] [68] [131] In these protocols, critical parameters, such as cell aggregate size, agitation rate and small molecule concentrations were optimized. As yet, no studies of the cardiac differentiation of PSCs in Vertical-Wheel™ bioreactors are available in the literature, but taking into account that these bioreactors provide gentler and more efficient mixing conditions than the conventional stirred tank bioreactors (see Section 1.3), the differentiation efficiency for this bioprocess was assumed to fall in that range reported for STBRs and spinner flasks if critical parameters are optimized. Hence, the differentiation yield used as default by the model corresponds to the medium value of that range, which is 79.5%.

As for the fold increase (FI), there are no growth curves nor information about cell growth in the aforementioned studies. Therefore, this value was based on the study conducted by Halloin and co-workers, in which 5×10^5/mL hiPSCs were inoculated to 500 mL STBRs and differentiated in CMs, obtaining about 1×10^6 cells/mL after 10 days, which corresponds to a 2 FI in cell number. Given that the differentiation process described in this model has the duration of 20 days, a 2 FI value can be regarded as a conservative value to consider as an input. The FI value is only respective to the differentiation stage, because it was assumed that cell growth in subsequent stages is negligible.

Regarding maturation, it was assumed that there are no cell losses. Therefore, maturation yield was not considered as an input parameter.

Both differentiation media studied in this model (RPMI/B27 and CDM3) were assumed to provide similar cell growth and differentiation efficiencies. Therefore, FI and all step yields are considered to be the same whether the selected differentiation medium is RPMI/B27 or CDM3, except for the case study in which the impact of increasing or decreasing CDM3 performance in terms of FI in relation to RPMI/B27 is assessed.

A batch failure rate of 30% was considered in the model to account for the costs of failing batches. It was also supposed a failure detection probability of 20%, which corresponds to the probability of detecting a failing batch in each intermediate quality control step. A small percentage was considered for this parameter because the only quality control performed in each intermediate step is flow cytometry. Thus, although flow cytometry is important to monitor the evolution of cardiac markers and decrease in pluripotency markers throughout the process, it may not be sufficient to detect batch failures in achieving certain quality targets, such as karyotypic normality and adequate contractile and electrophysiological

properties. It was assumed that failed batches not detected until the final quality control step would be detected at that step.

Table 3.1: Input parameters used as default by the bioprocess economics model.

Parameter	Value	Reference(s)
Target CM number per donor	1×10^9 CMs	[13]
Differentiation medium	RPMI/B27	-
Inoculation density	5×10^5 cells/mL	[68]
Fold increase (FI)	2	[68]
Differentiation yield	79.5%	[67], [68], [128], [131]
Purification yield	74.4%	[84]
Harvesting yield	95.2%	[55]
Cryopreservation yield	85.8%	[128]
Batch failure rate	30%	[108]
Failure detection probability	20%	Expert opinion

3.1.3.2 Biological variability

Because each batch corresponds to hiPSC-CMs derived from different donors, the bioprocess is inevitably subject to some degree of variability due to donor-to-donor biological differences. Therefore, variations in the differentiation, purification, harvesting and cryopreservation yields were accounted to assess the impact of these parameters in the process COGs.

Table 3.2 summarizes the minimum and maximum values considered for each of those biological associated parameters, as well as the default value considered for the baseline case scenario. All yields minimum and maximum percentages, except for differentiation yield, were defined based on the standard error of the mean of the values used as default (mean value), which were retrieved from the respective references. The minimum and maximum vales for the differentiation yield were based on reported values from differentiation of CMs from PSCs in STBRs or spinner flasks, as mentioned before.

Table 3.2: Minimum, default and maximum values for each bioprocess economics input parameters in order to account with biological variability inherent to the system.

Parameter	Min. Value	Default value	Max. value	Reference(s)
Differentiation yield	59.9%	79.5%	99%	[67], [68], [128],[131]
Purification yield	62.3%	74.4%	86.5%	[84]
Harvesting yield	91.2%	95.2%	99.2%	[55]
Cryopreservation yield	83.6%	85.8%	88%	[128]

3.1.3.3 Model workflow

The model is composed of modules and classes in order to organize the code properly and improve its readability. It consists of the ”database.py”, ”autologous.py”, ”allogeneic.py” and ”main.py” modules.

”database.py” contains the classes Datatable(), Facility() and CultureConditions(), which store the costs associated with reagents and the process step times, costs of facility management and default culture conditions, respectively.

”autologous.py” and ”allogeneic.py” contain the classes DifAutologous() and DifAllogeneic(), respectively, which define the differentiation process steps and cell numbers and costs calculations throughout the process using the information from the classes in the ”database.py” module for each cell therapy modality. Class objects’ are initialized based on parameters found in Table 3.1, which correspond to the model’s deterministic inputs. Default values for these model inputs are stored in CultureConditions() class from the ”database.py” module.

”main.py” module defines a text-based graphical user interface that allows the user to run the ”autologous.py” module using as inputs the preset culture conditions stored in the CultureConditions() class from the ”database.py” module when typing ”run” or to simulate the preset comparisons of different experimental setups when typing ”study” and then typing the name of the intended study (”yields”, ”CDM3”, ”qual”, ”allogeneic”). The ”yields” study compares the impact of different process yields in the autologous bioprocess costs in order to account for biological variability. The worst yield scenario, baseline scenario and best yield scenario were considered, which correspond to the processes with the minimum, default and maximum yield values in each step, respectively. Step yield values for these three scenarios are indicated in Table 3.2. The ”CDM3” study compares the autologous bioprocess costs of different CDM3 medium performance scenarios with the baseline autologous scenario. The ”qual” study assess the impact of batch failure rate and probability of failure detection probability in the autologous bioprocess costs. The ”allogeneic” study allows the comparison of autologous and allogeneic process costs at different production scales.

When running the aforementioned studies, important information is returned by the model, such as the bioreactor working volume, cell numbers in each step and bioprocess costs per step and category. Bioprocesses costs by step and category in each study are organized in bar charts to allow for a better visualization and comprehension of the data. All these studies and respective results will be analysed in detail in Section 4.1.

3.1.3.4 Model output equations

3.1.3.4.1 Direct costs Direct costs considered in the present model are the costs associated with consumables and reagents used for cell culture, storage, as well as intermediate and final quality controls. Consumable and reagent costs were taken from supplier information and are presented in Table 7.1.

3.1.3.4.2 Indirect costs Indirect costs considered in the model are equipment and facility depreciation costs, facility and equipment operational costs and labor costs. GMP facility, equipment and labor related main parameters and respective costs are presented in Table 3.3. All facility associated parameters and respective costs are shown in Table 7.2.

3.1.3.4.3 Equipment and Facility Depreciation Costs Assuming linear depreciation, facility and equipment depreciation costs are calculated by dividing their acquisition costs by their depreciation time

Table 3.3: GMP facility, equipment and labor related paramters.

Parameter	Value	Reference
Facility area	400 m^2	[108]
Clean room ratio	0.2	[108]
Facility depreciation period	15 years	[108]
Parallel processes	6	[108]
Equipment depreciation period	5 years	[108]
Employee amount	4	[108]
Daily worktime	8 h/day	This work
Salary per hour	12 €/h	[108]

and multiplying it by the process operation time [108], as follows:

$$COG_{dep} = \left(\frac{C_f}{t_{f,dep}} + \frac{C_{eq}}{t_{eq,dep}}\right) \times t_{operation} \tag{3.1}$$

COG_{dep} is the total cost of goods associated with facility and equipment depreciation, C_f and C_{eq} are the facility and equipment acquisition costs, respectively, $t_{f,dep}$ and $t_{eq,dep}$ are the GMP facility and equipment depreciation times (in days), respectively, and $t_{operation}$ is the total process operation time (in days).

3.1.3.4.4 Equipment and Facility Operation Costs Equipment and facility operation costs are associated with daily costs to keep the facility running [108]. They are calculated as follows:

$$COG_{operation} = \left(C_{gases} + C_{add,supplies} + C_{requal} + C_{maintenance} + C_{cleaning} + C_{garment}\right) \times t_{operation} \tag{3.2}$$

C_{gases} are the costs associated with necessary gases (oxygen, carbon dioxide, liquid nitrogen) for cell culture in incubators and bioreactors and storage. $C_{add,supplies}$ include the costs with additional office and laboratory supplies. C_{requal} is the cost of testing air quality and GMP compliance. $C_{maintenance}$ are the maintenance costs of equipment and facility. $C_{cleaning}$ are the costs of cleaning and disinfecting the facility. $C_{garment}$ are the costs associated with clean room personal protection equipment. [108]

3.1.3.4.5 Labor Costs Labor costs are calculated based on the number of workers, total worker time and total process operation time. It is calculated as follows:

$$COG_{labor} = n_{workers} \times C_{\frac{worker}{day}} \times t_{operation} \tag{3.3}$$

where $n_{workers}$ is the number of workers in the facility, $C_{\frac{worker}{day}}$ is the daily cost associated with each worker and $t_{operation}$ is the total process operation time (in days).

3.2 In-lab generation of hiPSC-derived cardiomyocytes

3.2.1 Culture of human induced pluripotent stem cells

3.2.1.1 Cell line

In this work, Gibco™ human episomal iPSC line was used. This line was derived from CD34-positive cord blood using a three-plasmid, seven-factor (SOKMNLT; SOX2, OCT4 (POU5F1), KLF4, MYC, NANOG, LIN28, and SV40L T antigen) episomal system.

3.2.1.2 Adhesion substrate

Matrigel (Corning®) was used as adhesion substrate. This matrix was derived from Engelbreth-Holm-Swarm mouse sarcoma and is composed of laminin (major component), collagen IV, entactin, heparin sulfate proteoglycans and a number of growth factors.

Matrigel was thawed in ice and aliquoted at -20°C. 12-well plates (Falcon ®) were coated with diluted Matrigel. For this purpose, aliquotes containing 60 μL of Matrigel per plate were thawed in ice and diluted 1:100 with DMEM/F12 (Thermo Fisher Scientific™) medium. Coated plates were left at room temperature for at least 2h prior to use or they were stored at 4°C for later use for a maximum of 2 weeks.

3.2.2 Culture Media

For hiPSC culture, three different media formulations were used: the commercially available mTeSR™1 (STEMCELL TECHNOLOGIES™) and E8 ™ (Gibco™) media and in-house prepared B8.

3.2.2.1 mTeSR™1 medium

Complete formulation of mTeSR™1 can be found in Table 7.4. mTeSR™1 5x supplement was thawed overnight at 4°C and then mixed with mTeSR™1 basal medium. Complete medium was aliquoted at -20°C. Before use, aliquots were thawed and 0.5% penicillin/streptomycin (PenStrep, Thermo Fisher Scientific™) was added. mTeSR™1 was pre-warmed at room temperature prior to medium exchange.

3.2.2.2 E8

Complete formulation for E8 can be found in Table 7.5. E8 50 x supplement was thawed overnight at 4°C and then mixed with E8TM basal medium. Complete medium was aliquoted at -20°C. Before use, aliquots were thawed and 0.5% PenStrep was added. E8 was pre-warmed at room temperature prior to medium exchange.

3.2.2.3 B8

B8 medium was prepared in house according to Kuo *et. al*. [60] Complete formulation of this medium and the brand from which each component was purchased can be found in Table 7.6. B8 medium was

aliquoted and stored at -20°C. Before use, aliquots were thawed and 0.5% PenStrep was added. B8 was pre-warmed at room temperature prior to medium exchange.

3.2.2.4 Washing medium

Washing medium was used to suppress enzymatic digestion or to maintain cells whenever they were processed in suspension. This solution is composed of DMEM/F12 with L-glutamine (Thermo Fisher Scientific™), 2.44 g/L of sodium bicarbonate (Sigma-Aldrich®) and supplemented with 10% (v/v) KO-SR (Thermo Fisher Scientific™), 1% (v/v) MEM non-essential amino acids (Thermo Fisher Scientific™) and 1% (v/v) penicillin/streptomycin. Washing medium was kept at 4°C and pre-warmed at room temperature before use.

3.2.3 Cell thawing

Cryovials (Thermo Fisher Scientific™) containing around 1 × 10^6 hiPSCs cryopreserved in liquid nitrogen were removed from the tank and warmed for about 30 s in a 37°C water bath. Afterwards, 1 mL of pre-warmed washing medium was slowly added to each cryovial to thaw cells. The cell suspension wasadded to a Falcon®tube containing 5 mL of washing medium and centrifuged for 3 min at 300×g. After removing the supernatant, the cells were ressuspended in 1 mL of mTeSR™1 medium and seeded in Matrigel-coated 6-well plates (Corning®) containing 0.5 mL of medium. Cells were placed in a CO2 incubator (SANYO, MCO-19AIC) and kept at 37°C, 5% CO2 and 20% O2.

3.2.4 hiPSC expansion as monolayers

hiPSC lines were routinely expanded in 6-well plates (Falcon®) coated with Matrigel with 1.5 mL of mTeSR™1 medium, E8 or B8 medium supplemented with 0.5% penicillin/streptomycin. mTeSR™1 and E8 were fully replaced daily, while B8 was exchanged 24h after cell passaging and every other day afterwards. Cells were maintained in a CO2 incubator at 37°C, 5% CO2 and 20% O2. When 80-90% confluency was reached, they were passaged as described in Section 3.2.5.

3.2.5 Cell passaging

Cell passaging was routinely performed using an EDTA solution (0.5 mM EDTA (Thermo Fisher Scientific™) and 1.8 g/L sodium chloride (Sigma-Aldrich®) in phosphate-buffered saline (PBS) solution (Thermo Fisher Scientific™). Cells were washed twice with 1 mL/well of EDTA solution and were incubated with 1 mL/well of EDTA solution for 5 min at room temperature for dissociation into small clumps. After removing the EDTA solution, the cells were flushed twice with 1 mL/well of culture medium and collected to a Falcon®tube. Culture medium was added to the Falcon®tube in sufficient amount to distribute the cell suspension in the wells of the new Matrigel-coated 6-well plate, that already had 0.5 mL/well of culture medium. Cells were passaged at a ratio of 1:4. Finally, newly plated cells were kept in a CO2 incubator at 37°C, 5% CO2 and 20% O2.

3.2.6 Cell harvesting and counting

To perform cell harvesting, cells were first washed with PBS and were singularized by incubation with Accutase for 7 min in a CO2 incubator. Washing medium was used to inactivate Accutase. Cells were collected to a Falcon®tube and the suspension was centrifuged at 300 x g for 3 min. After discarding the supernatant, cells were resuspended in 1 mL of washing medium per well. The cell suspension was thoroughly mixed and a sample of 10 µL was collected. This sample was mixed with 10 µL of Trypan Blue (Thermo Fisher Scientific™) and the resulting mixture was loaded in a hemocytometer and visualized under an inverted optical microscope (Leica Microsystems, Model DMI3000 B).

The quantity of cells in the original sample was calculated as follows:

$$Total\ cell\ number = \frac{Average\ cell\ number}{N_{squares} \times D_f \times\ 10^4 \times V_s} \tag{3.3}$$

Where $N_{squares}$ corresponds to the number of squares of the hemocytometer, D_f is the sample dilution factor and V_s is the volume of the original suspension of cells. 10^{-4} corresponds to the volume of a hemocytometer square in mL.

3.2.7 Cell cryopreservation

Cells were washed twice with 1 mL/well of EDTA and incubated with 1 mL/well of EDTA for 5 min at room temperature. Afterwards, cells were flushed twice with 1 mL/well of washing medium and collected into a Falcon®tube. The suspension was centrifuged at 300 x g for 3 min. After discarding the supernatant, cells were resuspended in 250 µL of KO-SR containing 10% (v/v) of dimethylsulfoxide (DMSO; Sigma-Aldrich®). Suspended cells were transferred to cryovials (250 µL/cryovial) and stored at -80°C for a maximum of 24 h before being transferred to liquid nitrogen (-196°C).

3.2.8 Cardiac differentiation of hiPSCs

3.2.8.1 Culture Medium

3.2.8.1.1 RPMI/B27 RPMI 1640 (Thermo Fisher Scientific™) was used as a basal medium for the differentiation of hiPSCs into CMs, which composition can be found in Table 7.7. This medium was either supplemented with 2% B-27 minus insulin (Thermo Fisher Scientific™) or B-27 (Thermo Fisher Scientific™), which were thawed at room temperature in the dark, and 0.5% penicillin/streptomycin to obtain RPMI/B27-insulin or RPMI/B27, respectively. Both media were stored at 4 °C protected from light for a maximum of 30 days.

3.2.8.1.2 CDM3 CDM3 medium was also used as a medium for differentiation. It was prepared as described by Burridge et. al. [76]. It consists of RPMI 1640 basal medium supplemented with 75 mg/mL of L-ascorbic acid 2-phosphate (Sigma-Aldrich®), 500 µg/mL of rice-derived recombinant human albumin

(Sigma-Aldrich®) and 0.5% penicillin/streptomycin. Medium was stored at 4 °C protected from light for a maximum of 30 days.

3.2.9 Differentiation of hiPSCs into cardiomyocytes via modulation of the canonical Wnt pathway

hiPSCs were differentiated into cardiomyocytes based on the protocol developed by Lian et. al. [72].

hiPSCs were seeded in Matrigel-coated 12-well plates at a density of 100,00 cells/cm^2 and expanded in 2D monolayer culture until a confluence of around 90-95% was attained and differentiation could be initiated. Cells were differentiated in RPMI medium supplemented with 2% (v/v) B-27 minus insulin and 0.5% PenStrep from day 0 to 7 and differentiated with RPMI supplemented with B-27 and 0.5% PenStrep from day 7 until the end of differentiation. GSK3 inhibitor CHIR99021 (Stemgent) was supplemented to the medium at day 0 at a concentration of 6 μM, and after 24 hours medium was changed to RPMI/B-27 minus insulin. At day 3, 750 μL/well of medium were removed and replaced with medium containing Wnt inhibitor IWP-4 (Stemgent) for 2 days to obtain a final concentration of 5 μM . From day 7, medium was changed every 3 days until harvesting. The performance of differentiation was assessed phenotypically by the exhibition of spontaneous contraction (first day of contraction and beating rate) and quantitatively by assessing the expression of cTnT by flow cytometry.

Figure 3.2 summarizes each condition tested for the differentiation of hiPSCs into cardiomyocytes in 2D culture conditions. Cells expanded in mTeSR^{TM}1, E8^{TM} or B8 medium were differentiated either in RPMI/B27 or CDM3 medium.

3.2.10 Characterisation of hiPSCs and hiPSC-derived cardiomyocytes

3.2.10.1 Flow cytometry

3.2.10.1.1 Sample collection Cells were harvested using Accutase, ressuspended in washing medium to inactivate Accutase and centrifuged at 300 x g for 3 min, as described in Section 3.2.6. After that, the supernatant was discarded and cells were washed with 1 mL of PBS. Another centrifugation for 3 min at 300 x g was performed and, after removing the supernatant, cells were fixed by ressuspension in 1 mL of 2% paraformaldehyde (PFA; Sigma-Aldrich®) in PBS for 20 min. The cell suspension was centrifuged, ressuspended in 1 mL of PBS and kept at 4 °C for a maximum of 2 weeks.

3.2.10.1.2 Cardiac Troponin T Cells in PBS were centrifuged at 300×g for 3 min. After discarding the supernatant, the pellet was resuspended and incubated during 15 min at 4 °C in 1 mL of 90% of cold methanol. The cell suspension was centrifuged and washed two times with flow cytometer buffer (FCB) 1 (0.5 % of BSA (Sigma-Aldrich®) in PBS). During this last washing step each representative sample was split in order for half of the cells serve as negative controls and the other half to be incubatedwith the primary anti-cTnT antibody: negative control samples were then resuspended in 100 μL of FCB2 (0.5% BSA and 0.1% Triton X-100 (Sigma-Aldrich®) in PBS) and the remaining samples were

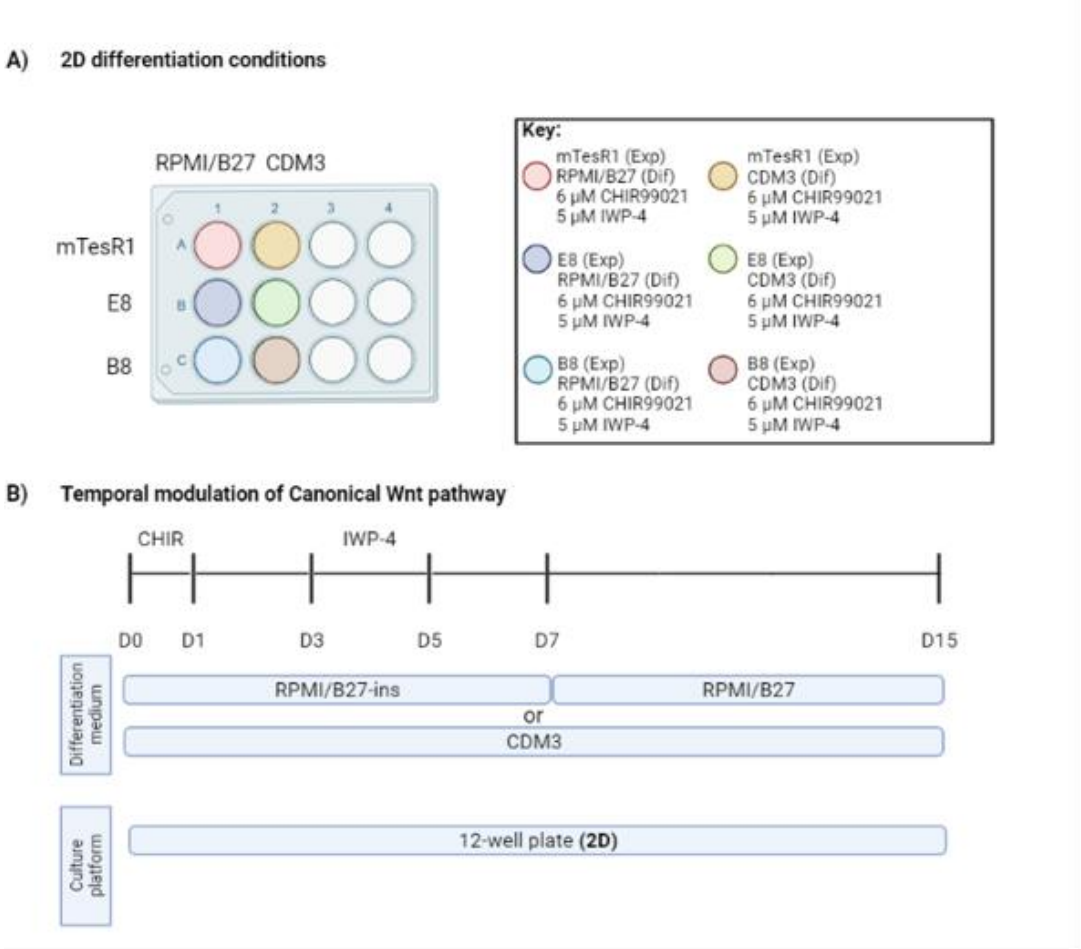

Figure 3.2: Differentiation via modulation of the canonical Wnt pathway in 2D conditions. A) 2D differentiation conditions. B) Temporal modulation of the canonical Wnt pathway. At the startof differentiation, culture medium (RPMI/B27 or CDM3) is supplemented with small molecule CHIR99021 for 1 day to activate Wnt pathway and promote mesendoderm formation. From day 3 to 5 medium is supplemented with IWP-4 to inactivate canonical Wnt pathway and promote cardiac mesoderm formation. Cells are differentiated in 12-well plates.

resuspended in 100 µL of FCB2 with 0.4 µL of mouse immunoglobulin (Ig) G anti-cTnT antibody (Thermo Fisher Scientific™, dilution of 1:250). Samples with the primary antibody were incubated for 1h at room temperature. Afterwards, cells were washed twice with 2 mL of FCB2 and incubated in the dark for 30 min with 100 µL of FCB2 containing 0.1 µL of Alexa Fluor®488-conjugated goat anti-mouse IgG secondary antibody (Thermo Fisher Scientific™, dilution of 1:300). After that period, cells were washed with 1 mL of FCB2 and then twice with 2 mL of the same solution. Finally, they were resuspended in 300 µL of FB1 and transferred to FACS tubes (Falcon®) to be analysed in a FACSCalibur™ flow cytometer (see section 3.2.10.1.3).

3.2.10.1.3 Sample analysis Cell samples were analysed with a FACSCalibur™ flow cytometer (Becton Dickinson, USA) and data was acquired using Cell Quest software (Becton Dickinson). The gate was selected to contain only 1% of false positives. Data was analysed with Flowing Software 2 (University of Turku, Finland). When possible, a minimum of 10,000 events were analysed for each sample.

4 | Results and Discussion

4.1 Cost of good analysis: Production of autologous hiPSC-CMs in Vertical-Wheel Bioreactors

4.1.1 Introduction

A cost analysis was conducted using Python to assess the impact of biological associated parameters (e.g fold increase in cell number during differentiation, differentiation yield, etc.), culture medium and batch failure rates using Vertical-Wheel™ bioreactors in the production of autologous hiPSC-CMs to treat a post-MI patient undergoing a clinical trial. The objective is to identify what are the bioprocess main cost drivers and suggest solutions to reduce the overall process costs to make it more economically viable.

The process outline can be consulted in Section 3.1.2. The considered facility has the capacity to run 6 parallel processes (i.e 6 VWBRs running at the same time), which means that 6 doses per patient can be produced in each facility run, since only one dose can be produced per batch due to the autologous modality.

4.1.2 Model application

4.1.2.1 Base case scenario analysis

The baseline case scenario consists of a bioprocess simulation where “default” values were assumed for the parameters associated with biological variability (Table 3.1). Under these conditions, Figure 4.1A shows the number of hiPSCs required for the production of the target number of CMs per donor and the cell numbers predicted after each process step. Figures 4.1B and 4.1C demonstrate the distribution of bioprocess costs per category and per step, respectively.

According to the model, only 1 batch is required in order to produce the target number of 1×10^9 CMs per donor in the conditions of the base case scenario. The working volume required to achieve that targetis 2070 mL. This value is compatible with the minimum working volume of the PBS 3 MAG bioreactor, which is 1800 mL. Thus, there is no excess production of CMs (Figure 4.1A).

The total bioprocess cost in base case scenario conditions is 40826 €. Reagents are the main cost driver (representing 55% of the total bioprocess cost), followed by facility (27%), labor (10%), consumables (4%) and quality controls (4%) (Figure 4.1B). Regarding cost breakdown per step, maturation and differentiation

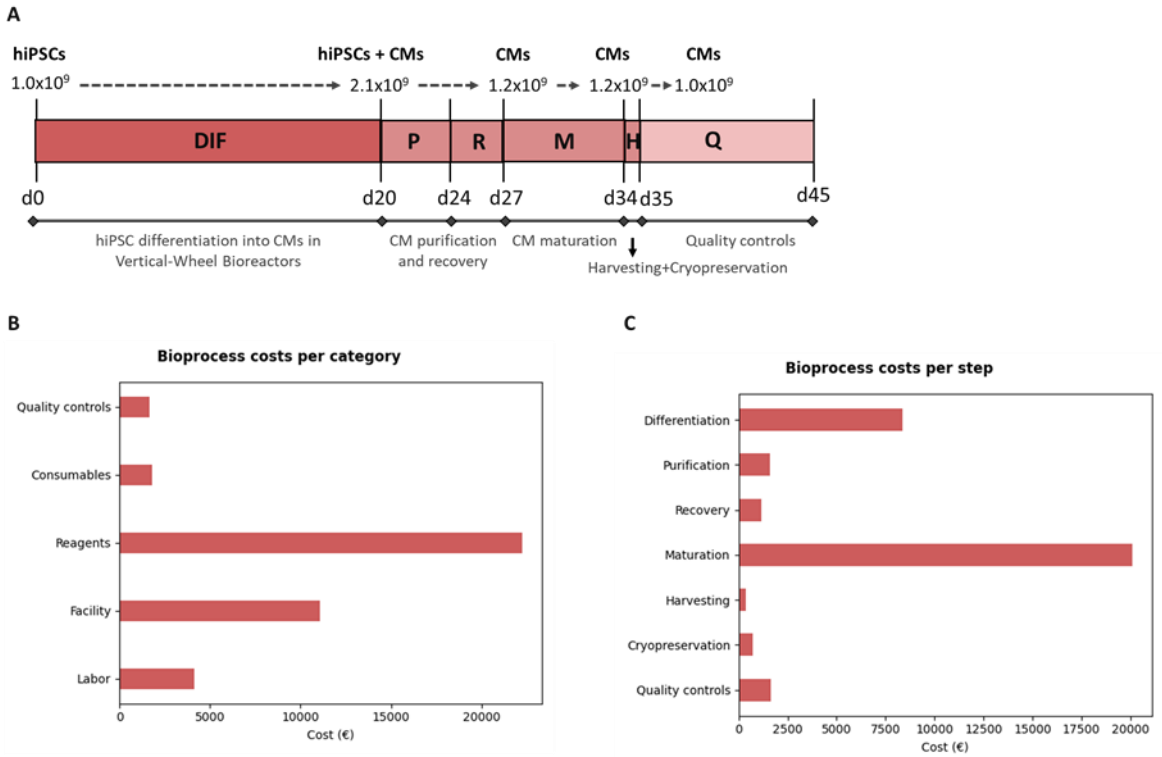

Figure 4.1: Base case scenario production and COGs. A-Number of hiPSCs required to achieve the target number of CMs per donor and number of cells after each process step. B- Breakdown of bioprocess costs per category. C-Breakdown of bioprocess costs per step.

are the major cost contributors, accounting for 49% and 20% of the total bioprocess cost, respectively (Figure 4.1C).

The greater contribution of reagents to the process cost is due to the fact that all the process since hiPSC inoculation and differentiation in Vertical-Wheel™ bioreactors and subsequent purification and maturation in the same bioreactors are based on extensive culture medium supplementation and frequent exchanges with fresh medium. The other bioprocess stages, especially quality controls, contribute as well to the high expenditure on reagents, because quality controls are performed throughout and at the end of the process. Increased reagents costs are also related with the percentage of batch failures (30%) and failure detection probability (20%) because of the extra batches that have to be carried out to make up for the failed ones. Within the reagents-related expenses, the maturation and differentiation stages have the greatest contribution to the process costs since they correspond to the stages of longerduration (20 days of differentiation and 7 days of maturation) and with more complex and expensive culture media and supplements. Maturation medium represents the highest expenditure with reagents, because it is a complex fatty-acid rich medium made up of several components (medium formulation canbe consulted in Table 7.9), which makes it very costly (about 1114 €/L, see Table 7.1). Given that 80% ofthe maturation medium is changed every 2 days (see Table 7.3), the expenses with maturation medium are very high. Since the costs associated with the maturation medium are extremely high, it would be highly relevant to investigate the feasibility of reducing the percentage of medium exchange and/or to reduce the medium changes, while maintaining the final product quality. For example, changing half of the maturation medium every 2 days instead of 80% would drive the total bioprocess cost to 35552 €,

representing a 13% decrease in relation to the base case scenario. The same type of strategies could be investigated for the culture medium feeding regimes used in the other bioprocess steps, in order to reduce the overall costs.

Since the facility also represents a significant portion of the process cost (27%), efforts to reduce the cost associated with it would be beneficial. In this model, it has been assumed that the facility equipment would only be used for the production autologous hiPSC-CMs. However, in reality, it is likely that the equipment is shared between multiple research activities. [114] To consider this, the facility associated costs were lowered to 75% of the facility costs from the base case value. In this situation, total bioprocess costs would be 38063 €, a 7% reduction relative to the baseline case. Combining the 25% reduction in facility costs and the aforementioned feeding medium regime of changing 50% of the maturation medium every 2 days would cause a 20% reduction in total bioprocess cost in relation to the baseline case (32661 € in this situation vs. 40826 € in the baseline scenario).

Taken together, the changes suggested herein, such as reducing the percentage and frequency of medium exchanges, especially in the maturation step, as well as reducing the costs associated with the facility may lead to effective solutions to significantly reduce the overall process cost.

4.1.2.2 Impact of process yield in bioprocess costs

The impact of the yield of different stages, in terms of cell number and CM purity, over the bioprocess costs was assessed. By combining the yields of the different process stages (see Table 3.2), it was possible to estimate the worst process yield, the baseline case process yield (with the ”default” yield values) and the best process yield. The values obtained are, respectively, 29%, 48% and 75%. Figure 4.2 shows the number of hiPSCs required for the production of the target number of CMs per donor and the cell numbers estimated after each process step for each yield scenario. Figures 4.3A and 4.3B demonstrate the total bioprocess costs and distribution of bioprocess costs per category, respectively.

For the worst yield scenario 2 batches are required to produce the target number of CMs, while for the baseline and best yield scenarios only 1 batch is required. The necessary working volume for the worst yield scenario, baseline yield scenario and best yield scenario is 3600 mL, 2069 mL and 1800 mL, respectively. Therefore, a significant higher amount of starting hiPSCs (1.8×10^9 cells) is required to achieve the desired target of CMs than for the baseline yield and best yield scenarios, which require 1×10^9 and 9×10^8 cells, respectively. In the best yield scenario, the real necessary working volume corresponds to the bioreactor minimum working volume (1800 mL). Therefore, in this case, a greater number of CMs than required target are generated (1.4×10^9 CMs, Figure 4.2).

Total bioprocess cost for the worst yield scenario, baseline yield scenario and best yield scenario is 75241€, 40826€ and 38220€, respectively (Figure 4.3A). From the worst yield scenario to the baseline yield scenario there is a reduction of approximately 46% in the bioprocess cost and a reduction of 49% to the best yield scenario. The reduction in process costs with an increasing yield is due to reduction of the bioreactor necessary working volume and, therefore, less expenses associated with reagents (Figure 4.3B). It should be noted that process costs for the best yield scenario might be reduced by do not performing the cryopreservation of CMs produced in excess, resulting in less expenses with

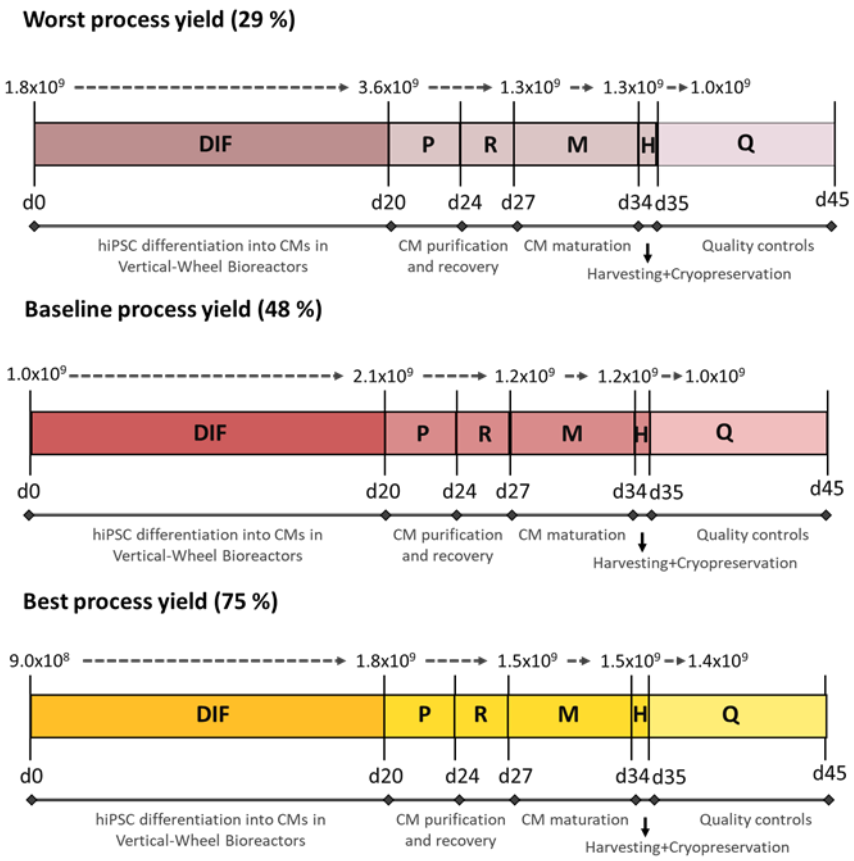

Figure 4.2: Impact of process yield in the number of hiPSCs required to achieve the target number of CMs per donor and number of cells after each process step for each yield scenario.

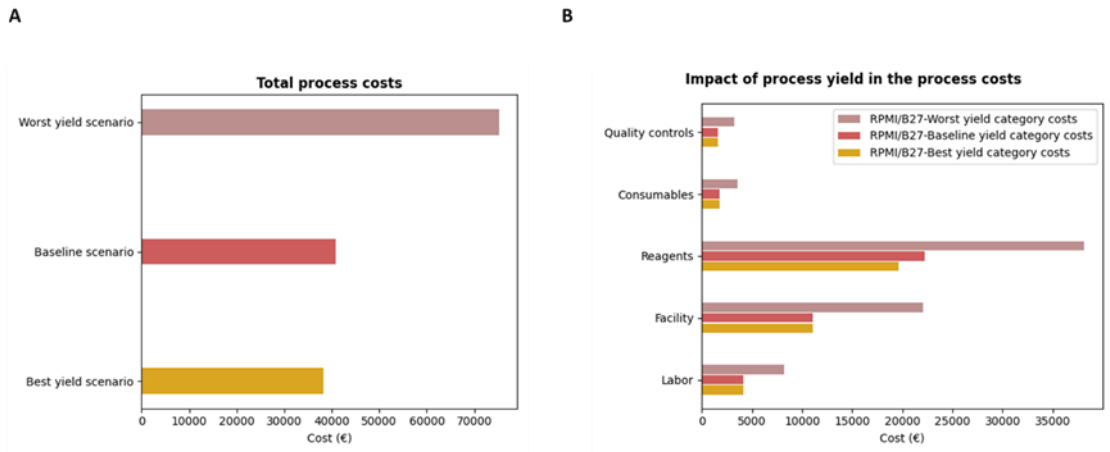

Figure 4.3: Impact of process yield in the process COGs. A-Total bioprocess costs for each yield scenario. B-Breakdown of bioprocess costs per step for each yield scenario.

cryopreservation medium. The pros and cons of cryopreserving the surplus cells generated (e.g storage of extra cells vs. increased costs) should be carefully evaluated. All categories costs' are higher for the worst yield scenario than the remaining scenarios because of the higher required number of batches. Quality controls, consumables, facility and labor costs are the same for the baseline and best yield scenarios because only 1 batch is required for both cases.

4.1.2.3 Impact of CDM3 medium performance in bioprocess costs

Cardiac differentiation of hiPSCs using the Wnt pathway modulation method was established and it is widely performed using RPMI/B27, a serum-free culture medium formulation consisting of RPMI basal medium supplemented with B27, a proprietary (Thermo Fisher Scientific) mixture of 21 components, including animal origin components, such as BSA. However, despite the efficient and robust performance of RPMI/B27 for cardiac differentiation, the clinical use of this medium is hindered by concerns regarding the use of animal origin components, due to the possible presence of animal pathogens and biological variability. An alternative culture medium was developed for hiPSC cardiac differentiation, named CDM3 (Chemically Defined Medium, 3 Components), which is a chemically defined and xeno-free medium more suitable for prospective clinical applications. [76] CDM3 medium has also the advantage of being cheaper than RPMI/B27; CDM3 medium costs 36€/L, whereas RPMI/B27 costs 420€/L (see Table 7.1). However, only limited quantitative information is currently available regarding the performance of CDM3 for hiPSC cardiac differentiation as 3D aggregates, either in terms of cell proliferation and differentiation efficiency.

In this section, to better understand the impact of CDM3 medium performance in bioprocess costs, four different scenarios were simulated: the baseline scenario (with RPMI/B27); CDM3 leads to the same FI in cell number than the baseline (named CDM3 (1x)); CDM3 leads to a FI in cell number that is lower than the baseline (0.75 times; named CDM3 (0.75x); CDM3 leads to a FI in cell number that is higher than the baseline 1.5 times (named CDM3 (1.5x)) and CDM3 leads to a FI in cell number that is higher than the baseline 2 times (named CDM3 (2x)) . For the remaining process steps, for each scenario, the yields were assumed to be those used as default by the model.

Figure 4.4 shows the number of hiPSCs required for the production of the target number of CMs per donor and cell numbers after each process step for each scenario. Figures 4.5A and 4.5B demonstrate the total bioprocess costs and distribution of bioprocess costs per category, respectively. For each scenario were considered the yields used as default by the model.

In all situations, 1 batch is required to produce the target number of CMs. For the CDM3 (0.75 x), a higher initial amount of hiPSCs (1.4×10^9 cells) is required, for the baseline and CDM3(1x) 1×10^9 cells are required and for the CDM3(1.5x) and CDM3(2x) 9×10^8 cells are required (Figure 4.4A). The necessary working volume is 2760 mL for CDM3 (0.75 x), 2070 mL for the baseline and CDM3(1x) and 1800 mL for the CDM3(1.5x) and CDM3(2x). In the latter scenarios (CDM3(1.5x) and CDM3(2x)) there is a surplus production of CMs, which increases alongside with FI (1.3×10^9 CMs for CDM3(1.5x) and 1.7×10^9 CMs for CDM3(2x), Figure 4.5A), because the necessary working volume is below the bioreactor minimum working volume.

Total process costs for the CDM3 (0.75x), baseline, CDM3 (1x), CDM3(1.5x) and CDM3(2x) scenarios are 47502 €, 40826 €, 40482 €, 37916 € and 38173 €, respectively (Figure 4.5A). This difference in costs is only caused by differences in reagents costs (Figure 4.5B); quality controls, consumables, facility and labor costs are equal for all scenarios because the same number of batches is required and the process duration is the same. The CDM3(0.75x) scenario cost is 15%, 14%, 20% and 19% higher than CDM3 (1x), baseline, CDM3 (1.5x) and CDM3 (2x) scenarios cost, due to the lower cell proliferation and, therefore, the requirement of a higher working volume. From the baseline scenario to the CDM3 (1x) scenario there

is a slight reduction (1 %) in process costs, which is only due to differences in CDM3 and RPMI/B27 medium costs, as medium performance is the same in both cases. Although medium performance is better in CDM3 (2x) when compared with CDM3 (1.5x), the first scenario process cost is 0.7% higher. This increase in costs is associated with the bioreactor's minimum working volume constraint. Thus, since the real working volume required is lower than 1800 mL, there is a surplus production of CMs which leads to higher expenses with cryopreservation medium, assuming the excess cells are cryopreserved

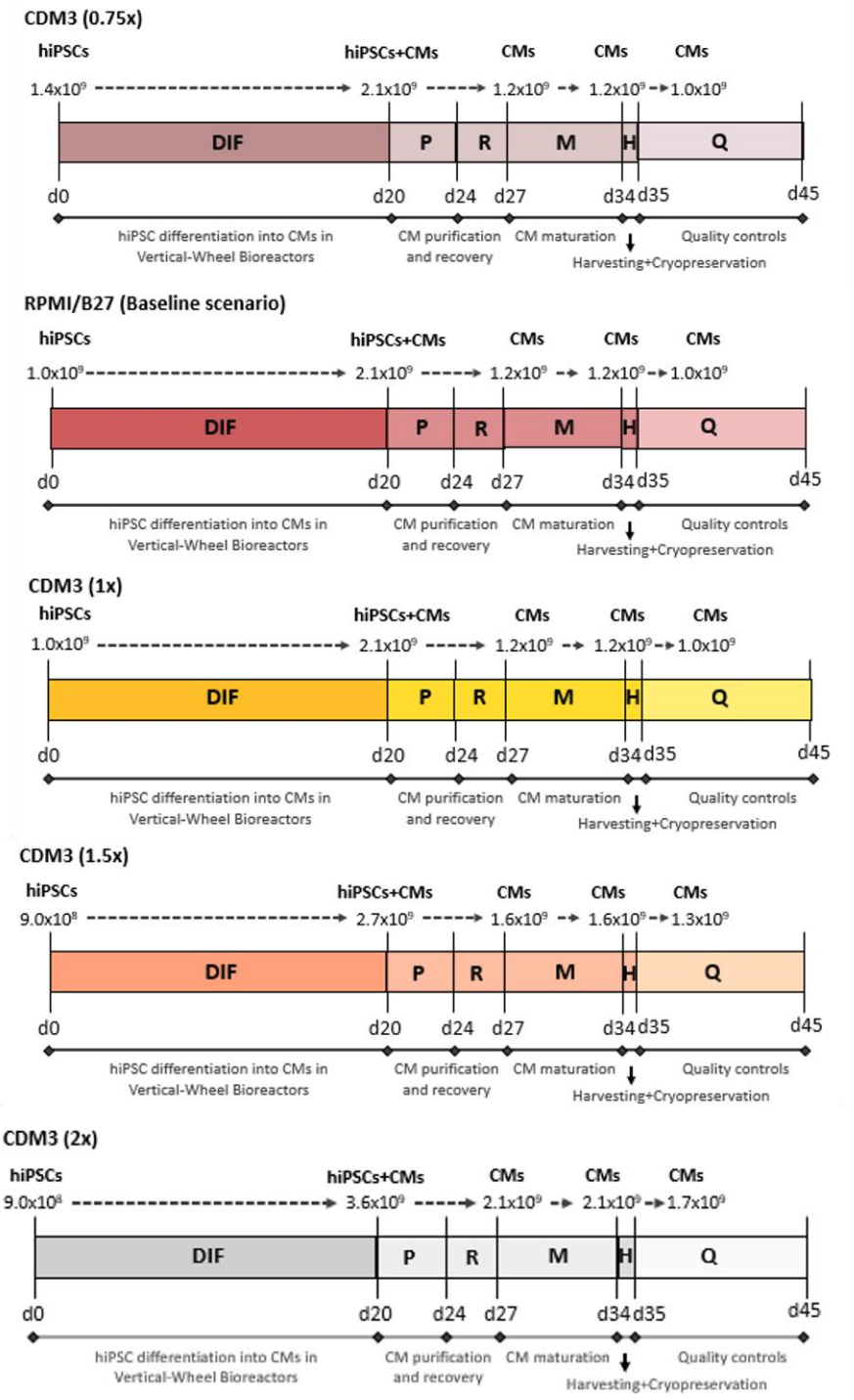

Figure 4.4: Impact of CDM3 medium efficiency in the number of hiPSCs required to achieve the target number of CMs per donor and number of cells after each process step for each fold increase scenario.

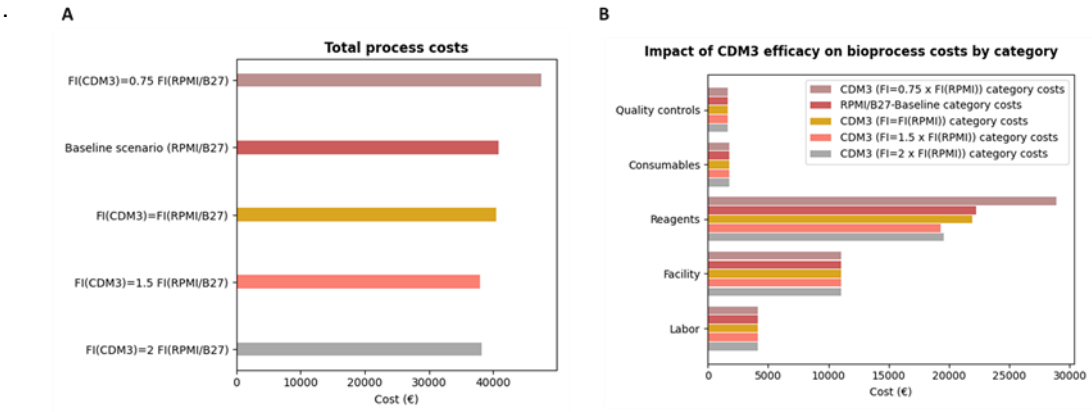

Figure 4.5: Impact of CDM3 medium efficiency in the process COGs. A-Breakdown of bioprocess costs per category for each culture medium efficiency scenario. B-Breakdown of bioprocess costs per step for culture medium efficiency scenario.

In order to reduce the process costs with an increasing medium performance while maintaining the same inoculation density (500,000 cells/mL), the solution would be to use the calculated necessary working volume instead of the 1800 mL minimum working volume of the 3L VWBRss.This would be possible by using VWBRs with smaller dimensions (PBS 0.1 MAG and/or PBS 0.5 MAG). Nonetheless, this approach has notable disadvantages since these smaller scale bioreactors are not equipped with automated monitoring and control systems and therefore, are not ideal to guarantee reproducibility between batches and homogeneity between cells generated. Thus, there is a clear limitation for autologous processes for which the necessary working volume is comprised between 500 mL and 1800 mL, since the 3L VWBR is, at the moment, the only available choice for a fully controlled VWBR in this scale. On the other hand, increasing medium performance (which consequently causes a decrease in the required working volume) leads to the production of CMs above the target number, since the bioreactor has to operate in its minimum working volume (1800 mL). Because of this limitation, an increased medium performance only translates into a clear reduction in overall process costs up to the point where the required working volume corresponds to the minimum working volume of the bioreactor; from this point, there will be an overproduction of CMs, which may be questionable in autologous processes, especially if the excess cells have to be discarded and will not be used to treat any other patients or for any other application. In cases where a high medium performance leads to an overproduction of CMs due to the bioreactor volume limitations, the inoculation density could be adjusted so that the required working volume matches the minimum working volume of the reactor. However, it is important to note that inoculation density affects the initial aggregate size and growth, which in turn impacts overall cell yields and differentiation efficiency. [66] [53] Therefore, adjustments to this parameter must be carefully tested and experimentally validated in combination with other parameters, such as agitation speed, in order to guarantee differentiation efficiency.

4.1.2.4 Impact of batch failure rate and probability of batch failure detection probability in bioprocess costs

The design of a bioprocess where hiPSC expansion and differentiation are performed in disposable bioreactor vessels, with some degree of automation and operation under a close environment, was

envisioned to minimize the risk of contaminations with microrganisms, which may lead to batch failure and loss of resources, with impact on process economic viability. Other causes that may lead to batch failure include problems with the cell inoculum, due to low quality cells or stochastic events that may lead to spontaneous differentiation or unpredicted cell death. The occurrence of these events may be minimized with a better process understanding. Nevertheless, to minimize the number of failed batches, quality control assays may be performed throughout the process steps. An effective quality control is expected to allow early detection of failed batches and therefore higher probability of batch failure detection.

The impact of batch failure rate and probability of batch failure detection in bioprocess costs was evaluated. Figure 4.6A represents the impact of batch failure rate in the process COGs, showing the total costs for a process with 30% of failed batches (baseline case) but also with no batch failures (0%), 50% batch failure or 70 % batch failure using RPMI/B27 medium and with a failure detection probability of 20%. The respective cost breakdown per category is shown in Figure 4.6B. The impact of running the bioprocess with 0 % batch failure detection probability was also evaluated. This scenario was compared with increasing probabilities of failure detection. Figure 4.6C shows the cost decrease or increase of varying failure detection probabilities (20%, 40%, 60%, 80%, 100%) in relation to the scenario of 30 % batch failure and no failure detection probability. Identical simulations were also performed with batch failure rates of 20%, 30% and 40%.

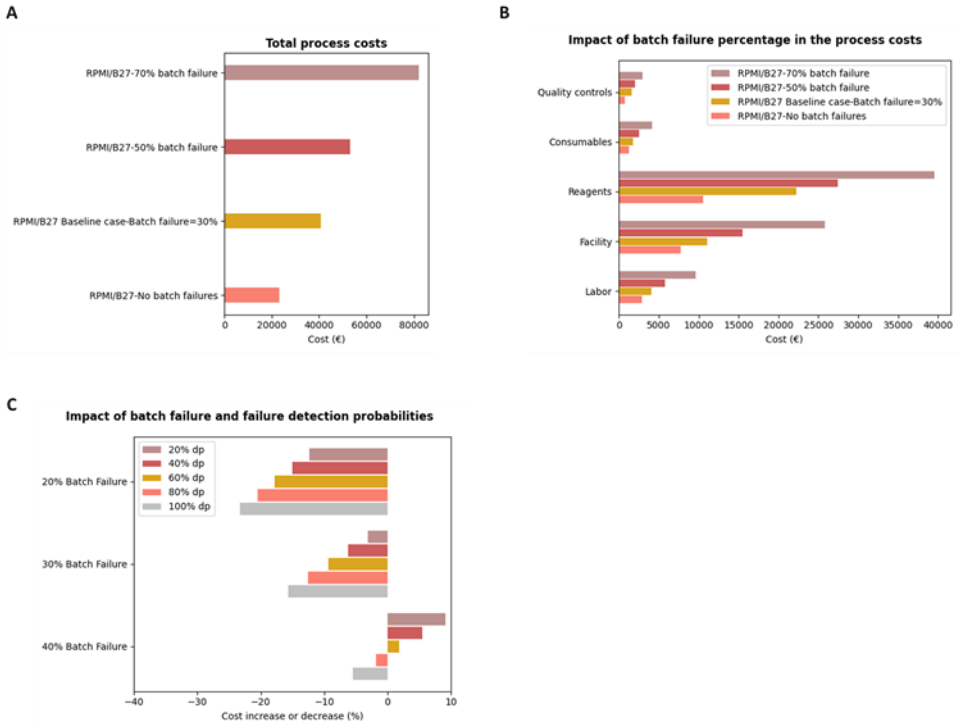

Figure 4.6: Impact of batch failure rates and failure detection probabilities in the process COGs. A-Total process costs for each batch failure rate scenario (in all cases, it was considered a 20% failure detection probability). B-Breakdown of bioprocess costs per step for each batch failure rate scenario. C-Impact of variation of batch failure rate and failure detection probability in the variation of process COGs in relation to the case of a process with 30% probability of batch failure and no failure detection probability. dp- failure detection probability

The total process costs of a process with 70%, 50%, 30% and no batch failures is 82058 €, 53195 €, 40826 € and 23188 €, respectively (Figure 4.6A). Therefore, batch failures have a significant impact on bioprocess total cost. If there were no batch failures, bioprocess total cost would be 43% less than the baseline process cost. On the other hand, if there were a 50% and 70% batch failure rate, bioprocess total costs would be 30% and 101% higher than the baseline process cost, respectively. The responsible factors for the difference in process costs between different batch failure rate scenarios are quality controls, consumables and reagents (Figure 4.6B), whose cost increases proportionally to the failure rate. The higher the batch failure rate, the greater is the number of extra batches that have to be carried out to compensate for those that failed, which entails high costs associated with reagents.

Figure 4.6C demonstrates the importance of investing in process quality controls in order to lower the batch failure rate and increase the failure detection probability by these quality controls. It is possible to observe that the increase in the failure detection probability leads to a significant reduction in process costs in relation to a process with a 30% batch failure and no failure detection, except for the case of processes with 40% batch failure and 20%, 40% and 60% failure detection probabilities. As for the remaining cases, there is a significant reduction in process costs; this reduction is greater the lower is batch failure probability and the higher the failure detection probability. Therefore, the highest cost reduction happens for a process with 20% batch failure rate and 100% failure detection probability; in this case, there is a cost reduction of about 23% in comparison with a process with 30% batch failure and no failure detection probability.

This study shows the importance of investing in quality controls to drive down COGs, because less batch failures and a higher failure detection probability lead to lower expenditures on reagents, which are the main cost drivers of the process.

4.1.2.5 Estimation of the total bioprocess cost

This thesis focused on the cost analysis of the differentiation stage of a bioprocess for autologous CM generation from hiPSC. While the estimation of costs for the expansion phase of hiPSCs aggregates is out of the scope of this thesis, these costs must be taken into consideration when estimating the COGs of the manufacturing of hiPSC-CMs. Unpublished data from SCERG (William Salvador MSc thesis), indicate that the COGs of expanding hiPSCs aggregates in VWBRs, using the standard commercially available medium mTesR1, up to the required cell number per donor for cardiac differentiation is about 32000 €. Adding this cost to the COGs of differentiating these hiPSC aggregates into pure and mature hiPSC-CMs (40826 €, baseline scenario) results in a total cost per donor, to reach the target CM number of 1×10^9 cells, of around 70000 € (i.e 70 € per million CMs). Assuming that COGs is 25% of the final price of a vial of cryopreserved CMs [108], the final price would be 280 € per million CMs. This is in line with reported prices for hiPSC-CMs in the market; FUJIFILM sells vials of 1×10^6 CMs (iCell Cardiomyocytes) at 495 $ (around 422€ as of September 2021) [132]; AXOL sells hiPSC-derived ventricular CMs at 280€/million cells [133]. It is important to note that reprogramming costs were not included in the calculation of the COGs for the production of autologous hiPSC-CMs in VWBRs.

4.1.3 Comparison of autologous vs. allogeneic process COGs at different production scales

In this section, the impact in process COGs of the transfer from an autologous therapy to an allogeneic therapy at different production scales is assessed. The different production scales correspond to 6, 12 and 18 parallel processes, which means that 6, 12 and 18 batches, respectively, are conducted at the same time for each production scale. In autologous cell therapy modalities, each batch produces cells to treat one patient, so the number of parallel processes corresponds to the maximum number of doses produced in a facility run. As for allogeneic modalities, the entire bioreactor working volume can be used to produce many patient doses, which means that higher number of doses can be produced at each facility full capacity than for autologous processes: 8, 17 and 26 doses for 6, 12 and 18 parallel processes, respectively. Model input parameters correspond to the ones used as default by the bioprocess economics model (Table 3.1).

Figure 4.7A shows the comparison of total costs per dose for each therapy modality at each production scale and Figure 4.7B depicts the breakdown of process costs per category for autologous and allogeneic therapies at a production scale of 6 parallel processes.

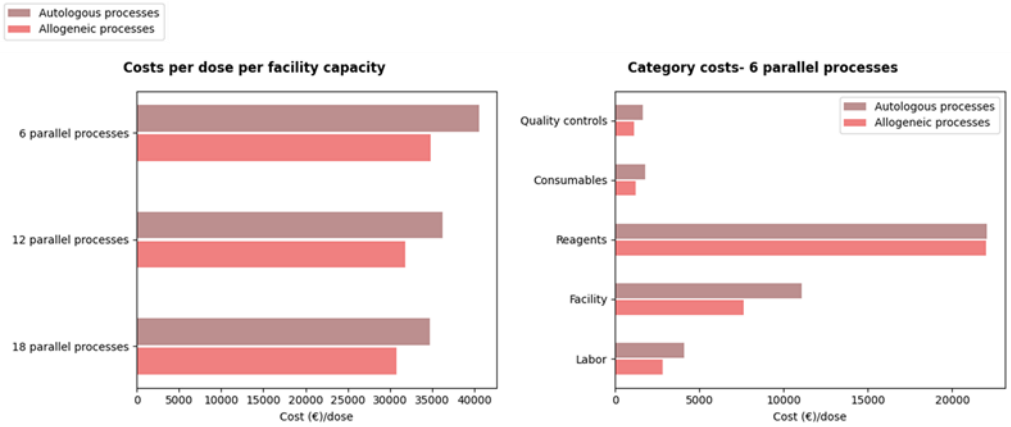

Figure 4.7: Impact of cell therapy modality (autologous vs. allogeneic) and production scale on the process COGs. A-COGs per dose for autologous and allogeneic processes at a production scale of 6, 12 and 18 parallel processes. B-Breakdown of process costs per category (quality controls, consumables, reagents, facility and labor) for autologous and allogeneic therapies at a production scale of 6 parallel processes.

In Figure 4.7A, it can be observed that the cost per dose for allogeneic processes is always lower than the cost per dose for autologous processes for each different scale. The COGs/dose for autologous therapies are 40602 €, 36207 € and 34743 € for 6, 12 and 18 parallel processes, respectively, and the COGs/dose for allogeneic therapies are 37865 €, 32535 € and 30895 € for 6, 12 and 18 parallel processes, respectively, which represent a 7%, 10% and 11% cost decrease in allogeneic scenarios in comparison with autologous scenarios. It can also be noticed that, as the production scale increases, the COGs/dose become lower for both therapy modalities, which is caused by lower facility costs per dose.

As the production scale increases the facility remains the same, except for the number of 3L VWBRs that increases according to the number of parallel processes, thereby resulting in costs being more spread out per dose. For autologous processes, there is a reduction in COGs/dose of 11% from 6 parallel processes to 12 parallel processes and of 14% to 18 parallel processes. As for allogeneic processes, there is a reduction in COGs/dose of 14% from 6 parallel processes to 12 parallel processes and of 18% to 18 parallel processes.

Figure 4.7B represents the differences in COGs/dose breakdown per category between the autologous and allogeneic processes for 6 parallel processes. The other production scales follow a similar pattern. Overall, the production of allogeneic therapies results in lower COGs/dose for each category at every scale. Quality control, consumables, facility and labor costs are equal for both scenarios at the same scale because the number of bioreactors and workers is equivalent and quality controls have a fixed cost per batch. However, these costs are spread by a higher number of doses in the allogeneic setting, resulting in lower COGs/dose in these categories. Total reagents cost is higher in allogeneic settings due to the higher number of doses produced. However, since quality control costs depend on the number of bioreactors and not on the number of produced doses, reagents costs per dose also decrease because of the lower quality controls costs per dose.

These results show that the production of allogeneic therapies is cheaper than autologous processes and that the cost per dose is more accessible per patient in the former context. Allogeneic therapies using hiPSC-CMs are particularly relevant to treat patients who suffered myocardial infarction, due to the high prevalence of this disease and the possible role of hiPSC-CMs in the heart's remuscularization, as suggested from some clinical studies using animal models (see Section 1.3.6). HLA-matched allogeneic cells can be used to produce large cell banks, allowing the existence of off-the-shelf products to treat HLA-compatible patients. For instance, it has been reported that the generation of 50 hiPSC lines would be sufficient to cover 90% of the Japanese population in the treatment of several diseases by differentiating these lines into several cell types, including hiPSC-CMs. [99] Although HLA-matching might reduce the intensive use of immunosupressive agents [99] and the cost per dose of allogeneic cell therapies is lower, the long-term cost effectiveness of each cell therapy must be evaluated, as in allogeneic therapies there are medical costs associated with immunosuppressive drugs, whereas in autologous therapies there is no risk of immunorejection due to the fact that patients' own cells are used.

4.1.4 Conclusions

The present study has demonstrated the importance of using bioprocess economics models as a decision tool to conduct the production of hiPSC-CMs in VWBRs.

The COGs of the baseline scenario was estimated to be 40826 € and the main process cost drivers were shown to be the reagents, for which the maturation medium accounts the most, and facility. Thus, in the establishment of a process of this type, which relies on frequent medium exchanges, it will be important to assess the reduction of the frequency and percentage of medium exchanges without compromising cell quality and viability in order to drive process costs down. Another factor that could drive process costs down would be using the facility for multiple research activities besides the production of autologous

hiPSC-CMs.

Biological variability was introduced in the model to account for differences in the process COGs derived from donor-to-donor biological differences (Table 3.2). Variations in differentiation, purification, harvesting and cryopreservation yield were considered, being differentiation yield the most variable factor. Cardiac differentiation is highly dependent on the cell line, which affects differentiation efficiency and cellular growth. [67] Apart from that, the cell density, aggregate size and timing and dose of supplementation with small molecules, namely CHIR and IWP-2, have an effect on hiPSC cardiac differentiation. [68] The increase in bioprocess yield resulted in lower process COGs due to lower working volumes required and, therefore, less expenses with reagents.

From this study it was concluded that improving the medium performance reduced the overall process costs up to a certain point: when an increase in medium performance causes a reduction in the working volume, the process costs decrease, since the expenses with reagents are reduced; however, increasing medium performance up to the point where the necessary working volume is less than the minimum working volume entails increasing costs with excess production and higher cryopreservation medium expenses. Changes in cell density could be evaluated in order for the working volume to be equal or higher than the bioreactor minimum working volume in order to avoid excess production, but the effects of changing this parameter must be assessed, since this parameter can compromise differentiation efficiency.

From the aforementioned case studies, it can be concluded that parameters that affect the required working volume should be carefully studied and validated in order to reduce reagents associated costs while maintaining cell quality and viability. These include medium feeding regimes, cellular density, medium performance in terms of cell growth and viability and process yields.

Batch failure rates were found to have a significant impact in total bioprocess costs, because a hypothetical process with no batch failures would cost 43% less than the baseline case (Figure 4.6A) . Failure detection probabilities also have a significant impact on process costs; the higher the failure detection probability is and the lower the batch failure detection rate is, the higher is the reduction in process costs. This is because of the lower number of batches that have to be carried out to compensate for the failing ones and, therefore, less expenses with quality controls, consumables and reagents. Thus, investing in quality controls is important to drive down the process COGs, since it would decrease batch failure rates and increase batch failure detection probabilities.

The production of allogeneic therapies resulted in COGs/dose at the production scales of 6, 12 and 18 parallel processes. This has to do with a better spread of quality control, consumables, facility, reagents and labor costs by the number of produced doses. However, the long-term cost effectiveness of each cell therapy must be evaluated, as in allogeneic therapies there are medical costs associated with immunosuppressive drugs, whereas in autologous therapies there is no risk of immunorejection due to the fact that patients' own cells are used.

4.2 Generation of hiPSC-CMs as monolayers via modulation of the canonical Wnt pathway

Gibco hiPSCs were cultured in mTesR^{TM}1, E8^{TM} or B8 medium and differentiated during 15 days in RPMI/B27 or CDM3 through the temporal modulation of the canonical Wnt signalling pathway (see Figure 3.2), as described by Lian et. al. [72]. Cell characterization was performed based on the expression of the intracellular marker cTnT via flow cytometry after differentiation. cTnT is an important cardiac marker, as it is involved in the calcium-mediated interaction between actin and myosin, which is responsible for cardiomyocyte contraction. [134] [135] The expression of pluripotent markers, such as transcription factors OCT4 and SOX2 and cell surface markers Tra-1-60 and SSEA-4, was not analyzed before starting differentiation due to insufficient cell numbers.

Figure 4.8 shows bright field microscopy images of cells at differentiation day 15 for each condition.

Figure 7.1 depicts the expression of cTnT marker, analyzed by flow cytometry, of cells grown in each culture condition at differentiation day 15.

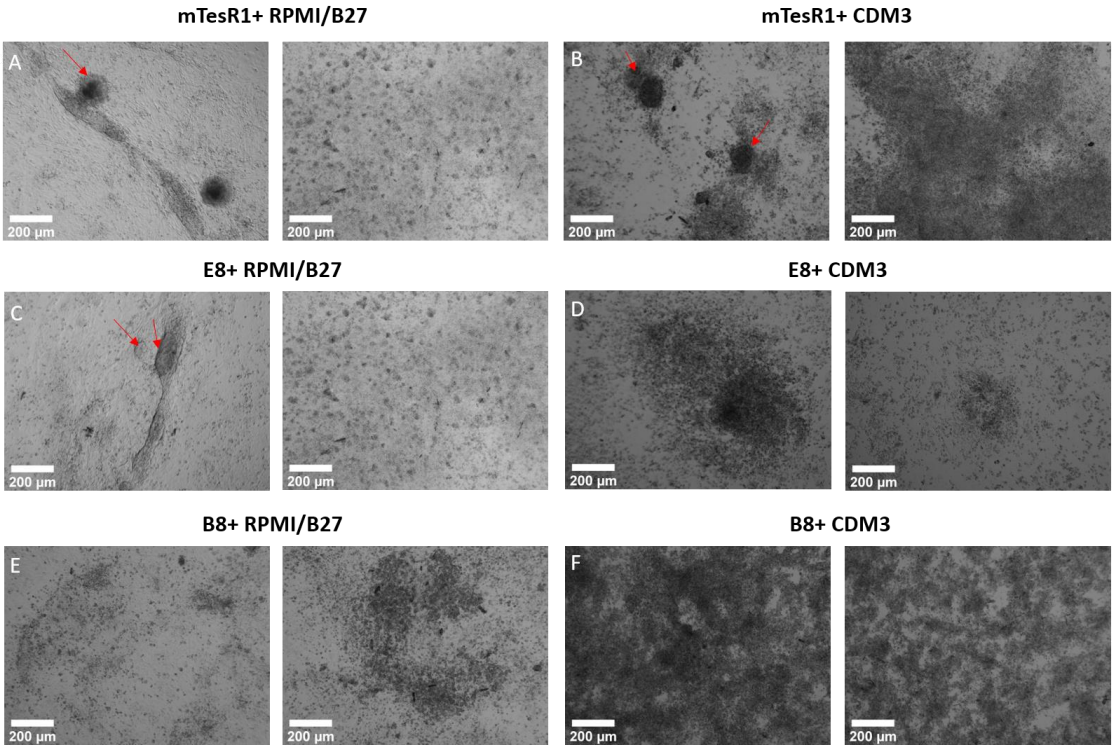

Figure 4.8: Bright field microscopy images of cells at differentiation day 15 for each condition. Gibco hiPSCs were cultured in mTesR^{TM}1 medium, E8^{TM} or B8 and differentiated during 15 days in RPMI/B27 or CDM3 through the temporal modulation of the canonical Wnt signalling pathway. Beating aggregates were first observed at day 14 for mTeSR1+RPMI/B27 condition and at day 15 for mTeSR1+CDM3 and E8+RPMI/B27 conditions. Red arrows represent areas of contracting cells.

Table 4.1 summarizes the results of the cardiac differentiation experiment for each culture condition.

Table 4.1: Summary of the results obtained for each culture condition of the differentiation experiment. Gibco hiPSCs were expanded in mTesR1, E8 or B8 medium and were seeded at a density of 400,000 cells/mL to be differentiated either in RPMI/B27 or CDM3 medium into CMs via the temporal modulation of the wingless-type mouse mammary tumour virus integration site (WNT) signalling pathway. The first day of spontaneous contraction, the beating rate of cells and the percentage of $cTnT^+$ cells, which was evaluated through flow cytometry, is presented for each condition. The beating rate of cells was measured from 2, 5, and 3 beating colonies for mTeSR1+RPMI/B27, mTeSR1+CDM3 and E8+RPMI/B27, respectively, which are presented as mean ±standard deviation. bpm- beatings per minute.

Condition	First day of spontaneous contraction	Beating rate (bpm)	% $cTnT^+$ cells
mTeSR1+RPMI/B27	14	7 ±1 bpm	15.56 %
mTeSR1+CDM3	15	43 ±5 bpm	13.50%
E8+RPMI/B27	15	5 ±3 bpm	17.70 %
E8+CDM3	-	-	32.60 %
B8+RPMI/B27	-	-	18.50 %
B8+CDM3	-	-	14.35 %

During the 15 days of the cardiac differentiation protocol, spontaneous contractions were only observed for cells expanded under mTesR™1 medium and differentiated in RPMI/B27 or CDM3 and for cells expanded using E8™ medium and differentiated in RPMI/B27. As for the remaining conditions, no spontaneous contractions were observed and extensive cell death occurred, as it can be observed in Figure 4.8. Spontaneous contractions were first observed at day 14 for mTeSR1+RPMI/B27 condition and at day 15 for mTeSR1+CDM3 and E8+RPMI/B27 conditions. Nevertheless, even for those conditions, extensive cell death could be observed. Moreover, contracting regions were small and the cells tended to group as aggregates instead of forming a monolayer of beating cells (Figure 4.8A, B and C, left). This might suggest poor cell survival and adhesion to Matrigel™ substrate.

In fact, very low percentages of $cTnT^+$ cells were obtained in those conditions which presented spontaneous contractions, which were 15.6 %, 13.5 % and 17.7 % for mTeSR1+RPMI/B27, mTeSR1+CDM3 and E8+RPMI/B27 conditions (Table 4.1, Figure 7.1). These results are not in line with the results obtained by Lian and co-workers in the original protocol, which generated 80-98% $cTnT^+$ cells after 2 weeks. Another significant difference is the first day of observed spontaneous contractions, which were observed at day14 or 15 in the present work and between day 8 and 10 (depending on the cell line) in Lian and colleagues' work. Although spontaneous contractions were not observed in the remaining conditions, flow cytometry results indicate the presence of 32.6 %, 18.5 % and 14.4 % (Table 4.1, Figure 7.1) $cTnT^+$ cells for E8+CDM3, B8+RPMI/B27 and B8+CDM3 conditions, respectively. It is important to note, however, that very few events were captured for CDM3 conditions and, therefore, these values have to be confirmed with further experiments.

The beating rate of differentiated cells was 7 ±1, 43 ±5, 5 ±3 beatings per minute (bpm) in all the experiments for mTeSR1+RPMI/B27, mTeSR1+CDM3 and E8+RPMI/B27 conditions, respectively. Adult cardiomyocytes generally have a beating rate between 60 and 90 bpm. [136] Therefore, the generated cardiomyocytes had an immature contractile phenotype after 15 days. The beating rate for the mTeSR1+CDM3 condition was significantly higher than in mTeSR1+RPMI/B27 and E8+RPMI/B27, which

suggests that cardiomyocytes in the former condition may have a higher degree of maturation.

Despite the low efficiency in comparison to the original protocol, the present results suggest that different culture medium formulations in expansion and differentiation affect differentiation efficiency. It is known that the extracellular matrix and its properties, such as stiffness and biochemical composition, soluble biochemical cues and cell-cell interactions act in concert to regulate cell fate. [137] Thus, it is presumable that the interaction between cells, Matrigel and different biochemical cues present in each culture medium led to different differentiation outcomes. Matrigel is derived from the ECM produced by Engelbreth-Holm-Swarm mouse sarcoma cells and, as a consequence, it is variable in its mechanical and biochemical properties between batches and within a single batch, which can lead to a lack of reproducibility between experiments. This might explain, in part, the far lower number of $cTnT^+$ cells in this work than in the original protocol, even for the mTeSR1+RPMI/B27 condition (15.6 % vs. 80-98 % $cT\ nT^+$ cells), in which the same culture media were used. Unlike Matrigel, synthetic substrates are chemically defined and can be modified for their mechanical, physical and biological properties, which would allow for more reproducible results and a better comparison of the differentiation efficiency in different culture media. [138]

Apart from the culture medium and substrate in which cells grow, other factors can affect cardiac differentiation efficiency, such as bulk cell density and small molecule CHIR99021 concentration. Kempf et. al. showed that different bulk cell densities and concentrations of the chemical WNT pathway activator CHIR99021 guide hPSCs towards different cell fates along the primitive streak (definitive endoderm, cardiac mesoderm and presomitic mesoderm) through different paracrine microenvironments. [139] Therefore, these parameters should be optimized for each culture condition. Recently, a study revealed that cardiac differentiation protocols using an initial high cell density might benefit from a negative feedback on Wnt signaling by the secretion of auto/paracrine factors that inhibit Wnt pathway (e.g DKK1, DKK4, Cerberus) and suppress anti-cardiac mesoderm genes, while at low cell densities (1% confluence) these factors are not present in sufficient amount to suppress anti-cardiac mesoderm. Performing an earlier inhibition of the canonical Wnt pathway in low cell density cultures, by adding IWP2 to the culture from day 1 to day 3 instead of day 3 to day 5, allowed the inhibition of anti-cardiac mesoderm genes and promoted the expression of cardiac genes, improving differentiation efficiency from 4% to 80%. [140] It is possible that, in the present experiment, the negative feedback on Wnt signaling caused by the high cell density effect was neglected due to the low cell survival in Matrigel substrate since the beginning of the experiment. Earlier supplementation of IWP2 to the culture could have probably resulted in better differentiation efficiencies.

4.2.1 Conclusions

hiPSCs present an enormous potential for regenerative medicine, drug screening and disease modelling, due to their unique features. Contrary to hESCs, they can be reprogrammed from adult somatic cells, which avoids ethical concerns, and personalized medicine can be accomplished by the generation of patient-specific cells. Particularly, hiPSC-CMs present an exciting possibility for cardiac cell-based therapies because of the high prevalence of CVDs and long wait-lists for cardiac transplant, as high numbers of cells can be produced in a relatively short time. The human heart has a very limited regenerative capacity and it is incapable of restoring the high number of cells lost in a failing heart, about 1 billion cardiomyocytes. [13]

This part of the work aimed to assess the differentiation of hiPSC-CMs via temporal modulation of the canonical Wnt pathway in two different culture media (RPMI/B27 or CDM3), that had been previously expanded in three different culture media (mTesR1, E8 or B8). The comparison of different culture media formulations in terms of differentiation performance is particularly important from an economic perspective, since culture media are the main cost drivers of bioprocesses. The higher is the cardiomyocyte yield per hiPSC input, the lower the number of initial hiPSCs that is required and, therefore, less culture media volume is spent, which reduces the COGs. On the other hand, for prospective clinical applications it is crucial to validate xeno-free and chemically defined alternatives, which are safer and do not constitute risk of infection to patients with animal-derived components upon transplantation. Among the culture media tested, expansion media B8 and E8 and differentiation media CDM3 are xeno-free and chemically defined, while the other medium formulations are not xeno-free, as animal-derived components, such as bovine serum albumin, are present in mTesR1 and B27 supplement of RPMI 1640.

The results showed that the differentiation potential varied under the different culture medium formulations tested. However, one the main limitations of this work is the lack of replicates due to time constraints and insufficient supply of reagents due to the pandemics. More replicates would be necessary to obtain more robust conclusions. Another limitation is related to the use of Matrigel, which itself presents variable mechanical and biochemical properties within a single batch. In addition, Matrigel did not seem to properly support cell growth and adhesion, as cells tended to group as aggregates instead of forming monolayers during differentiation. Even in the expansion phase, a variable growth of hiPSCs was observed between passages, probably due to the variability of Matrigel, which made it impossible to collect some cells for analysis of pluripotency markers before starting differentiation. This variability and lack of cell adhesion to the substrate might explain the far lower percentage of $cTnT^+$ cells (up to 32.6 %) obtained than the 80-98 % $cTnT^+$ cells obtained by Lian. et. al. in the original protocol after 15 days of differentiation. [72] The use of chemically defined synthetic substrates would allow the comparison of different culture media performances without biased factors arising from substrate inherent variability. For example, laminin-based matrices have been demonstrated to maintain long-term adhesion during CDM3 cardiac differentiation. [76]

Overall, it was demonstrated that the interaction between cells, Matrigel and different biochemical cues present in each culture medium can lead to different cardiac differentiation outcomes, either in terms of the percentage of $cTnT^+$ cells or qualitative maturity degree assessed by the number of bpm.

5 | Future work

The bioprocess economic model developed in this work was of great value to provide an estimate of the COGs of producing hiPSC-CMs in 3L VWBRs. However, an extensive process knowledge is still required to turn this model more reliable. Important parameters, such as process step yields and fold increase, were assumed from the few studies reporting the differentiation of hiPSC into CMs via modulation of the canonical Wnt pathway in STBRs, since no studies of this process in VWBRs were published yet. Because of this gap in the literature, the present model was kept deterministic and some sensitivity analysis were performed to understand the impact of parameters in the COGs. In stochastic models, however, input parameters are randomly sampled from probabilistic distributions, which give a better idea of the most likely range where the process costs fall. In order to develop a stochastic economic model, it would be essential to determine the probability distributions of process inputs, which is only feasible after sufficient data is generated from the cardiac differentiation of hiPSCs in VWBRs.

Regarding the in-lab generation of hiPSC-CMs as monolayers via modulation of the canonical Wnt pathway and the comparison of differentiation efficiency under different culture media formulations, more replicates and chemically defined substrates would be desirable to draw proper conclusions. It would also be interesting to assess the robustness of these conclusions when using different cell lines. Furthermore, the study of differentiation efficiency under different culture medium formulations together with other factors that affect the differentiation efficiency of hiPSCs into CMs, such as different concentration and timing of modulation with small molecules and bulk cell density, would be of value to further optimize cardiac differentiation for each condition in monolayer culture. The same type of optimization could be done for 3D culture and differentiation of cells as aggregates, as this culture format better resembles the cells' natural microenvironment and has been proved to allow for more efficient and faster differentiation in comparison to 2D cultures. In these culture systems, it is essential to control aggregate size due to diffusional limitations of nutrients, growth factors and oxygen in the center of the aggregates. VWBRs are promising platforms for cardiac differentiation, as they allow a gentle mixing and control of aggregate size under low shear stress conditions.

6 | Bibliography

1. Zakrzewski, W., Dobrzyński, M., Szymonowicz, M. & Rybak, Z. Stem cells: past, present, and future. *Stem cell research & therapy* **10,** 1-22 (2019).
2. Singh, V. K., Kalsan, M., Kumar, N., Saini, A. & Chandra, R. Induced pluripotent stem cells: applications in regenerative medicine, disease modeling, and drug discovery. *Frontiers in cell and developmental biology* **3,** 2 (2015).
3. Prodinger, C. M., Reichelt, J., Bauer, J. W. & Laimer, M. Current and future perspectives of stem cell therapy in dermatology. *Annals of dermatology* **29,** 667-687 (2017).
4. Evans, M. J. & Kaufman, M. H. Establishment in culture of pluripotential cells from mouse embryos. *nature* **292,** 154-156 (1981).
5. Martin, G. R. Isolation of a pluripotent cell line from early mouse embryos cultured in medium conditioned by teratocarcinoma stem cells. *Proceedings of the National Academy of Sciences* **78,** 7634-7638 (1981).
6. Shapiro, T. J. I.-E. J., JJ, S. W. M. S., *et al.* Embryonic stem cell lines derived from human blastocysts. *Science* **282,** 1145-7 (1998).
7. Takahashi, K. & Yamanaka, S. Induction of pluripotent stem cells from mouse embryonic and adult fibroblast cultures by defined factors. *cell* **126,** 663-676 (2006).
8. Takahashi, K. *et al.* Induction of pluripotent stem cells from adult human fibroblasts by defined factors. *cell* **131,** 861-872 (2007).
9. Yu, J. *et al.* Induced pluripotent stem cell lines derived from human somatic cells. *science* **318,** 1917-1920 (2007).
10. Daley, G. Q. & Scadden, D. T. Prospects for stem cell-based therapy. *Cell* **132,** 544-548 (2008).
11. Shi, Y., Inoue, H., Wu, J. C. & Yamanaka, S. Induced pluripotent stem cell technology: a decade of progress. *Nature reviews Drug discovery* **16,** 115-130 (2017).
12. Mahla, R. S. Stem cells applications in regenerative medicine and disease therapeutics. *International journal of cell biology* **2016** (2016).
13. Ieda, M. & Zimmermann, W.-H. *Cardiac Regeneration* (Springer, 2017).
14. Cyranoski, D. 'Reprogrammed'stem cells approved to mend human hearts for the first time. *Nature* **557,** 619-619 (2018).

15. Sun, C. & Kontaridis, M. I. Physiology of cardiac development: from genetics to signaling to therapeutic strategies. *Current opinion in physiology* **1,** 123-139 (2018).

16. Tan, C. M. J. & Lewandowski, A. J. The transitional heart: from early embryonic and fetal development to neonatal life. *Fetal diagnosis and therapy* **47,** 373-386 (2020).

17. Paige, S. L., Plonowska, K., Xu, A. & Wu, S. M. Molecular regulation of cardiomyocyte differentiation. *Circulation research* **116,** 341-353 (2015).

18. Bulatovic, I., Månsson-Broberg, A., Sylvén, C. & Grinnemo, K.-H. Human fetal cardiac progenitors: the role of stem cells and progenitors in the fetal and adult heart. *Best Practice & Research Clinical Obstetrics & Gynaecology* **31,** 58-68 (2016).

19. Günthel, M., Barnett, P. & Christoffels, V. M. Development, proliferation, and growth of the mammalian heart. *Molecular Therapy* **26,** 1599-1609 (2018).

20. Burridge, P. W., Sharma, A. & Wu, J. C. Genetic and epigenetic regulation of human cardiac reprogramming and differentiation in regenerative medicine. *Annual review of genetics* **49,** 461-484 (2015).

21. Di Baldassarre, A., Cimetta, E., Bollini, S., Gaggi, G. & Ghinassi, B. Human-induced pluripotent stem cell technology and cardiomyocyte generation: Progress and clinical applications. *Cells* **7,** 48 (2018).

22. Mummery, C. L. *et al.* Differentiation of human embryonic stem cells and induced pluripotent stem cells to cardiomyocytes: a methods overview. *Circulation research* **111,** 344-358 (2012).

23. Hartman, M. E., Dai, D.-F. & Laflamme, M. A. Human pluripotent stem cells: Prospects and challenges as a source of cardiomyocytes for in vitro modeling and cell-based cardiac repair. *Advanced drug delivery reviews* **96,** 3-17 (2016).

24. *Cardiovascular diseases (CVDs)* https://www.who.int/news-room/fact-sheets/detail/cardiovascular-diseases-(cvds) (2021).

25. Choi, D., Hwang, K.-C., Lee, K.-Y. & Kim, Y.-H. Ischemic heart diseases: current treatments and future. *Journal of controlled release* **140,** 194-202 (2009).

26. Zhao, W., Zhao, J. & Rong, J. Pharmacological Modulation of Cardiac Remodeling after Myocardial Infarction. *Oxidative Medicine and Cellular Longevity* **2020** (2020).

27. Minicucci, M. F., Azevedo, P. S., Polegato, B. F., Paiva, S. A. & Zornoff, L. A. Heart failure after myocardial infarction: clinical implications and treatment. *Clinical cardiology* **34,** 410-414 (2011).

28. Zannad, F., Agrinier, N. & Alla, F. Heart failure burden and therapy. *Europace* **11,** v1-v9 (2009).

29. *Types of Heart Medications* https://www.heart.org/en/health-topics/heart-attack/treatment-of-a-heart-attack/cardiac-medications (2020).

30. Beaupré, R. A. & Morgan, J. A. *Donation after cardiac death: a necessary expansion for heart transplantation* in *Seminars in thoracic and cardiovascular surgery* **31** (2019), 721-725.

31. Funakoshi, S. *et al.* Enhanced engraftment, proliferation and therapeutic potential in heart using optimized human iPSC-derived cardiomyocytes. *Scientific reports* **6,** 1-14 (2016).

32. Wu, S. M., Chien, K. R. & Mummery, C. Origins and fates of cardiovascular progenitor cells. *Cell* **132,** 537-543 (2008).

33. Birket, M. J. & Mummery, C. L. Pluripotent stem cell derived cardiovascular progenitors-a developmental perspective. *Developmental biology* **400,** 169-179 (2015).

34. Cyganek, L., Chen, S., Borchert, T. & Guan, K. Cardiac progenitor cells and their therapeutic application for cardiac repair (2013).

35. Witman, N., Zhou, C., Beverborg, N. G., Sahara, M. & Chien, K. R. *Cardiac progenitors and paracrine mediators in cardiogenesis and heart regeneration* in *Seminars in cell & developmental biology* **100** (2020), 29-51.

36. Später, D. *et al.* A HCN4+ cardiomyogenic progenitor derived from the first heart field and human pluripotent stem cells. *Nature cell biology* **15,** 1098-1106 (2013).

37. Elsheikh, E., Genead, R., Mansson-Broberg, A., Bulatovic, I., Ljung, K., *et al.* Human Embryonic Non-haematopoietic SSEA-1+ Cells are Cardiac Progenitors Expressing Markers of Both the First and Second Heart Field. *J Cytol Histol* **4,** 192 (2013).

38. Menasché, P. *et al.* Human embryonic stem cell-derived cardiac progenitors for severe heart failure treatment: first clinical case report. *European heart journal* **36,** 2011-2017 (2015).

39. Yang, L. *et al.* Human cardiovascular progenitor cells develop from a KDR+ embryonic-stem-cell-derived population. *Nature* **453,** 524-528 (2008).

40. Chong, J. J. *et al.* Progenitor cells identified by PDGFR-alpha expression in the developing and diseased human heart (2013).

41. Skelton, R. J. *et al.* SIRPA, VCAM1 and CD34 identify discrete lineages during early human cardiovascular development. *Stem cell research* **13,** 172-179 (2014).

42. Bearzi, C. *et al.* Human cardiac stem cells. *Proceedings of the National Academy of Sciences* **104,** 14068-14073 (2007).

43. Van Berlo, J. H. *et al.* C-kit+ cells minimally contribute cardiomyocytes to the heart. *Nature* **509,** 337-341 (2014).

44. Sultana, N. *et al.* Resident c-kit+ cells in the heart are not cardiac stem cells. *Nature communications* **6,** 1-10 (2015).

45. Takamiya, M., Haider, K. H. & Ashraf, M. Identification and characterization of a novel multipotent sub-population of Sca-1+ cardiac progenitor cells for myocardial regeneration. *PLoS One* **6,** e25265 (2011).

46. Le, M. N. T. & Hasegawa, K. Expansion culture of human pluripotent stem cells and production of cardiomyocytes. *Bioengineering* **6,** 48 (2019).

47. Dakhore, S., Nayer, B. & Hasegawa, K. Human pluripotent stem cell culture: current status, challenges, and advancement. *Stem cells international* **2018** (2018).

48. Alexander, B. *Methods in iPSC Technology* (Advances in Stem Cell Biology, 2021).

49. Polanco, A., Kuang, B. & Yoon, S. Bioprocess Technologies that Preserve the Quality of iPSCs. *Trends in Biotechnology* (2020).

50. Serra, M., Brito, C., Correia, C. & Alves, P. M. Process engineering of human pluripotent stem cells for clinical application. *Trends in biotechnology* **30,** 350-359 (2012).

51. Villa-Diaz, L., Ross, A., Lahann, J. & Krebsbach, P. Concise review: the evolution of human pluripotent stem cell culture: from feeder cells to synthetic coatings. *Stem cells* **31,** 1-7 (2013).

52. Lambshead, J. W., Meagher, L., O'Brien, C. & Laslett, A. L. Defining synthetic surfaces for human pluripotent stem cell culture. *Cell Regeneration* **2,** 1-17 (2013).

53. Kropp, C., Massai, D. & Zweigerdt, R. Progress and challenges in large-scale expansion of human pluripotent stem cells. *Process Biochemistry* **59,** 244-254 (2017).

54. Rodrigues, C. A., Nogueira, D. E. & Cabral, J. M. Next-generation stem cell expansion technologies. *Cell and Gene Therapy Insights* **4,** 791-804 (2018).

55. Borys, B. S. *et al.* Overcoming bioprocess bottlenecks in the large-scale expansion of high-quality hiPSC aggregates in vertical-wheel stirred suspension bioreactors. *Stem Cell Research & Therapy* **12,** 1-19 (2021).

56. *Innovative Vertical-WheelTM technology* https://www.pbsbiotech.com/vertical-wheel.html.

57. Croughan, M., Giroux, D., Fang, D. & Lee, B. Novel single-use bioreactors for scale-up of anchorage-dependent cell manufacturing for cell therapies, 105-139 (2016).

58. *MagDrive Technology* https://www.pbsbiotech.com/magdrive.html.

59. *AirDrive Technology* https://www.pbsbiotech.com/airdrive.html.

60. Kuo, H.-H. *et al.* Negligible-cost and weekend-free chemically defined human iPSC culture. *Stem cell reports* **14,** 256-270 (2020).

61. Beers, J. *et al.* Passaging and colony expansion of human pluripotent stem cells by enzyme-free dissociation in chemically defined culture conditions. *Nature protocols* **7,** 2029-2040 (2012).

62. Rivera, T., Zhao, Y., Ni, Y. & Wang, J. Human-Induced Pluripotent Stem Cell Culture Methods Under cGMP Conditions. *Current Protocols in Stem Cell Biology* **54,** e117 (2020).

63. Nogueira, D. Engineering Characterisation of Bioreactors for Human Pluripotent Stem Cell Expansion and Cardiac Differentiation. *DBE, IST, Lisbon, PT, PhD dissertation* (2021).

64. Nogueira, D. E. *et al.* Strategies for the expansion of human induced pluripotent stem cells as aggregates in single-use Vertical-Wheel™ bioreactors. *Journal of biological engineering* **13,** 1-14 (2019).

65. Manstein, F. *et al.* High density bioprocessing of human pluripotent stem cells by metabolic control and in silico modeling. *Stem cells translational medicine* (2021).

66. Kempf, H., Andree, B. & Zweigerdt, R. Large-scale production of human pluripotent stem cell derived cardiomyocytes. *Advanced Drug Delivery Reviews* **96,** 18–30 (2016).

67. Laco, F. *et al.* Selection of human induced pluripotent stem cells lines optimization of cardiomyocytes differentiation in an integrated suspension microcarrier bioreactor. *Stem cell research & therapy* **11,** 1–16 (2020).

68. Halloin, C. *et al.* Continuous WNT control enables advanced hPSC cardiac processing and prognostic surface marker identification in chemically defined suspension culture. *Stem cell reports* **13,** 366–379 (2019).

69. Kehat, I. *et al.* Human embryonic stem cells can differentiate into myocytes with structural and functional properties of cardiomyocytes. *The Journal of clinical investigation* **108,** 407–414 (2001).

70. Laflamme, M. A. *et al.* Cardiomyocytes derived from human embryonic stem cells in pro-survival factors enhance function of infarcted rat hearts. *Nature biotechnology* **25,** 1015–1024 (2007).

71. Lian, X. *et al.* Robust cardiomyocyte differentiation from human pluripotent stem cells via temporal modulation of canonical Wnt signaling. *Proceedings of the National Academy of Sciences* **109,** E1848–E1857 (2012).

72. Lian, X. *et al.* Directed cardiomyocyte differentiation from human pluripotent stem cells by modulating Wnt/β-catenin signaling under fully defined conditions. *Nature protocols* **8,** 162–175 (2013).

73. Cao, N. *et al.* Highly efficient induction and long-term maintenance of multipotent cardiovascular progenitors from human pluripotent stem cells under defined conditions. *Cell research* **23,** 1119–1132 (2013).

74. Moore, G. E., Gerner, R. E. & Franklin, H. A. Culture of normal human leukocytes. *Jama* **199,** 519–524 (1967).

75. Zhang, J. *et al.* Extracellular matrix promotes highly efficient cardiac differentiation of human pluripotent stem cells: the matrix sandwich method. *Circulation research* **111,** 1125–1136 (2012).

76. Burridge, P. W. *et al.* Chemically defined generation of human cardiomyocytes. *Nature methods* **11,** 855–860 (2014).

77. Habas, R. & Dawid, I. B. Dishevelled and Wnt signaling: is the nucleus the final frontier? *Journal of biology* **4,** 1–4 (2005).

78. Clevers, H. Wnt/β-catenin signaling in development and disease. *Cell* **127,** 469–480 (2006).

79. Nusse, R. & Clevers, H. Wnt/β-catenin signaling, disease, and emerging therapeutic modalities. *Cell* **169,** 985–999 (2017).

80. Ban, K., Bae, S. & Yoon, Y.-s. Current strategies and challenges for purification of cardiomyocytes derived from human pluripotent stem cells. *Theranostics* **7,** 2067 (2017).

81. Xu, C., Police, S., Rao, N. & Carpenter, M. K. Characterization and enrichment of cardiomyocytes derived from human embryonic stem cells. *Circulation research* **91,** 501–508 (2002).

82. Klug, M. G., Soonpaa, M. H., Koh, G. Y., Field, L. J., *et al.* Genetically selected cardiomyocytes from differentiating embronic stem cells form stable intracardiac grafts. *The Journal of clinical investigation* **98,** 216–224 (1996).

83. Dubois, N. C. *et al.* SIRPA is a specific cell-surface marker for isolating cardiomyocytes derived from human pluripotent stem cells. *Nature biotechnology* **29,** 1011–1018 (2011).

84. Tohyama, S. *et al.* Distinct metabolic flow enables large-scale purification of mouse and human pluripotent stem cell-derived cardiomyocytes. *Cell stem cell* **12,** 127–137 (2013).

85. Miki, K. *et al.* Efficient detection and purification of cell populations using synthetic microRNA switches. *Cell stem cell* **16,** 699–711 (2015).

86. Ahmed, R. E., Anzai, T., Chanthra, N. & Uosaki, H. A brief review of current maturation methods for human induced pluripotent stem cells-derived cardiomyocytes. *Frontiers in cell and developmental biology* **8,** 178 (2020).

87. Karbassi, E. *et al.* Cardiomyocyte maturation: advances in knowledge and implications for regenerative medicine. *Nature Reviews Cardiology* **17,** 341–359 (2020).

88. Kamakura, T. *et al.* Ultrastructural maturation of human-induced pluripotent stem cell-derived cardiomyocytes in a long-term culture. *Circulation Journal* **77,** 1307–1314 (2013).

89. Fukushima, H. *et al.* Specific induction and long-term maintenance of high purity ventricular cardiomyocytes from human induced pluripotent stem cells. *PloS one* **15,** e0241287 (2020).

90. Horikoshi, Y. *et al.* Fatty acid-treated induced pluripotent stem cell-derived human cardiomyocytes exhibit adult cardiomyocyte-like energy metabolism phenotypes. *Cells* **8,** 1095 (2019).

91. Cao, N. *et al.* Ascorbic acid enhances the cardiac differentiation of induced pluripotent stem cells through promoting the proliferation of cardiac progenitor cells. *Cell research* **22,** 219–236 (2012).

92. Parikh, S. S. *et al.* Thyroid and glucocorticoid hormones promote functional T-tubule development in human-induced pluripotent stem cell-derived cardiomyocytes. *Circulation research* **121,** 1323–1330 (2017).

93. Ribeiro, A. J. *et al.* Contractility of single cardiomyocytes differentiated from pluripotent stem cells depends on physiological shape and substrate stiffness. *Proceedings of the National Academy of Sciences* **112,** 12705–12710 (2015).

94. Branco, M. A. *et al.* Transcriptomic analysis of 3D cardiac differentiation of human induced pluripotent stem cells reveals faster cardiomyocyte maturation compared to 2D culture. *Scientific reports* **9,** 1–13 (2019).

95. Ronaldson-Bouchard, K. *et al.* Advanced maturation of human cardiac tissue grown from pluripotent stem cells. *Nature* **556,** 239–243 (2018).

96. Duelen, R. & Sampaolesi, M. Stem cell technology in cardiac regeneration: a pluripotent stem cell promise. *EBioMedicine* **16,** 30–40 (2017).

97. Mazzola, M. & Di Pasquale, E. Toward cardiac regeneration: combination of pluripotent stem cell-based therapies and bioengineering strategies. *Frontiers in Bioengineering and Biotechnology* **8,** 455 (2020).

98. Redd, M. A. *et al.* Patterned human microvascular grafts enable rapid vascularization and increase perfusion in infarcted rat hearts. *Nature communications* **10,** 1-14 (2019).

99. Hulot, J.-S. *et al.* Considerations for pre-clinical models and clinical trials of pluripotent stem cell-derived cardiomyocytes. *Stem cell research & therapy* **5,** 1-7 (2014).

100. Garbern, J. C., Escalante, G. O. & Lee, R. T. Pluripotent stem cell-derived cardiomyocytes for treatment of cardiomyopathic damage: current concepts and future directions. *Trends in cardiovascular medicine* **31,** 85-90 (2021).

101. Lipsitz, Y. Y., Timmins, N. E. & Zandstra, P. W. Quality cell therapy manufacturing by design. *Nature biotechnology* **34,** 393-400 (2016).

102. Lipsitz, Y. Y. *et al.* A roadmap for cost-of-goods planning to guide economic production of cell therapy products. *Cytotherapy* **19,** 1383-1391 (2017).

103. Luo, Y., Kurian, V. & Ogunnaike, B. A. Bioprocess systems analysis, modeling, estimation, and control. *Current Opinion in Chemical Engineering* **33,** 100705 (2021).

104. Karnieli, O. & Gur-Lavie, B. Cell therapy: early process development and optimization of the manufacturing process are critical to ensure viability of the product, quality, consistency and cost efficiency. *Journal of Commercial Biotechnology* **21,** 83-91 (2015).

105. Nath, S. C., Harper, L. & Rancourt, D. E. Cell-Based Therapy Manufacturing in Stirred Suspension Bioreactor: Thoughts for cGMP Compliance. *Frontiers in Bioengineering and Biotechnology* **8** (2020).

106. Csaszar, E., Mills, S. & Zandstra, P. W. Process evolution in cell and gene therapy from discovery to commercialization. *The Canadian Journal of Chemical Engineering* (2021).

107. Farid, S. S. Process economics of industrial monoclonal antibody manufacture. *Journal of Chromatography B* **848,** 8-18 (2007).

108. Bandeiras, C. TESSEE-Tool for Early Stem Cells Economic Evaluation. *DBE, IST, Lisbon, PT, PhD dissertation* (2019).

109. Raychaudhuri, S. *Introduction to monte carlo simulation* in *2008 Winter simulation conference* (2008), 91-100.

110. *Logical process designs for stem cell manufacturing: computational support tools for improved cost-effectiveness* https://www.regmednet.com/logical-process-designs-for-stem-cell-manufacturing-computational-support-tools-for-improved-cost-effectiveness/ (2017).

111. Nießing, B., Kiesel, R., Herbst, L. & Schmitt, R. H. Techno-Economic Analysis of Automated iPSC Production. *Processes* **9,** 240 (2021).

112. Bandeiras, C., Cabral, J. M., Gabbay, R. A., Finkelstein, S. N. & Ferreira, F. C. Bringing Stem Cell-Based Therapies for Type 1 Diabetes to the Clinic: Early Insights from Bioprocess Economics and Cost-Effectiveness Analysis. *Biotechnology journal* **14,** 1800563 (2019).

113. Wallner, K. *et al.* Stem cells and beta cell replacement therapy: a prospective health technology assessment study. *BMC endocrine disorders* **18,** 1-12 (2018).

114. Jenkins, M., Bilsland, J., Allsopp, T. E., Ho, S. V. & Farid, S. S. Patient-specific hiPSC bioprocessing for drug screening: Bioprocess economics and optimisation. *Biochemical Engineering Journal* **108,** 84-97 (2016).

115. Weil, B. D. *et al.* An integrated experimental and economic evaluation of cell therapy affinity purification technologies. *Regenerative medicine* **12,** 397-417 (2017).

116. Darkins, C. L. & Mandenius, C.-F. Design of large-scale manufacturing of induced pluripotent stem cell derived cardiomyocytes. *Chemical Engineering Research and Design* **92,** 1142-1152 (2014).

117. Glen, K. E., Cheeseman, E. A., Stacey, A. J. & Thomas, R. J. A mechanistic model of erythroblast growth inhibition providing a framework for optimisation of cell therapy manufacturing. *Biochemical Engineering Journal* **133,** 28-38 (2018).

118. Misener, R. *et al.* Stem cell biomanufacturing under uncertainty: a case study in optimizing red blood cell production. *AIChE Journal* **64,** 3011-3022 (2018).

119. Simaria, A. S. *et al.* Allogeneic cell therapy bioprocess economics and optimization: Single-use cell expansion technologies. *Biotechnology and bioengineering* **111,** 69-83 (2014).

120. Mizukami, A. *et al.* Technologies for large-scale umbilical cord-derived MSC expansion: Experimental performance and cost of goods analysis. *Biochemical Engineering Journal* **135,** 36-48 (2018).

121. Harrison, R. P., Medcalf, N. & Rafiq, Q. A. Cell therapy-processing economics: small-scale microfactories as a stepping stone toward large-scale macrofactories. *Regenerative medicine* **13,** 159-173 (2018).

122. Hassan, S. *et al.* Allogeneic cell therapy bioprocess economics and optimization: downstream processing decisions. *Regenerative medicine* **10,** 591-609 (2015).

123. Hassan, S. *et al.* Process change evaluation framework for allogeneic cell therapies: impact on drug development and commercialization. *Regenerative medicine* **11,** 287-305 (2016).

124. Chilima, T. D. P., Moncaubeig, F. & Farid, S. S. Impact of allogeneic stem cell manufacturing decisions on cost of goods, process robustness and reimbursement. *Biochemical Engineering Journal* **137,** 132-151 (2018).

125. Bandeiras, C., Cabral, J. M., Finkelstein, S. N. & Ferreira, F. C. Modeling biological and eco- nomic uncertainty on cell therapy manufacturing: the choice of culture media supplementation. *Regenerative medicine* **13,** 917-933 (2018).

126. De Sousa Pinto, D. *et al.* Scalable Manufacturing of Human Mesenchymal Stromal Cells in the Vertical-Wheel Bioreactor System: An Experimental and Economic Approach. *Biotechnology journal* **14,** 1800716 (2019).

127. Ng, K. S. *et al.* Bioprocess decision support tool for scalable manufacture of extracellular vesicles. *Biotechnology and bioengineering* **116,** 307-319 (2019).

128. Chen, V. C. *et al.* Development of a scalable suspension culture for cardiac differentiation from human pluripotent stem cells. *Stem cell research* **15,** 365-375 (2015).

129. Hamad, S. *et al.* Generation of human induced pluripotent stem cell-derived cardiomyocytes in 2D monolayer and scalable 3D suspension bioreactor cultures with reduced batch-to-batch variations. *Theranostics* **9,** 7222 (2019).

130. *How to Dissociate and Plate Human Pluripotent Stem Cell-Derived Cardiomyocytes for Micro-electrode Array (MEA) Assay* https://www.stemcell.com/how-to-dissociate-and-plate-human-pluripotent-stem-cell-derived-cardiomyocytes-for-microelectrode-array-mea-assay.html.

131. Kempf, H. *et al.* Controlling expansion and cardiomyogenic differentiation of human pluripotent stem cells in scalable suspension culture. *Stem cell reports* **3,** 1132-1146 (2014).

132. *iCell Cardiomyocytes, 11713* https://www.fujifilmcdi.com/icell-cardiomyocytes-11713-gcmc11713.

133. *Human iPSC-Derived Ventricular Cardiomyocytes (Male)* https://www.axolbio.com/shop/product/human-ipsc-derived-ventricular-cardiomyocytes-male-154591?category=39.

134. Sehnert, A. J. *et al.* Cardiac troponin T is essential in sarcomere assembly and cardiac contractility. *Nature genetics* **31,** 106-110 (2002).

135. Sharma, S., Jackson, P. & Makan, J. *Cardiac troponins* 2004.

136. Kannel, W. B., Kannel, C., Paffenbarger Jr, R. S. & Cupples, L. A. Heart rate and cardiovascular mortality: the Framingham Study. *American heart journal* **113,** 1489-1494 (1987).

137. Macri-Pellizzeri, L. *et al.* Substrate stiffness and composition specifically direct differentiation of induced pluripotent stem cells. *Tissue Engineering Part A* **21,** 1633-1641 (2015).

138. Aisenbrey, E. A. & Murphy, W. L. Synthetic alternatives to Matrigel. *Nature Reviews Materials* **5,** 539-551 (2020).

139. Kempf, H. *et al.* Bulk cell density and Wnt/TGFbeta signalling regulate mesendodermal patterning of human pluripotent stem cells. *Nature communications* **7,** 1-13 (2016).

140. Le, M. N. T., Takahi, M. & Ohnuma, K. Auto/paracrine factors and early Wnt inhibition promote cardiomyocyte differentiation from human induced pluripotent stem cells at initial low cell density. *Scientific reports* **11,** 1-9 (2021).

141. Serra, M., Chan, A., Dubey, M. & Shea, T. B. A low-cost interface for multi-electrode array data acquisition systems. *BioTechniques* **45,** 451-456 (2008).

142. Thomson, J. A. & Ludwig, T. *Culture medium containing gamma-aminobutyric acid, pipecolic acid or lithium for the maintenance of stem cells in an undifferentiated state* US Patent 8,426,203. Apr. 2013.

143. Chen, G. *et al.* Chemically defined conditions for human iPSC derivation and culture. *Nature methods* **8,** 424–429 (2011).

7 | Appendix

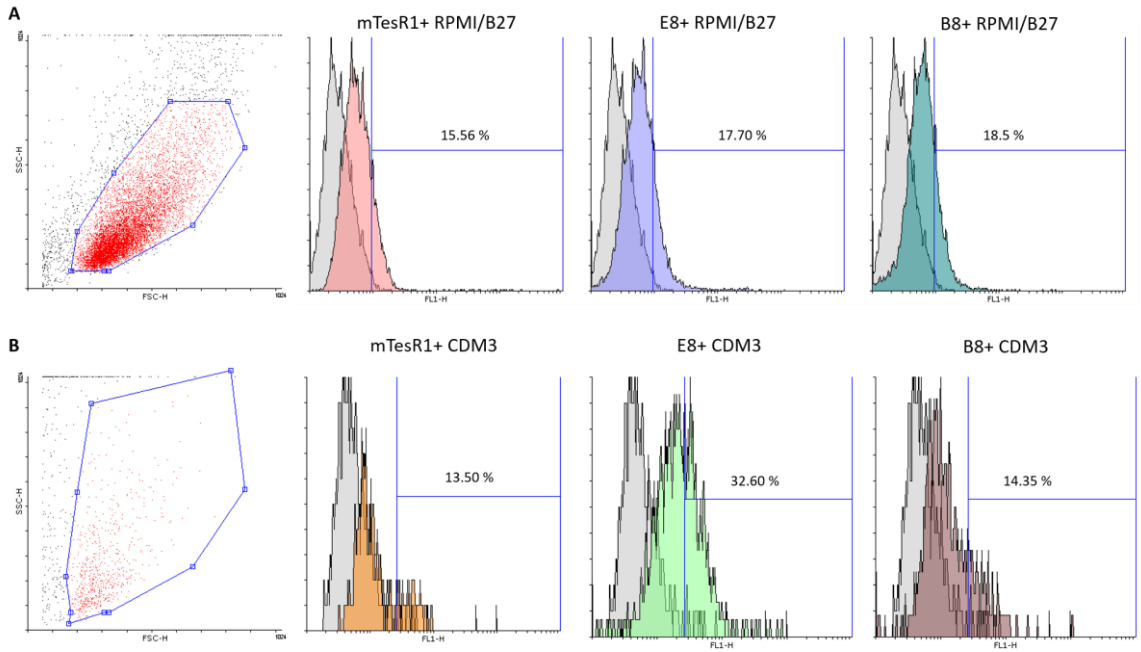

Figure 7.1: Flow cytometry analysis of cardiac differentiated cells from Gibco hiPSCs via modulation of the canonical Wnt pathway under different expansion and differentiation media. A: hiPSCs grown in mTesR1, E8 or B8 medium and differentiated in RPMI/B27 medium; B: hiPSCs grown in mTesR1, E8 or B8 medium and differentiated in CDM3 medium. For each condition, representative images of a 2D dot plot show population gating and histograms of cTnT, including negative controls (grey) are shown.For RPMI/27 conditions at least 10,000 events were captured. However, for CDM3 conditions, very few events (in some cases, less than 1000) were captured due to low cell numbers.

Table 7.1: Reagents and respective costs considered in the bioprocess economic model of the production of autologous hiPSC-CMs in Vertical-Wheel™ Bioreactors

Reagents	Cost	Reference	Observations
Reagents for Differentiation			
RPMI	36.06 €/L	TFS (21875034)	-
B-27	384.00 €/L	TFS (A1486701)	Dilution of 1:50 in RPMI
B-27 (-) Insulin	398.00 €/L	TFS (A3695201)	Dilution of 1:50 in RPMI
Rice-derived recombinant human albumin	0.04 €/L	SA (A9731-5G)	Concentration of 500 μg/L in RPMI
L-ascorbic acid 2-phosphate	0.01 €/L	SA (A8960-5G)	Concentration of 213 μg/L in RPMI
CHIR-99021	42.52 €/L	SA (SML1046-25MG)	Concentration of 6 μM in CM
Y-27632	64.83 €/L	SCT (72304)	Concentration of 5 μM in CM
IWP-4	71.12 €/L	SA (SML1114-25MG)	Concentration of 5 μM in CM
Reagents for Purification			
Sodium L-lactate	0.01 €/L	SA (L7022-5G)	Concentration of 4 μM in CM
Reagents for Maturation			
DMEM no glucose	41.50 €/L	TFS (11966025)	-
HEPES 1M	52.09 €/L	TFS (15630080)	Concentration of 10 mM in DMEM
L-Carnitine inner salt	7.74 €/L	SA (C0158-5G)	Concentration of 2 mM in DMEM
Creatine	458.96 €/L	SA (C0780-100G)	Concentration of 5 mM in DMEM
Taurine	287.85 €/L	SA (T0625-100G)	Concentration of 5 mM in DMEM
MEM non essential amino acids solution	43.18 €/L	TFS (11140050)	Dilution of 1:100 in DMEM
ITS-G	63.23 €/L	TFS (41400045)	Dilution of 1:100 in DMEM
Linoleic Acid-Oleic Acid-Albumin	159.68 €/L	SA (L9655-5ML)	Dilution of 1:100 in DMEM
Reagents for Harvesting			
Accutase	450.00 €/L	SA (SCR005)	-
Reagents for Cryopreservation			
Cryostor CS10	4080.00 €/L	SCT (07930)	-

Reagents for Flow Cytometry			
PBS	39.30 €/L	SA (806552-1L)	-
Trypsin-EDTA	365.80 €/L	TFS (15400054)	Dilution of 1:2 in PBS
4% FBS	95.38 €/L	SA (F2442-50ML)	Dilution of 1:25 in PBS
1% NGS	262.30 €/L	SA (566380-10ML)	Dilution of 1:100 in PBS
3% NGS	708.30 €/L	SA (566380-10ML)	Dilution of 3:100 in PBS
2% PFA	40.56 €/L	SA (158127-500G)	Concentration of 20 g/L in PBS
1% Saponin	53.44 €/L	SA (47036-50G-F)	Dilution of 1:200 in PBS
1% BSA	1539.60 €/L	TFS (15561020)	0.5% in PBS
1% Triton X-100	103.01 €/L	SA (T8787-100ML)	Dilution of 1:100 in PBS
OCT4 Antibody	11,50 €/L	TFS (MA1-104)	Dilution of 1:300 in 3% NGS
SOX2 Antibody	22,60 €/L	TFS (MA1-014)	Dilution of 1:150 in 3% NGS
Nanog Dylight 488 Antibody	35201.22 €/L	TFS (MA1-017-D488)	Dilution of 1:100 in 3% NGS
Sarcomeric α-Actinin PE Antibody	20934.13 €/L	MB (130-119-766)	Diluition of 1:50 in 3% NGS
cTnT Antibody	15646.68 €/L	TFS (MA5-17192)	Dilution of 1:250 in FB2
MYL7 Antibody	44801.22 €/L	TFS (MA5-26390)	Dilution of 1:100 in 3% NGS
MLC2v Antibody	39701.22 €/L	TFS (PA5-86045)	Dilution of 1:100 in 3% NGS
Anti-mouse IgG1 AF488 Secondary Antibody	50449.19 €/L 10086.40 €/L	TFS (A-21121)	Dilution of 1:20 in 3% NGS Dilution of 1:100 in FB2*
Anti-human IgG1 AF488 Secondary Antibody	60084.07 €/L	TFS (A10631)	Dilution of 1:10 in 3% NGS
Anti-rabbit IgG AF488 Secondary Antibody	25149.19 €/L	TFS (A-11008)	Dilution of 1:20 in 3% NGS
Reagents for qRT-PCR			
RNA Kit	15.20 €/use	TFS (12183020)	10 preparations
cDNA Kit	2.09 €/use	TFS (4368814)	200 reactions
TaqMan™ Gene Expression Master Mix	493.00 €	TFS (4369016)	200 reactions
SOX2 TaqMan™ probe	1.14 €/use	TFS (4331182)	75 reactions
OCT4 TaqMan™ probe	1.14 €/use	TFS (4351372)	75 reactions
Nanog TaqMan™ probe	1.14 €/use	TFS (4331182)	75 reactions
Nkx2-5 TaqMan™ probe	1.14 €/use	TFS (4331182)	75 reactions
TNNT2 TaqMan™ probe	1.14 €/use	TFS (4351372)	75 reactions
MYL7 TaqMan™ probe	1.14 €/use	TFS (4331182)	75 reactions
MYL2 TaqMan™ probe	1.14 €/use	TFS (4331182)	75 reactions

Reagents for Immunocytochemistry			
5% NGS	1.15 €/L	SA (566380-10ML)	Dilution of 1:20 in PBS
10% NGS	2.27 €/L	SA (566380-10ML)	Dilution of 1:10 in PBS
4% PFA	41.81 €/L	SA (158127-500G)	Concentration of 40 g/L in PBS
0.1% Triton X-100	39.78 €/L	SA (X100-100ML)	Dilution of 1:1000 in PBS
DAPI	55.95 €/L	SA (D9542-1MG)	Concentration of 1.5 mg/L in PBS
SOX2 Antibody	15558.85 €/L	TFS (14-9811-82)	Dilution of 1:100 in SS
OCT4 Antibody	158971.00 €/L	TFS (MA5-31458)	Diluition of 1:25 in SS
MYL7 Antibody	40988.85 €/L	TFS (PA5-102011)	Dilution of 1:100 in SS
Sarcomeric α-Actinin Antibody	18774.15 €/L	Ab (ab137346)	Dilution of 1:100 in SS
cTnT Antibody	5945.61 €/L	RDS (MAB1874)	Dilution of 1:2000 in SS
Reagents for Microelectrode Array			
DMEM/F12	84.00 €/L	SA (SCM162)	-
Geltrex matrix	485.66 €/L	TFS (A1413201)	Dilution of 1:100 in DMEM/F12

Table 7.2: Facility associated parameters and respective costs considered in the bioprocess economic model of the production of autologous hiPSC-CMs in Vertical-Wheel™ Bioreactors

Parameter	Value	Reference
Facility area	400 m^2	[108]
Clean room ratio	0.2	[108]
Cost per clean room area	4652.00 €/m^2	[108]
Cost per non clean room area	2713.60 €/m^2	[108]
Facility depreciation period	15 years	[108]
Parallel processes	6	This work
Equipment depreciation period	5 years	[108]
Incubator amount	8	This work
Unit incubator cost	9604.00 €	TFS (15650667)
Centrifuge amount	4	This work
Unit centrifuge cost	7163.00 €	TFS (15808722)
BSC amount	4	This work
Unit BSC cost	10865.00 €	TFS (10445753)
Flow cytometer amount	1	This work
Unit flow cytometer cost	94700.00 €	TFS (15310677)
Spectrophotometer amount	1	This work
Unit spectrophotometer cost	10169.39 €	TFS (10506405)
qRT-PCR system amount	1	This work
Unit qRT-PCR system cost	20560.00 €	TFS (15341295)
Microscope amount	2	This work
Unit microscope cost	1396.00 €	TFS (15723725)
Fluorescence microscope amount	1	This work
Unit fluorescence microscope cost	20660.35 €	TFS (11960279)
PBS MINI base unit amount	18	This work
Unit PBS MINI base cost	2473.00 €	PBS Biotech
PBS 3 MAG base unit amount	6	This work
Unit PBS 3 MAG base cost	65550.00 €	PBS Biotech
MEA platform amount	1	This work
Unit MEA platform cost	24000.00 €	[141]
CO2 daily cost	13.14 €/day	[108]
Other gases daily cost	34.17 €/day	[108]
Additional supplies daily cost	17.3 €/day	[108]
Requalification daily cost	143.24 €/day	[108]
Maintenance daily cost	115.65 €/day	[108]
Cleaning daily cost	61.33 €/day	[108]
Garment daily cost	4.38 €/day	[108]
Employee amount	4	This work
Daily worktime	8 h/day	[108]
Salary per hour	12 €/h	[108]

Table 7.3: Medium feeding regimes considered in the bioprocess economic model of the production of autologous hiPSC-CMs in Vertical-Wheel™ Bioreactor

Step	Medium exchange regime
Differentiation	Total medium change at day 3 and from day 5 onwards 80% of the medium is changed
Purification	50% of the medium is changed everyday
Recovery	50% of the medium is changed everyday
Maturation	80% of the medium is changed every 2 days

Table 7.4: mTeSR1™ medium formulation. [142]

Component	Concentration (mM)	Component	Concentration (mM)
Inorganic salts			
Calcium chloride (anhydrous)	8.24×10^{-1}	Potassium chloride	3.26
HEPES	1.18×10^{1}	Sodium bicarbonate	1.80×10^{1}
Lithium chloride	9.80×10^{-1}	Sodium chloride	9.46×10^{1}
Magnesium chloride (anhydrous)	2.37×10^{-1}	Disodium phosphate (anhydrous)	
Magnesium sulfate	3.19×10^{-1}	Monosodium phosphate (monohydrate)	3.55×10^{-1}
Trace Minerals			
Ferric nitrate (nonahydrate)	9.71×10^{-5}	Chromium(III) chloride	1.98×10^{-6}
Ferric sulfate (heptahydrate)	1.18×10^{-3}	Silver nitrate	9.81×10^{-7}
Cupric sulfate (pentahydrate)	4.08×10^{-6}	Aluminium chloride (hexahydrate)	4.87×10^{-6}
Zinc sulfate (heptahydrate)	1.18×10^{-3}	Barium acetate	9.79×10^{-6}
Ammonium metavanadate	1.09×10^{-5}	Cobalt(II) chloride	9.81×10^{-6}
Mangenous sulfate (monohydrate)	1.97×10^{-6}	Germanium dioxide	4.97×10^{-6}
Nickel(II) sulfate (hexahydrate)	9.70×10^{-7}	Potassium bromide	9.89×10^{-7}
Selenium	1.77×10^{-4}	Potassium iodide	1.00×10^{-6}
Sodium metasilicate (nonahydrate)	9.66×10^{-4}	Sodium fluoride	9.83×10^{-5}
Tin(II) chloride	1.24×10^{-6}	Rubidium chloride	9.81×10^{-6}
Molybdic acid, ammonium salt	1.97×10^{-6}	Zirconyl chloride (octahydrate)	9.80×10^{-6}
Cadmium chloride	1.22×10^{-5}		
Energy Substrates			
D-Glucose	1.37×10^{1}	Sodium Pyruvate	3.92×10^{-1}
Lipids			
Linoleic acid	1.88×10^{-4}	Myristic acid	8.59×10^{-5}
Lipoic acid	4.00×10^{-4}	Oleic acid	6.94×10^{-5}
Arachidonic acid	1.29×10^{-5}	Palmitic acid	7.65×10^{-5}
Cholesterol	1.12×10^{-3}	Palmitoleic acid	7.71×10^{-5}
DL-α tocopherol-acetate	2.90×10^{-4}	Stearic acid	6.89×10^{-5}
Linolenic acid	6.99×10^{-5}		

Component	Concentration (mM)	Component	Concentration (mM)
Aminoacids			
L-alanine	1.37×10^{-1}	L-leucine	3.54×10^{-1}
L-arginine hydrochloride	5.48×10^{-1}	L-lysine hydrochloride	3.91×10^{-1}
L-asparagine (monohydrate)	1.37×10^{-1}	L-methionine	9.06×10^{-2}
L-aspartic acid	1.37×10^{-1}	L-phenylalanine	1.69×10^{-1}
L-cysteine hydrochloride (monohydrate)	7.83×10^{-2}	L-proline	2.16×10^{-1}
L-cysteine dihydrochloride	7.83×10^{-2}	L-serine	2.94×10^{-1}
L-glutamic acid	1.37×10^{-1}	L-threonine	3.52×10^{-1}
L-glutamine	2.94	L-tryptophane	3.46×10^{-2}
Glycine	2.94×10^{-1}	L-tyrosine disodium salt (dihydrate)	1.68×10^{-1}
L-histidine hydrochloride (monohydrate)	1.18×10^{-1}	L-valine	3.55×10^{-1}
L-isoleucine	3.26×10^{-1}		
Vitamins			
Ascorbic acid	2.53×10^{-1}	i-Inositol	5.49×10^{-2}
Biotin	1.12×10^{-5}	Niacinamide	1.30×10^{-2}
B12	3.94×10^{-4}	Pyridoxine hydrochloride	7.62×10^{-3}
Choline chloride	5.03×10^{-2}	Riboflavin	4.56×10^{-4}
D-Calcium pantothenate	3.69×10^{-3}	Thiamine hydrochloride	2.42×10^{-2}
Folic acid	4.71×10^{-3}		
Growth Factors/Proteins			
GABA	9.79×10^{-1}	Human Insulin	3.92×10^{-3}
Pipecolic Acid	9.84×10^{-4}	Human Holo-Transferrin	1.37×10^{-4}
bFGF	5.77×10^{-6}	Human Serum Albumin	1.95×10^{-1}
TGFβ1	2.35×10^{-8}	Glutathione (reduced)	6.38×10^{-3}
Other Components			
Hypoxanthine Na	1.18×10^{-2}	2-mercaptoethanol	9.80×10^{-2}
Phenol red	1.69×10^{-2}	Pluronic F-68	2.33×10^{-2}
Putrescine-2HCl	3.95×10^{-4}	Tween 80	3.29×10^{-4}
Thymidine	1.18×10^{-3}		

Table 7.5: Formulation for E8 medium. [143]

Components	E8
DMEM/F12 with HEPES	1
Insulin	19.4 mg/L
L-ascorbic acid 2-phosphate magnesium	64 mg/L
Transferrin	10.7 mg/L
Sodium selenium	14 μg/L
FGF2	100 μg/L
TGFB1	2 μg/L
Sodium bicarbonate	543 mg/L
pH	7.4
Osmolarity	340 mOsm/L

Table 7.6: Formulation for B8 medium. [60]

Components	B8	Brand
DMEM/F12 with HEPES	1	
Insulin	20 μg/mL	
Ascorbic acid 2-phosphate	200 μg/mL	Sigma-Aldrich
Transferrin	20 μg/mL	
Sodium selenite	20 ng/mL	
FGF2-G3	40 ng/mL	
TGFβ3	0.1 ng/mL	
NRG1	0.1 ng/mL	
Sodium bicarbonate	2438 μg/mL	
pH	7.1	-
Osmolarity	310 mOsm/L	-

Table 7.7: Formulation for RPMI 1640 medium. [74]

Component	Concentration (mg/L)
Aminoacids	
l-Arginine	200
l-Asparagine	50
l-Aspartic acid	20
l-Cystine	50
l-Glutamic acid	20
l-Glutamine	300
Glutathione, reduced	1
Glycine	10
l-Histidine	15
l-Hydroxyproline	20
l-Isoleucine	50
l-Leucine	50
l-Lysine hydrochloride	40
l-Methionine	15
l-Phenylalanine	15
l-Proline	20
l-Serine	30
l-Threonine	20
l-Tryptophan	5
l-Tyrosine	20
l-Valine	20
Vitamins	
para-Aminobenzoic acid	1
Biotin	0.2
Calcium pantothenate	0.25
Choline chloride	3
Cyanocobalamin	0.005
Folic acid	1
i-Inositol	35
Nicotinamide	1
Pyridoxine hydrochloride	1
Riboflavin	0.2
Thiamine hydrochloride	1
Salts	
Calcium nitrate tetrahydrate	100
Disodium phosphate heptahydrate	1512
Magnesium sulfate heptahydrate	100
Potassium chloride	400
Sodium bicarbonate	2000
Sodium chloride	6000
Miscellaneous	
Glucose	2000
Phenolsulfonphthalein	5

Table 7.8: Formulation for CDM3 medium. [76]

Component	Concentration (μg/L)
RPMI 1640 basal medium	1 x L-
ascorbic acid 2-phosphate	213 μg/L
rice-derived recombinant albumin	500 μg/L

Table 7.9: Fatty acid-rich medium formulation for the metabolic maturation of hiPSC-CMs. [90]

Component	Concentration
DMEM, no Glucose	1 x
HEPES	10 mM
L-carnitine inner salt	2 mM
Creatine	5 mM
Taurine	5 mM
MEM (non-essential amino acids) Solution	100 x
Insulin, Transferrin, Selenium Solution (ITS-G)	100 x
Linoleic Acid-Oleic Acid-albumin	100 x
Penicillin-Streptomycin	100 x